Soybean Nodulin 26: A Channel for Water and Ammonia at the Symbiotic Interface of Legumes and Nitrogen-fixing Rhizobia Bacteria

A Dissertation

Presented for the

Doctor of Philosophy

Degree

The University of Tennessee, Knoxville

Jin Ha Hwang

May 2013

ACKNOWLEDGEMENTS

First of all, I would like to express my utmost appreciation to my mentor, Dr. Daniel M. Roberts, who has been more than just a supervisor. He has always supported and encouraged me in my endeavors both in life and in science. He is the best research mentor I have ever met in the entire period of my life. He has guided me and shown me exactly where I have to go in the field of science. Even though I occasionally had doubt, his guidance always turned out to be right after all. Now, I really respect him for that from the bottom of my heart. One more serious note, and one that I will not ever forget in my whole life, when I found myself in a difficult situation due to my family issues, he supported my decision to take a much needed one-year break so that I could take care of my family before returning to take the huge step of earning a Ph.D. Again, on behalf of my family members, I would like to thank Dan.

I would also like to thank my doctoral committee: Dr. Elias Fernandez, Dr. Gladys Alexandre, Dr. Brad Binder, and Dr. Juan Luis Jurat-Fuentes for guidance and assistance during my time in graduate school. Through the committee meetings, their careful advice and constructive criticism have helped foster my scientific growth. Additionally, I want to thank Dr. Albrecht von Arnim for providing me with lots of assistance concerning my graduate studies, family issues, and life in general.

I am setting aside the best for last: my labmates. I have had wonderful privilege to work with a number of people in the lab. Special thanks to Pintu,

Ansul and their wives (Pradnya, and Anisha). These Indian brothers (not just friends) have always been supportive and we did not hesitate to share all of our emotions through the good and the bad of our lives in Knoxville. I also would like to thank other lab members. I cannot forget about smart Tian. She has mainly collaborated with me in yeast work, and has shared great memories in lab life. I was also really happy to work with Pratyush, a postdoc in our lab. He is the most careful and detailed scientist I have ever had the benefit to work with. I have to also thank handsome Craig (now undoubtedly as my American brother) for his valuable efforts into detailed revision on my dissertation writing. He actually worked on almost all of my English writing. There are too many to name them all, but there are a few former graduates with whom I spent truly memorable times in the lab: Won-Gyu Choi, Ian Wallace, and Eric Vincill. I wish them all success in their future careers.

On a more personal note, I want to thank my family in Korea. My father, my mother, my late sister and her family members have also supported me. Thank you. Finally, I sincerely thank my wife, Sejin Moon, and son, Daniel Jae-oong Hwang. They have been patient and have happily supported me through the hardest times. Obviously, without these two, it would not have been possible to complete my study and to build up all things together.

Finally, I am thankful to God for the strength to complete my work at the University of Tennessee.

ABSTRACT

During the infection and nodulation of legume roots by soil bacteria of the *Rhizobiaceae* family, the invading endosymbiont becomes enclosed within a specialized nitrogen-fixing organelle known as the "symbiosome". In mature nodules the host infected cells are occupied by thousands of symbiosomes, which constitute the major organelle within this specialized cell type. The symbiosome membrane is the outer boundary of this organelle which controls the transport of metabolites between the symbiont and the plant host. These transport activities include the efflux of the primary metabolic product of nitrogen fixation and the uptake of dicarboxylates as an energy source to support bacterial nitrogen fixation.

Soybean nodulin 26, a member of the aquaporin superfamily, is the major protein component of the symbiosome membrane that encloses nitrogen-fixing bacteroids in root nodules. Previous work has demonstrated that nodulin 26 facilitates the transport of water as well as other uncharged solutes such as glycerol and formamide. In addition, it is clear that the protein is a target for developmental and environmental sensitive posttranslational phosphorylation which may regulate transport activity.

The present research project provides evidence that nodulin 26 is an “aquaglycero-ammoniaporin” that is specifically localized to the symbiosome membrane, where it could play a potential role in osmoregulatory and metabolic functions in the symbiosis. First, it is shown that purified nodulin 26 reconstituted

into liposomes possesses an ammonia permease activity that is favored approximately 4-fold over its aquaporin activity. Second, it is shown that nodulin 26 serves as a docking site for the ammonia assimilatory enzyme, cytosolic glutamine synthetase on the surface of the symbiosome membrane. Third, it is shown that phosphorylation of nodulin 26 exerts opposite effects on the regulation of ammonia and water transport activities. Fourth, it is demonstrated that phosphorylation of nodulin 26 in mature nitrogen-fixing nodules is tightly controlled by various environmental osmotic stimuli that regulate the rate of nitrogen-fixation as well as modulation of the oxygen diffusion barrier inside nodules. A model for how nodulin 26 phosphorylation could contribute to the regulation of these physiological processes is devised.

TABLE OF CONTENTS

LIST OF TABLES

LIST OF FIGURES

CHAPTER I

INTRODUCTION

Overview of water channels

Water is a simple chemical substance containing one oxygen and two hydrogen atoms which is an indispensable molecule in biological systems. Since water molecules compose the most abundant part and primary unit of living cells, they define the environment for many biological processes. This aqueous environment of living systems is structurally organized into distinct cells and organelles by the hydrophobic barriers of lipid bilayers. In terms of water homeostasis, the maintenance of metabolic and osmotic equilibrium in aqueous conditions is crucial to counterbalance and prevent the cells from disarranging changes (Ho, 2006). Biological membrane barriers spontaneously formed by the lipid bilayers structurally compartmentalize organelles and enable cells to transport water molecules and various metabolites in and out of organelles and cells. Water flux across subcellular, cellular and transcellular barriers plays a key role in homeostatic regulation processes.

Water flux across membranes occurs in two ways, which can be defined by using two quantitative biophysical parameters. First, water can diffuse

nonspecifically directly through the membrane lipid bilayer matrix. This diffusion rate is quantified by the diffusive permeability coefficient (P_d). The second mechanism for membrane water flux is by osmosis-driven facilitated transport through proteinaceous channels. This facilitated transport is quantified by the osmotic permeability coefficient (P_f) (Baylis, 1988). The ratio of P_f/P_d can be used as an indicator to determine if water movement is simply diffusive (if close to 1) or facilitated (if greater than 1) (Finkelstein, 1987).

Activation energy (E_a) reflects the temperature dependence of water movement and can distinguish facilitated transport from simple bilayer diffusion, since facilitated transport, which mimics movement in aqueous media, is energetically favored (Zeidel et al., 1992; King and Agre, 1996). Diffusive water transport through a hydrophobic membrane requires a relatively higher activation energy of more than 10 kcal/mol (King and Agre, 1996). In contrast, channel-mediated water movement is characterized by lower activation energy, usually less than 5 kcal/mol (King and Agre, 1996). Having identified that biological membranes often exhibit lower E_a than simple diffusion, early studies sought to identify a proteinaceous transporter for water. Additional evidence for proteinaceous transport in biological membranes was provided by the observation of mercurial inhibition of the water flow. Simple bilayer diffusion through model membranes is not inhibited by Hg^{2+}, and the effect of this reagent on water transport through biological membranes was proposed to result from interaction with and modification of sulfhydryls of cysteines present in water

channel proteins (Macey, 1984). Taking this combined evidence into account, a higher ratio of P_f over P_d, lower energy cost and mercurial inhibition of water transport lead to the prediction of protein-facilitated water flux across biological membrane barriers.

A major breakthrough in the molecular understanding of facilitated water flux came from the seminal work of Peter Agre's laboratory. In the late 1980s, a major integral membrane protein, known as CHIP28, was identified from human red-blood cells and rat kidney membranes (Agre et al., 1987; Denker et al., 1988). Agre's group found that CHIP28 is a selective water-transporting channel by using a *Xenopus* oocyte expression system. Specifically, it was observed that expression of erythrocyte CHIP28 protein in *Xenopus* oocytes resulted in a large increase in the permeability of the plasma membrane for water (Preston and Agre, 1991; Preston et al., 1992). In support of this finding, reconstitution of purified CHIP28 into proteoliposome vesicles resulted in a highly increased P_f and exhibited the biochemically defined characteristics of water channels such as mercurial sensitivity and a low activation energy for water transport (Zeidel et al., 1992). In 1997, the aquaporin nomenclature workshop of the Human Genome Nomenclature committee renamed CHIP28 as aquaporin 1 (AQP1) (Agre, 1997). In 2003, Peter Agre was awarded the Nobel Prize in Chemistry for his groundbreaking work on aquaporins (Agre, 2003).

Major Intrinsic Proteins (MIPs): diversity and structural features

Since the initial characterization of the first aquaporins, and with the substantial advances in functional genomics, it became clear that aquaporins are members of an ancient family of structurally similar integral membrane channels known as “the major intrinsic proteins” (MIPs). The MIPs are ubiquitously expressed in all organisms from prokaryotes to higher eukaryotes (El Karkouri et al., 2005; Zardoya, 2005), and are especially prevalent and diverse in plants (Johanson et al., 2001). MIPs are responsible for the selective bidirectional flux of water and neutral uncharged solutes across cellular membranes (King et al., 2004; Maurel et al., 2008; Hachez and Chaumont, 2010). Mammals contain 13 MIP genes (Agre et al., 1998). With regard for transport specificity, mammalian MIPs were originally clustered into two different subsets: the aquaporins and aquaglyceroporins (Agre et al., 1998). The aquaporins possess a high degree of water specificity, and exclude other solutes and protons. In contrast, the aquaglyceroporins are permeable to water and small uncharged molecules such as polyols (including glycerol) and other uncharged solutes such as urea (Maurel et al., 1994; Luyten et al., 1995; Rivers et al., 1997; Hubert et al., 2005). AQP1, the original CHIP28 protein, belongs to the water-specific class and is completely selective for water transport (Preston et al., 1992). AQP2, AQP4 and AQP5 are also classified as typical water-specific aquaporins (Echevarria and Ilundain, 1998; Carbrey and Agre, 2009).

Unlike the water-specific aquaporins, mammalian AQP3, AQP7, AQP9 and AQP10, are representatives of the multifunctional aquaglyceroporins, and have been demonstrated to be permeable to uncharged small solutes like glycerol and urea in addition to water (Ishibashi et al., 1994; Ishibashi et al., 1997; Tsukaguchi et al., 1998; Ishibashi et al., 2002). Aquaglyceroporins are expressed in a variety of different tissues, and emerging reports suggest that several of them may play numerous physiological or pathophysiological roles in a wide range of metabolism and metabolic diseases in mammals (Rojek et al., 2008).

Analysis of the MIP superfamily by sequence alignment, secondary structure predictions and ultimately by crystallographic structural studies have shown a highly conserved topology and structural fold shared by all family members (Gonen and Walz, 2006). MIPs generally assemble into homotetramers with individual subunits (molecular weights between 25 and 30 kDa) forming the transport pore. Each subunit consists of six transmembrane helices linked by five loops (A to E) with amino- and carboxy-terminal cytoplasmic extensions (Fig. 1.1). Loops B and E contain small helices that have highly conserved asparagine, proline and alanine sequences (Asn-Pro-Ala) called the NPA motifs. Structural studies show that these motifs fold back into center of the membrane-embedded pore forming two opposing half helices where the two Asn side chains meet in middle of pore (Fig. 1.1).

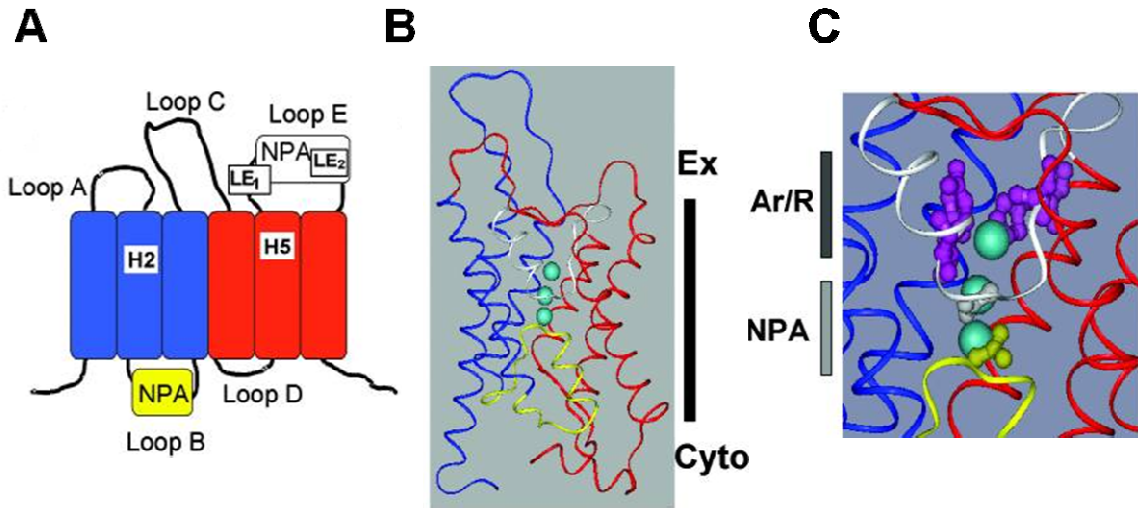

Figure 1.1. Conserved structural topology of Major Intrinsic Proteins. (A) Conserved topological diagram of the MIP family. Transmembrane α-helices 1 to 3 shown in blue and 4 to 6 shown in red based on Wallace and Roberts (2004). Two NPA half helices are shown in yellow (in loop B) and white (in loop E). Helix H2 and H5, and loop E (LE_1 and LE_2) indicate positions from which ar/R tetrad forms. **(B)** Crystal structure of bovine AQP1 (PDB: 1J4N) (Sui et al., 2001) with same color codes from **A**. Three water molecules in the channel pore are shown as aqua spheres. The extracellular (Ex) and cytosolic (Cyto) faces of the bilayer are indicated, and the width of the lipid bilayer is represented as a black bar. **(C)** Representation of the ar/R and NPA constrictions with trapped water molecules in the channel pore. Ar/R is shown in magenta, and side chains of NPA Asn residues are shown in white and yellow.

The selectivity filter is formed by four amino acids that come together to form a narrow constriction in the channel pore (de Groot and Grubmuller, 2001).

Due to this narrowing in the pore architecture as well as the symmetrical two-fold topology of the 6 membrane domains and the 7th pseudo-transmembrane helix, the structural fold of the MIP family has been highly conserved and can be represented as an “hourglass” (Fig. 1.1) (Jung et al., 1994). The narrowest constriction is termed the aromatic/argnine region (ar/R) (de Groot and Grubmuller, 2001), which consists of a group of 4 amino acids in close proximity within the channel pore including a conserved arginine and the presence of aromatic amino acid side chains. The ar/R is composed of amino acids from the 2nd and 5th helices (H2 and H5) and two other residues (LE_1 and LE_2) from loop E (Fig. 1.1). In water-selective AQP1, these residues are Phe (H2), His (H5), Cys (LE_1) and Arg (LE_2). The His and Arg residues form three hydrogen bond contacts with an entering water molecule, facilitating high flux of water through the filter. In addition, the AQP1 ar/R constricts the pore to 3 Å, approximately the diameter of one water molecule, allowing specificity (Sui et al., 2001).

The structural basis for aquaglyceroporin transport is best represented by the bacterial glycerol facilitator GlpF. GlpF was cloned in *E. coli* and characterized by *Xenopus* oocyte analysis and showed selectivity for glycerol transport with a very low intrinsic water transport rate (Sweet et al., 1990; Maurel et al., 1994). From the x-ray crystal structure (Fu et al., 2000), the ar/R of GlpF is

composed of two aromatic residues Trp (H2) and Phe (LE_1), and the conserved Arg (LE_2) characteristic of most ar/R, and a small side chain Gly (H5). This results in a wider (3.6 Å) and more hydrophobic selectivity filter compared to AQP1. The amphipathic properties of the GlpF ar/R allow the Phe and Trp residues to form hydrophobic interactions with the hydrocarbon backbone of glycerol, while the Arg forms hydrogen bond contacts with the hydroxyl group of glycerol (Fu et al., 2000). In addition to these features necessary to interact with transported glycerol, the increase in the hydrophobicity of the GlpF ar/R accommodates a barrier to water transport because of reduced ability to form hydrogen bond contacts with transported water molecules (Fu et al., 2000).

Major Intrinsic Proteins (MIPs): classification in plants

Since the first characterization of *Arabidopsis* tonoplast intrinsic protein γ (γ-TIP) (Maurel et al., 1993) as an aquaporin, many other plant MIPs have been investigated. For example, whole genome sequencing has uncovered 35 full-length MIP genes encoded in *Arabidopsis* (Johanson et al., 2001), 33 in rice (Sakurai et al., 2005) and 55 in poplar (Gupta and Sankararamakrishnan, 2009), compared to 13 in humans and 2 in *E. coli*. In plants, aquaporin-mediated water flux is a key physiological process in cell elongation, osmoregulation, seed germination and continuous water utilization (Maurel, 2007). In addition, plants are more likely to be exposed to environmental osmotic stresses such as drought and salinity because their sessile life style accords limited ability to escape from

these adverse environmental conditions (Chrispeels and Maurel, 1994). In addition, water relations are critical for common aspects of plant cell growth and development-relating turgor-driven cell expansion (Cosgrove, 1986). Therefore, plants require efficient and rapid regulation of bulk water flow to adapt to environmental challenges and to undergo fundamental developmental processes. Accordingly, it is not surprising that plants evidently have larger numbers of MIP genes as compared to animals and bacteria. However, it is also clear that the diversification of plant MIPs has led to the acquisition of additional transport functions besides water flux (Ludewig and Dynowski, 2009).

The *Arabidopsis* MIPs have been classified into four plant-specific phylogenetic subgroups based on their sequence similarity: the plasma membrane intrinsic proteins (PIPs), the tonoplast intrinsic proteins (TIPs), the small basic intrinsic proteins (SIPs) and the nodulin 26-like intrinsic proteins (NIPs) (Johanson et al., 2001; Quigley et al., 2002). PIPs and TIPs possess aquaporin activities and are localized in plasma membrane and vacuolar (named also tonoplast) membrane, respectively (Chaumont et al., 2005). The NIP subgroups are homologs of soybean nodulin 26, a protein that is uniquely expressed in the symbiosome membrane of rhizobia-infected nitrogen-fixing root nodules (Fortin et al., 1987; Weaver et al., 1991). This subgroup is the focus of this dissertation and will be discussed further in more detail below. The SIPs which are a unique subset of MIPs due to their short amino-terminus and high frequency of basic residues at the carboxy-terminus are localized to the

endoplasmic reticulum (ER) membrane (Hanton et al., 2005; Ishikawa et al., 2005). Their transport selectivities and biological functions still remain as of yet unresolved.

Besides an increase in phylogenetic diversity, structural modeling of plant MIPs has shown diversification of pore selectivity (ar/R) sequences that transcend the traditional aquaporin and aquaglyceroporin paradigms. For example, Wallace and Roberts (2004) showed by homology modeling-based structural analysis for the ar/R selectivity regions of *Arabidopsis* MIPs that they can be classified into eight different subgroups based upon properties of each residue forming the ar/R tetrad, suggesting functional diversification of plant MIPs (Wallace and Roberts, 2004). Among the plant MIPs, only PIPs have one conserved ar/R signature characteristic of water-selective aquaporins (Wallace and Roberts, 2004). In contrast, TIPs are the most diverse with three separate conserved ar/R subgroups. NIPs are categorized into two distinct ar/R sequences, one that is similar to the soybean nodulin 26 as NIP subgroup I, and another that is characteristic of NIP subgroup II (Wallace and Roberts, 2004). The SIP subfamily possesses two separate ar/R regions (Wallace and Roberts, 2004). Additionally, subsequent analysis of MIP gene families in higher plants such as rice, maize (Bansal and Sankararamakrishnan, 2007) and poplar (Gupta and Sankararamakrishnan, 2009) as well as the moss *Physcomitrella patens* (Danielson and Johanson, 2008) have supported the unusual pore ar/R diversity of plant MIPs. For example, homology modeling and sequence analysis of rice,

maize (Bansal and Sankararamakrishnan, 2007) and poplar (Gupta and Sankararamakrishnan, 2009) MIPs discovered even more diverse ar/R signatures than those found in *Arabidopsis* (Wallace and Roberts, 2004).

Members of these MIP subfamilies are highly conserved through all sequenced plant genomes, but their structural and topological diversities including distinct ar/R compositions have been proposed to result in a variety of transport selectivities in addition to water transport activity (Wallace and Roberts, 2004; Bansal and Sankararamakrishnan, 2007; Ludewig and Dynowski, 2009). For example with one of the four MIP subfamilies, NIPs are unique to plant species, and each subgroup of the NIPs has different transport substrates based on the functional analysis and characterization with distinct ar/R constriction regions. NIP subgroup I transports water, glycerol (Dean et al., 1999) and lactic acid (Choi and Roberts, 2007), whereas NIP subgroup II is permeable to additional larger solutes such as urea (Wallace and Roberts, 2005) and boric acid (Takano et al., 2006; Tanaka et al., 2008). The additional divergent NIP subgroup III in rice functions as transporters for silicic acid (Ma et al., 2007; Mitani et al., 2008), arsenite (Ma et al., 2008) and selenite (Zhao et al., 2010).

The principle focus of this dissertation is the nodulin 26-like proteins (NIPs) and specifically legume nodulin 26. Nodulin 26 is the archetype of the NIP subfamily which was originally discovered as a protein specifically induced during the infection of soybean roots by soil rhizobia (Fortin et al., 1987), a

process that establishes a nitrogen-fixing symbiosis. In the next section, the process of nodulation and symbiotic nitrogen fixation are reviewed.

Biological nitrogen fixation in microorganisms

Nitrogen is one of the most important fundamental components comprising amino- and nucleic-acids and is an essential mineral nutrient to all organisms in nature. Nitrogen is abundant in the biosphere in diverse chemical forms. Molecular nitrogen (N_2) represents up to 80% in the atmosphere. For plant growth, however, nitrogen is often the most limiting macronutrient because biologically available nitrogen sources such as nitrate or ammonia are insufficient in the natural environment and plants can not directly utilize molecular nitrogen (N_2) found in the atmosphere (Gutierrez, 2012). Limitations in nitrogen is a major issue for sustainable agricultural productivity and the need for synthetic forms of nitrogen nutrients such as urea and ammonium nitrate is responsible for up to 50% of the operational costs in global agriculture (Hirel et al., 2011).

There are three distinct pathways through which molecular nitrogen is converted into biologically accessible forms of nitrogen: 1. biological enzymatic fixation of N_2 to ammonia; 2. atmospheric reactions by lightning discharge which converts N_2 to nitric (HNO_2) and nitrous (HNO_3) acids which are promptly accumulated into the biosphere by rain as nitrite (NO_2^-) and nitrate (NO_3^-); 3. the industrial Harber-Bosch fixation of N_2 to ammonia which is the source of most commercial fertilizers (Marschner, 1995). Fixed nitrate or ammonia can be

further assimilated by plants into organic biosynthetic metabolites such as amino acids, nucleotides, urea, and other N-associated biomolecules.

Biological nitrogen fixation is performed by diazotrophic bacteria, which are present either in a free-living form or as symbionts associated with different host organisms. Bacterial *Rhizobia*, actinobacteria *Frankia* and cyanobacteria are examples of symbiotic diazotrophs (Postgate, 1998; Vessey et al., 2005; Stal et al., 2010). Diazotrophs contain a metalloenzyme nitrogenase which catalyzes the reduction of N_2 to ammonia (Hu and Ribbe, 2011). The nitrogenase enzyme is composed of two separate enzymatic components. These include the heterotetrameric molybdenum-iron (MoFe) protein which is called dinitrogenase, and a homodimeric iron (Fe) protein called dinitrogenase reductase (Dixon and Kahn, 2004). Dinitrogenase reductase plays an important role as an electron donor in transferring high potential electrons to the dinitrogenase component. The dinitrogenase coordinates the FeMo cofactor near its N_2-binding active site and mediates the catalyzed reduction of N_2 to NH_3 (Eady and Postgate, 1974; Dixon and Kahn, 2004; Seefeldt et al., 2004). The overall N_2 reduction reaction catalyzed by this enzyme is as follows in equation 1.1:

$$N_2 + 8\,H^+ + 8e^- + 16\,ATP \longrightarrow 2\,NH_3 + H_2 + 16\,ADP + 16\,Pi \qquad \text{(Eq. 1.1)}$$

Chemically, the reaction of N_2 fixation requires hydrolysis of 16 moles of ATP as a source of chemical energy to compensate for the high energetic cost of N_2

reduction (N_2 bond energy is 225 kcal/mole) and produces one molecule of hydrogen gas (H_2) and two ammonia molecules (NH_3) (Igarashi and Seefeldt, 2003). The nitrogenase enzyme is extremely susceptible to inactivation by molecular oxygen (O_2), which oxidizes the iron-sulfur (Fe-S) cofactor and results in irreversible inhibition of the enzyme activity (Bergersen et al., 1976; Goldberg et al., 1987). These observations lead to the paradox encountered by nitrogen-fixing organisms: 1. the need for high respiration rates to supply energy for nitrogen fixation; and 2. the oxygen sensitivity of the nitrogenase.

In order to overcome the deleterious effects of the molecular oxygen, nitrogen-fixing microorganisms generally occupy microaerobic or anaerobic environments (Hill, 1988). Symbiotic diazotrophs adapt themselves to cooperative mutualistic associations with host organisms (for example, plants and fungi) that allow protection of nitrogenase from oxygen access, while simultaneously maintaining a high respiratory rate.

Symbiotic association between legume plants and *Rhizobia* and formation of symbiotic organelles

Under conditions of limiting soil-nitrogen, symbiosis between host legume plants and rhizobia results in formation and development of a new organ, the nodule which usually occurs on plant roots but also rarely occurs on stems (D'Haeze et al., 2000). Legume plants can gain the reduced nitrogen source required for their growth and development from nitrogen-fixing bacteria while the

host plants supply reduced carbon to the bacterial symbionts (Udvardi and Day, 1997; Yurgel and Kahn, 2004). *Pisum sativum* (pea) and *Medicago truncatula* (barrel clover) are representative temperate legume species that form an elongated indeterminate nodule containing an active apical meristem where continuous cell differentiation occurs. On the other hand, *Lotus japonicus* and *Glycine max* (soybean) belong to tropical legumes bearing spherical determinate nodules in which the nodule growth is due to a cell expansion process resulting in maturation immediately after initiation of the nodule formation (Crespi and Galvez, 2000).

Among legumes, *Medicago truncatula* has been considered one of outstanding genetic legume models since it has compact diploid genome and rapid generation time and is amenable to genetic transformation thus, allowing various sets of mutants available for functional characterization study (Tadege et al., 2008). In addition, completion of the genome sequencing projects aided in utilizing whole genetic information of the *Medicago truncatula* and *Lotus japonicus* (Sato et al., 2008; Young et al., 2011). As a crop legume, large-scale shotgun genome sequencing of soybean (*Glycine max*) had been also completed (Schmutz et al., 2010). Appreciable work on the sequenced genome with further establishment of transcriptome database for these legume plants has lead to better understanding and deciphering of functions and roles of individual genes associated with development and metabolism of the nitrogen-fixing symbiotic nodules (Stacey et al., 2006; Libault et al., 2010; Moreau et al., 2011).

The symbiotic association is initiated by reciprocal signal exchange between free-living soil rhizobia and plant roots (Oldroyd and Downie, 2008). Flavonoid compounds, such as apigenin, daidzein, genistin and luteolin are released as exudates from plant roots and induce transcriptional up-regulation of nodulation (*nod*) genes of compatible soil rhizobia bacteria (Begum et al., 2001; Maj et al., 2010). This drives the subsequent production of nodule-inducing (Nod) factors, which are composed of a lipochito-oligosaccharides (LCOs) with a structural backbone of four to five N-acetylated glucosamines, with additional fatty acyl or other substitutions at the non-reducing end (Gualtieri and Bisseling, 2000; Streng et al., 2011). Depending on the various types of legume species and their compatible rhizobia symbionts, the nod factors are differentially modified by carrying diverse substituents and thus impose species-specificity upon recognition and following symbiotic interaction between them (Gualtieri and Bisseling, 2000; Oldroyd and Downie, 2008; Streng et al., 2011).

Nod factors excreted from the rhizobia interact with lysine motif (LysM) domain-containing receptor-like kinases (RLKs) on root epidermal cell layers of the plant host (Madsen et al., 2003; Radutoiu et al., 2003). Perception process for the nod factors in the plant cells is linked to calcium spiking signal in the nucleus (Ehrhardt et al., 1996), which triggers activation of a calcium and calmodulin dependent protein kinase (CCaMK) (Gleason et al., 2006) resulting in activation of the nodule developmental program (Journet et al., 2001; Andriankaja et al., 2007). In the early infection process these include plant root

hair curling (Esseling et al., 2003), cell wall invagination, deposition of new cell wall material (Brewin, 2004) and eventually development of a tube-like structure called “infection thread” within the root hair (Monahan-Giovanelli et al., 2006). In addition, nod factor signaling leads to an induction of root cortical cell division leading to the appearance of nodule primordia which are defined as square-shaped cells remaining aligned in the same cell layer with adjacent non-induced inner cortical cells (Timmers et al., 1999). The infection thread contains dividing bacteria surrounded by plant cell wall and penetrates into outer root tissues, growing toward the nodule primordia. Ultimately, bacteria are released from the infection thread and are endocytosed into a specialized polyploidy “infected host cell” within the nodule primordia. This entry process results in formation of the organelle-like vesicle comprised of a specialized plant-derived membrane which encloses the bacteroids.

Endocytosis is followed by further morphologic differentiation of the bacteria into bacteroids as well as developmental changes in the plant-derived “symbiosome membrane (SM)” that encloses the bacteroids (Roth, 1988). The SM separates the bacteroids from the infected plant cell cytosol, eventually completing formation of a new symbiotic organelle called the "symbiosome" and differentiation of infected cells into a mature state where nitrogen fixation actively occurs (Verma and Hong, 1996; Oldroyd and Downie, 2008).

As the developing nodule grows and the rhizobia maintain cell division or enlargement inside the membrane envelope, there is a great need for membrane

biosynthesis in order for the symbiosome membrane to increase quantity and become compatible with newly given structural functions (Verma and Hong, 1996). The SM therefore, not only retains common properties from both plasma and vacuolar membrane, but also includes distinct features and composition compared to other endomembranes of plant cells (Roth and Stacey, 1989; Verma and Hong, 1996).

Besides its primary function to structurally segregate the bacteroids from the plant cytoplasm and protect the bacteroids from plant defense responses (Udvardi and Day, 1997; Day et al., 2001), the symbiosome membrane (SM) mediates exchange of various molecules indispensable for the symbiosis (Udvardi and Day, 1997; White et al., 2007). These include the primary metabolic exchange at the heart of the symbiosis: the efflux of fixed nitrogen in exchange for the uptake of a reduced carbon source that serves as the energy source supporting nitrogen fixation. In addition, the SM mediates the uptake of other essential metabolites and cofactors provided by the host to the endosymbiont.

In relation to the nodule developmental program activated by nod factor signaling, a number of host-encoded genes, termed "*nodulins*", are specifically expressed during nodule organogenesis and development (Legocki and Verma, 1980). Among these nodulins, are a number of gene products targeted to the symbiosome and perform functions necessary for the establishment and maintenance of the symbiosis. These include a set of transporters and channel

proteins that are targeted to the SM and facilitate the metabolic exchanges to maintain proper function of symbiosis between the host and endosymbionts (White et al., 2007). The biochemical and transport activities of the SM are reviewed in the following section below.

Transport activities of the symbiosome membrane

The SM accommodates a number of nodule-specific membrane transporters that are responsible for supporting high fluxes of metabolites and fixed-nitrogen compounds between the host plant and bacterial symbiont. Transcriptomics analysis followed by metabolite profiling of developing nodules supported the correlation between expression of transporters and active changes in metabolism by the fact that gene expression levels of transporters and transcripts involved in metabolic pathways of the root nodule are highly up-regulated compared to unnodulated root tissue (Colebatch et al., 2004; Benedito et al., 2008). A summary of examples of transport activities and transport proteins that have been found on mature SM is shown in table 1.1. Brief descriptions of key transport processes demonstrated on the symbiosome membrane are listed below.

Carbon uptake: Among metabolite exchanges across the SM is the uptake of reduced carbon in the form of C_4 dicarboxylates provided by host plants to the symbionts as a catabolic substrate essential to support the nitrogen fixation process (Udvardi and Day, 1997). As mentioned above, due to the high

Table 1.1. Transport activities on the symbiosome membrane

Transporter (mambrane nodulin)	Transport activities	Reference
Nodulin 26	Water, glycerol	Rivers et al., 1997; Dean et al., 1999; Guenther and Roberts, 2000
GmN70	Chloride, nitrite, nitrate	Vincill et al., 2005
Non-selective cation channel	Ammonium, potassium, calcium	Tyerman et al., 1995; Roberts and Tyerman, 2002; Obermeyer and Tyerman, 2005
H^+-ATPase	Protons (ATP-dependent)	Udvardi and Day, 1989
GmZIP1	Zinc	Moreau et al., 2002
Ca^{2+}-ATPase	Calcium (ATP-dependent)	Andreev et al., 1999
GmDMT1	Fe^{2+}, Mn^{2+}, Cu^{2+}, Zn^{2+}	Kaiser et al., 2003
Dicarboxylate transporter	Malate, succinate	Ou Yang et al., 1990
SST1	Sulfate	Wienkoop and Saalbach, 2003; Krusell et al., 2005;
Vacuolar H^+-ATPase	Protons (ATP-dependent)	Wienkoop and Saalbach, 2003; Catalano et al., 2004
H^+-transporting ATP synthase	Protons	Catalano et al., 2004

energetic cost of nitrogen fixation, it is not surprising that bacteroid symbionts require an energetically efficient carbon source for their respiration to support nitrogen fixation (White et al., 2007). Consistent with this, it has been demonstrated that rhizobia bacteroids express a dicarboxylate transport (Dct) system which consists of a dicarboxylate carrier protein, DctA, and a two component kinase regulatory system, DctB/DctD (Yurgel and Kahn, 2004). This system is indispensible for N_2 fixation, and isolated bacteroids are able to readily utilize the dicarboxylates for their respiration by uptake through the transport system (Poole and Allaway, 2000). Biochemical evidence for a dicarboxylate transporter on the SM came from kinetic and inhibitor studies with isolated soybean symbiosomes that showed selective uptake of radioisotopic malate and succinate (Udvardi et al., 1988). Additional experiments for various carbon substrates revealed selectivity for malate and succinate (Ou Yang et al., 1990), whereas no detectable transport activity of sugars or amino acids were detected (Udvardi et al., 1990). This channel-mediated uptake of the reduced carbon into the symbiosome is likely through a SM secondary transporter with uptake driven by an electrochemical gradient across the SM (Ou Yang et al., 1990; Udvardi et al., 1991). The symbiosome space is acidic and preserves a positive membrane potential ($\Delta\Psi$), compared to the cytosolic compartment of infected cell (Udvardi and Day, 1989; Udvardi et al., 1991). The molecular identity of the SM dicarboxylate transporter remains unknown presently.

ATPase: The SM is an energized membrane (Udvardi and Day, 1989) via a proton pumping H^+-ATPase which plays a critical role in the energizing mechanism that drives active transport of metabolites across the SM. The SM proton pumping H^+-ATPase pumps protons (H^+) from the cytosol into symbiosome space, consuming ATP molecules from the cytosolic side. This imposes changes in pH (ΔpH) and membrane potential ($\Delta\Psi$) within the lumen of the symbiosome, which is more acidic and positively charged inside compared to the cell cytosol (Udvardi and Day, 1989). This proton motive force leads to continuous secondary uptake of negatively charged metabolites in (e.g. dicarboxylates) (Ou Yang et al., 1990) and also controls cation (e.g. NH_4^+) release from the symbiosome space (Tyerman et al., 1995; Roberts and Tyerman, 2002).

Nonselective cation channel: Tyerman et al. (1995) used direct patch clamp recording of isolated soybean symbiosomes to demonstrate a voltage-activated rectified nonselective cation channel (NSCC) on symbiosome membranes. The channel is voltage-dependent with activation observed at negative potentials (with respect to the cytosolic side) and showed permeability to K^+, Na^+ and NH_4^+. This channel protein showed rectification with cation movement only observed in an inward (towards the cytosol) direction (Tyerman et al., 1995). The gating particle controlling rectification was shown to be divalent cations such as Mg^{2+} and Ca^{2+} (Tyerman et al., 1995; Roberts and Tyerman, 2002) or polyamines (Whitehead et al., 2001) which act from the cytosolic side of the SM (Tyerman et

al., 1995; Obermeyer and Tyerman, 2005). A similar channel was also found in *Lotus japonicus* symbiosomes, which also showed a finite Ca^{2+} permeability (Roberts and Tyerman, 2002). Given the electrochemical properties of the SM, and the large gradient of NH_4^+ between the symbiosome space and cell cytosol (Streeter, 1989), a role of the NSCC in the efflux of fixed NH_4^+ was proposed (Tyerman et al., 1995). In addition, in association with the electrogenic H^+-ATPase, the NSCC could also play a critical role in regulating SM potential homeostasis and the symbiosome electrochemical gradient (Roberts and Tyerman, 2002).

Inorganic anions: Early work demonstrated the presence of a SM nodulin protein in *Lotus japonicus* (LjN70), which shows characteristics of the major facilitator superfamily (MFS) of secondary transporters (Szczyglowski et al., 1998). Vincill et al. (2005) used two-electrode voltage clamp recoding of *Xenopus* oocytes expressing soybean GmN70 (an ortholog of *Lotus japonicus* LjN70) and demonstrated that the GmN70 is an inorganic anion/nitrate transport channel of the SM, and renamed N70-like proteins as nodulin-like anion transporters (NLAT) (Vincill et al., 2005). It was suggested that this anion transporter on the SM may play a significant role coordinated with H^+-ATPase in controlling the symbiosome membrane potential and pH inside the symbiosome (Vincill et al., 2005), and could account for an inorganic anion permeability previously observed on isolated symbiosomes (Udvardi and Day, 1989).

Metal cofactors and sulfate: GmZIP1 was characterized as a symbiosis-specific zinc transporter (Moreau et al., 2002). Evidence for localization of GmZIP1 to the SM came from the observation that GmZIP1 antibodies blocked symbiosome uptake of Zn^{2+}, and SM-specific expression of the GmZIP1 was demonstrated by immunoblot assay with isolated SM (Moreau et al., 2002). A second heavy divalent cation transporter, GmDMT1, was shown to be responsible for uptake of ferrous iron (Fe^{2+}), zinc (Zn^{2+}), copper (Cu^{2+}), and manganese (Mn^{2+}) by heterologous expression in the yeast metal-transport deficient mutants (Kaiser et al., 2003). Location of the GmDMT1 on the SM was verified by both immunoblot assay and immunolocalization using N-terminus specific antibody (Kaiser et al., 2003). These channel activities on the SM were proposed to be necessary for uptake of divalent metal ions as essential cofactors for bacteroid metabolism.

A sulfate transporter was proposed as a SM nodulin based on proteomic analysis (Wienkoop and Saalbach, 2003). Further map-based cloning approach of fix^- mutants of *Lotus japonicus* functionally identified a SM sulfate transporter, SST1 (Krusell et al., 2005). Transport of sulfate (SO_4^{2-}) was also proposed to be critical because bacterial nitrogenase complex protein consists of a large number of sulfur-containing amino acids as well as four metal clusters containing sulfur (Dos Santos et al., 2004).

Based on proteomics analysis, a number of additional regulatory and transport proteins were proposed to be associated with the symbiosome membranes from *Lotus japonicus* (Wienkoop and Saalbach, 2003) and *Medicago*

truncatula (Catalano et al., 2004) (Table 1.1), suggesting even greater complexity of transporters associated the SM. However, functional confirmation of these proteins in most cases remains uninvestigated.

Nodulin 26: a symbiosome membrane specific MIP

Initially discovered in soybean, nodulin 26 is one of a number of nodule-specific or nodule-enhanced proteins, which are members of the major intrinsic protein/aquaporin (MIP) superfamily of integral membrane protein channels and constitutes the major protein component of the symbiosome membrane in soybean root nodules (Fortin et al., 1987; Weaver et al., 1991; Wallace et al., 2006).

Nodulin 26 was originally discovered by Fortin et al. (1987) by immunoprecipitation of polysome complexes using antibodies raised against a purified soybean SM fraction, followed by *in vitro* translation which revealed a major 26 kDa polypeptide. In subsequent work by Weaver et al. (1991), generation of nodulin 26-specific antibodies enabled its detection and quantitation on isolated SM. From this work, it was clear that nodulin 26 is the major protein component of the SM, constituting up to 15% of the total protein mass of the membrane (Weaver et al., 1991; Rivers et al., 1997). Sequence analysis and structural investigation showed that nodulin 26 is a member of MIP superfamily (Sandal and Marcker, 1988; Wallace et al., 2006). Based on mRNA and protein expression, immunolocalization, and developmental profiles, it is

clear that nodulin 26 is a common component of legume SM and that it is uniquely expressed and targeted to this membrane (Wallace et al., 2006).

The finding of a member of the MIP/aquaporin that is a symbiosome-specific protein argues for a functional role in transport and/or homeostasis in support of the symbiosis. In order to characterize its transport functions, various approaches such as heterologous expression system using *Xenopus* oocytes (Rivers et al., 1997; Guenther et al., 2003), isolation of symbiosome membrane vesicles (Rivers et al., 1997) and reconstitution of purified nodulin 26 into proteoliposomes (Dean et al., 1999) were developed.

Initial functional characterization of nodulin 26 was conducted by expression in *Xenopus* oocytes as well as analysis of isolated symbiosome vesicles (Rivers et al., 1997). These studies showed that oocytes expressing nodulin 26 and isolated SM vesicles have elevated water permeability (P_f) with low activation energy and mercurial inhibition of the activity, characteristic of aquaporins. Additionally, isolated SM also showed high transport activity for nonelectrolyte solutes such as formamide and glycerol (Rivers et al., 1997). Dean and coworkers adopted an unequivocal approach by purifying and reconstituting native soybean nodulin 26 into liposomes for water and solute flux studies (Dean et al., 1999). It was obvious that nodulin 26 is a water permeable transporter with low E_a, and also that nodulin 26 proteoliposomes showed rapid glycerol efflux in a mercurial-sensitive manner that accounts for the permeability of the SM to glycerol (Dean et al., 1999). Overall, these functional studies

support that nodulin 26 is a unique multifunctional aquaglyceroporin on the SM with a high permeability to water and uncharged solutes such as glycerol. However, the intrinsic water transport rate of nodulin 26 (3.8×10^{-15} cm^3/s) is comparably lower than well-known active water transporter like mammalian AQP1 (117×10^{-15} cm^3/s) (Zeidel et al., 1992; Rivers et al., 1997). Nevertheless, the large expression and specific localization of the nodulin 26 to the SM is responsible for the high intrinsic P_f of symbiosomes.

In addition to being identified as the major protein component of the SM, nodulin 26 was identified as a major target for calcium-dependent phosphorylation by a SM-associated kinase (Weaver et al., 1991). Given that the cytosolic carboxyl-terminus of nodulin 26 contains a putative phosphorylation consensus motif for calcium dependent protein kinase (CDPK), it was proposed that this is the location for the phosphorylation. This was demonstrated by using a 14 amino acid synthetic peptide comprising the C-terminal sequence of the nodulin 26 and showing that it is a CDPK substrate (Weaver et al., 1991). Additionally, native nodulin 26 of the symbiosome membrane was able to be phosphorylated *in vivo* as well as *in vitro* (Weaver et al., 1991). It was further verified that a symbiosome membrane-associated CDPK specifically phosphorylated a serine 262 within the predicted CDPK site in the C-terminus of the native nodulin 26 (Weaver and Roberts, 1992).

The protein expression and phosphorylation state of soybean nodulin 26 were analyzed during nodule development and in response to environmental

cues by using nodulin 26- and phospho nodulin 26-specific antibodies (Guenther et al., 2003). The expression of nodulin 26 protein first becomes detectable in immature infected cells at 16 days post infection, which coincides with the endocytosis of the bacteroids and early stages of the formation of the symbiosome membrane. In contrast, the phosphorylation of nodulin 26 lagged behind its appearance and becomes detectable 25 days post infection, which coincides with the maturation of infected cells and the onset of nitrogen fixation (Guenther et al., 2003). The phosphorylation of nodulin 26 is also modulated in response to a number of environmental stimuli, showing enhancement under osmotic stress conditions such as salinity and drought (Guenther et al., 2003). The CDPK-mediated phosphorylation of nodulin 26 under osmotic stress conditions is consistent with the finding that osmotic stress signals trigger calcium signaling in plants (Knight et al., 1997). With respect to nodule physiology and membrane function, calcium-dependent phosphorylation of nodulin 26 may serve an osmoregulatory function to maintain water homeostasis of the infected cell cytosol (Guenther et al., 2003).

Goal of the present research

The symbiosome membrane represents a specialized interface that legumes have evolved to establish and manage nitrogen-fixing rhizobia symbiosis. As summarized above, plants target a number of nodule-enhanced or nodule-specific transport proteins to the SM to enable regulation of metabolic

exchange, modulation of proton motive force, and carry out other transport and homeostatic processes, in support of the symbiosis. Nodulin 26, a plant-specific member of the MIP/aquaporin superfamily is specifically targeted to the SM and is the sole member of the family that resides on this membrane.

Since the initial isolation and identification of nodulin 26 from soybean root nodules (Fortin et al., 1987), specific functions of nodulin 26 that may be associated with symbiotic processes have been the subject of considerable studies. From the previous biophysical functional analyses, soybean nodulin 26 was identified as a multifunctional aquaglyceroporin that transports multiple substrates including water, glycerol and formamide (Rivers et al., 1997; Dean et al., 1999). In addition, it is clear that the protein is a target for developmental and environmental sensitive posttranslational phosphorylation which may regulate transport activity (Guenther et al., 2003).

In the present work, we used proteoliposome reconstitution of recombinant nodulin 26 to investigate new transport activities of the nodulin 26 including ammonia transport. In addition, we investigated how nodulin 26 phosphorylation affects its transport activity and selectivity in response to environmental signals with respect to functional properties of nodulin 26 transport at the symbiotic interface. Finally, we used a screening technique to identify interacting partners of the nodulin 26 from cytosolic part of the infected cells, and studied signals triggering gene expression of nodulin 26. Overall, the present

study provides new information on the functional properties of nodulin 26 and its regulation in response to environmental stimuli.

CHAPTER II

MATERIALS AND METHODS

Soybean growth and Rhizobia culture conditions

Soybean (*Glycine max*, cv. USG 5601T) seeds were grown in medium grade vermiculite in a growth chamber at 24°C conditioned with long day light cycles (18-hour light/6-hour dark). The light intensity during the day light cycle was 350 ~ 400 mol/m^2/s. Seeds were watered at the time of planting with Herridge's solution (K_2HPO_4, 22 mg/L; KH_2PO_4, 17 mg/L; $MgSO_4 \cdot 7H_2O$, 250 mg/L; $CaCl_2 \cdot 2H_2O$, 37 mg/L; ferric monosodium EDTA, 9 mg/L; H_3BO_3 0.71 mg/L; $MnCl_2 \cdot 4H_2O$, 0.45 mg/L; $ZnCl_2$, 0.03 mg/L; $CuCl_2 \cdot 2H_2O$, 0.01 mg/L; $NaMoO_4 \cdot 2H_2O$, 0.005 mg/L) (Eskew et al., 1993).

Bradyrhizobium japonicum, USDA110 was grown in Bergersen's minimal medium (BMM) (270 mg/L $NaH_2PO_4 \cdot 7H_2O$; 80 mg/L $MgSO_4 \cdot 7H_2O$; 3 mg/L $FeCl_3 \cdot 6H_2O$; 3.7 mg/L ferric monosodium EDTA; 30 mg/L $CaCl_2 \cdot 2H_2O$; 0.0025 mg/L $MnSO_4 \cdot 4H_2O$; 0.03 mg/L H_3BO_3; 0.03 mg/L $ZnSO_4 \cdot 7H_2O$; 0.0025 mg/L $NaMoO_4 \cdot 2H_2O$; 0.1 mg/L biotin; 1 mg/L thiamine; 10g/L mannitol; 0.5 g/L sodium glutamate; 0.5 g/L yeast extract; pH 6.8 ~ 7.0). For the bacterial seed culture, 50 ml of BMM was inoculated with a single bacterial colony and was grown to mid-

log phase (A_{600} = 0.6) at 28°C with shaking at 250 rpm. This small culture was used to inoculate a large 450 mL BMM culture which was grown for 2 to 3 days at 28°C with shaking.

The culture was diluted 1:10 with Herridge's solution, and was used to inoculate 10 day-old soybean plants. After inoculation, plants were maintained under the growth conditions described above and were watered on alternating weeks with Herridge's solution or water. To repress nodulation in uninoculated control soybean plants, 5 mM KNO_3 was used to supplement the Herridge's solution as a nitrogen source.

For flooding treatment, pure N_2 gas was bubbled into a water container 30 minutes prior to submersion of soybean roots. Soybean plant roots were submerged in the water with continuous N_2 gas bubbling during whole period of the flooding treatment. The dissolved oxygen content (%) of water in the container was measured at each time point using an oxygen probe (Model 55, Yellow Springs Instrument), and was converted into dissolved oxygen (DO) content (%) expressed as a % of ambient O_2 (Table 2.1).

For hypoxia treatment, whole soybean plants were placed into an anaerobic jar (BD Diagnostic Systems) and were subjected to anaerobic conditions by using a BD BBL GasPak 100 System with a BBL dry anaerobic indicator strip (BD Diagnostic Systems).

For additional treatments of soybean plants with varying oxygen concentrations (either hypoxia for sub-ambient oxygen concentration or

Table 2.1. Dissolved oxygen content (%) of water in the container

Flooding time [a]	(-) 0.5 hr [c]	0 hr	1 hr	2 hr	3 hr	6 hr	12 hr	24 hr
Oxygen (O_2) content (%) in water	5.0	2.5	2.0	2.0	2.0	2.5	2.0	2.0
DO (%) [b]	23.9	12.0	9.6	9.6	9.6	12.0	9.6	9.6

a. Time point of O_2 measurement according to flooding stress treatment.

b. Dissolved oxygen.

c. (-) 0.5 hr indicates the time point at which nitrogen gas (N_2) was blown for 30 minutes prior to submersion of soybean roots.

hyperoxia for supra-ambient oxygen concentration), various mixtures of N_2 and O_2 gases were utilized. Soybean plants were placed into a modified gas jar system with a couple of layers of wet paper towels on the bottom to prevent dryness. The jar was fitted with inlet (1 cm diameter) and outlet (0.5 cm diameter) holes on opposite sides. Pure N_2 or 50% O_2 gas mixtures were used for sub-ambient or for supra-ambient O_2 conditions, respectively. Oxygen concentrations were measured by an oxygen monitor and showed a concentration of 2% O_2 under sub-ambient conditions and over 50% O_2 under supra-ambient conditions. For ambient control experiments, plants were placed in a plastic jar opened to the atmosphere.

Isolation of membrane fractions from soybean nodules

Microsomal fractions from soybean nodules were isolated as described by Guenther et al. (2003) with minor modifications. Nodules from the 35 day-old soybean plants were harvested on ice and were crushed in 25 mM 3-(N-morpholino) propanesulfonic acid (MOPS)-NaOH, pH 7.2, 10 mM EDTA, 10 mM $MgSO_4$, 5 mM iso-ascorbic acid, 5 mM dithiothreitol (DTT), 1% (w/v) polyvinylpyrroldone-40 (PVP-40), 1 μg/mL leupeptin, and 0.5 mM phenylmethylsulfonyl fluoride (PMSF), using an ice-cold mortar and pestle. Extracts were centrifuged at 100g in a Sorvall SS-34 rotor at 4°C for 10 minutes. The supernatant fraction was collected and was passed through a 25 gauge needle three times. The sample was centrifuged at 700g in a Sorvall SS-34 rotor

at 4°C for 20 minutes. The 700g supernatant fraction was then centrifuged at 100,000g in a Beckman Ti-60 rotor at 4°C for 1 hour. The microsomal membrane 100,000g pellet fraction was resuspended in 20 mM MOPS-NaOH, pH 7.0, 150 mM KCl, 1 mM EDTA, 1 μg/mL leupeptin, and 0.1 mM PMSF, and kept at -80°C until analysis.

Soybean symbiosome membranes were isolated as previously described (Weaver et al., 1991; Weaver et al., 1994; Rivers et al., 1997). Typically, nodules were harvested from soybean plants 25 days post-inoculation. Nodules were crushed on ice using an ice-cold motar and pestle in 25 mM MOPS-NaOH, pH 7.2, 10 mM EDTA, 10 mM $MgSO_4$, 5 mM iso-ascorbic acid, 5 mM DTT, 1% (w/v) PVP-40, 1 μg/mL leupeptin, and 0.5 mM PMSF. The nodule extracts were then passed through two layers of Miracloth and intact symbiosomes were isolated on discontinuous Percoll (Sigma) gradients as described by Udvardi and Day (1989). Isolated symbiosomes were broken by extrusion through a 25 gauge needle three times, and symbiosome membranes were separated from the bacteroids and symbiosome space fraction by differential centrifugation. The final purified symbiosome membrane fraction was stored at -80°C in 20 mM MOPS-NaOH pH 7.0, 150 mM KCl, 100 μM PMSF, 1 μM leupeptin, 1 μM pepstatin A until further analysis.

Intact symbiosome membrane vesicles for transport studies were prepared from the soybean nodule extracts as described by Christiansen et al. (1995) using an aqueous two-phase partitioning method. Soybean nodules were

extracted on ice using an ice-cold motar and pestle in 250 mM sucrose, 50 mM HEPES-KOH, pH 7.5, 5 mM EDTA, 0.1 mM EGTA, 20 mM iso-ascorbic acid, 5 mM DTT, 1% (w/v) PVP-40, 1 μg/mL leupeptin, and 0.5 mM PMSF. Cell debris were removed by centrifugation at 100g in a Sorvall SS-34 rotor at 4°C for 10 minutes. To remove bacteroids, the symbiosomes were ruptured by vortexing at the highest setting for 2 minutes in resuspension buffer (330 mM sucrose and 5 mM KH_2PO_4 at pH 7.8), and the symbiosome vesicles were isolated by the centrifugal two-phase partitioning. For vesicles used for stopped-flow spectrometry analysis, 100 μM carboxyfluorescein (CF) dye was added into the resuspension buffer before vortexing isolated symbiosomes. The final pellet of symbiosome vesicles was resuspended in dye-free resuspension buffer and was stored at 4°C or -80°C until analysis.

Phosphorylation and dephosphorylation treatment of isolated symbiosome vesicles

For calcium-dependent phosphorylation of nodulin 26 in intact symbiosome membrane vesicles, isolated symbiosome vesicles were incubated for 1 hour at 30°C in 10 mM Mg-acetate, 25 mM MOPS-NaOH, pH 7.0, 250 mM sorbitol, 2 mM ATP, and 1 mM $CaCl_2$. For dephosphorylation of nodulin 26, isolated symbiosome vesicles were incubated with 20 units/mL shrimp alkaline phosphatase (SAP, Promega) for 1 hour at 30°C in 25 mM Tris-HCl, pH 8.0, 3 mM $MgCl_2$, and 250 mM sorbitol. After phospho- and dephospho-treatments, the

symbiosome vesicles were centrifuged at 100,000g at 4°C for 1 hour. The final pellet of symbiosome vesicles was resuspended in either 250 mM sorbitol, 30 mM KCl, 10 mM HEPES-KOH, pH 6.8 for ammonia permeability measurements or 330 mM sucrose, 5 mM HEPES-KOH, pH 7.0, 100 μM $CaCl_2$ for osmotic water permeability measurements, and was stored at 4°C until analysis.

Isolation of symbiosome membrane vesicles from flooding samples

For analysis of the effects of flooding treatments on ammonia and water permeabilities in symbiosome vesicles, soybean plant roots were submerged in the water for 6 hours with continuous N_2 gas bubbling. Intact symbiosome membrane vesicles for transport studies were prepared from the flooding-treated soybean nodule extracts as described above, using an aqueous two-phase partitioning method. For stopped-flow spectrometry analysis, symbiosome vesicles were loaded with 100 μM CF. The final pellet of symbiosome vesicles was resuspended in dye-free resuspension buffer (330 mM sucrose, 5 mM KH_2PO_4, pH 7.8) and was stored at 4°C or -80°C until analysis.

Molecular cloning techniques for construction of His_6-nodulin 26 in *Pichia pastoris* expression vectors

Soybean nodulin 26 ORF was amplified by PCR reaction from nodule cDNA with the primer set shown in figure 2.1. For nodule cDNA preparation, total RNA was isolated from soybean nodules 25 days post inoculation by using

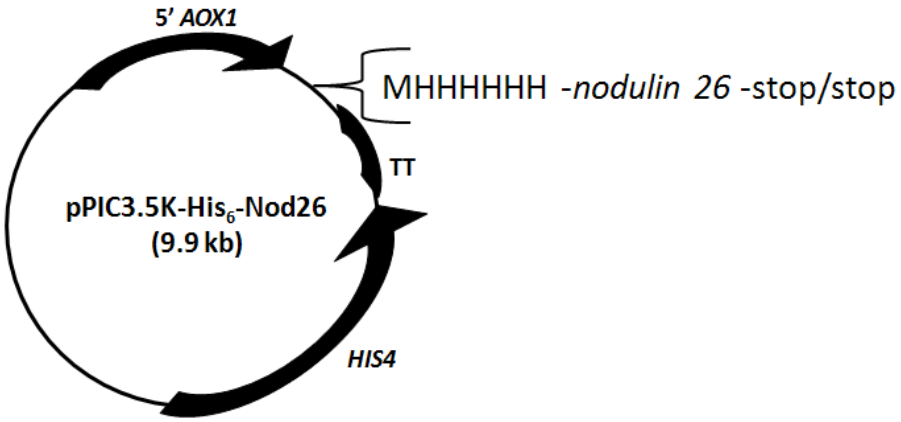

Primer sets for Pichia expression of nodulin 26

<Forward> CA/BamHI/Kozak/**His6**/Nodulin26
5′-CA/GGATCC/ACCATG/**CATCACCACCACCATCAT**/ATGGCTGATTATTCAGCAGG -3′

<Reverse> GTATTCAAT/NotI/***stop***/***stop***/Nodulin26
5′- GTATTCAAT/GCGGCCGC/***CTA***/***TTA***/TTTGGAGGCAGCACGGCCTTTGA -3′

Figure 2.1. Construction of *Pichia* expression system for nodulin 26. Schematic representation of *Pichia* expression vector inserted with a six histidine tag and nodulin 26 coding sequences containing two stop codons. The sequence of PCR primer set used for nodulin 26 cDNA amplification is indicated in the box below. The *BamH*I and *Not*I restriction sites are underlined and the region encoding a six histidine amino terminal tag and two stop codons are shown in bold. Kozak consensus sequence was designed to add a start codon. The reverse primer has two stop codons following a *Not*I restriction site. ***5'AOX1***, an 937 bp fragment containing the alcohol oxidase promoter, allowing methanol-inducible high level expression; **TT**, native transcription termination and polyadenylation signal from *AOX1* gene; ***HIS4***, *Pichia* wild-type gene coding for histidinol dehydrogenase and used to complement *Pichia his4* strains.

the Plant RNA Purification Reagent (Invitrogen) followed by RNAse-free DNase I treatment with the DNA-free™ kit (Ambion) using the manufacturer's instructions. Four μg of total RNA was reverse-transcribed into cDNA with the SuperScript™ first-strand synthesis system for reverse transcription-PCR (Invitrogen). PCR reaction was performed using the following parameters: 1 cycle of 5 min at 94°C, 5 cycles of 30 sec at 94°C, 40 sec at 57°C, 2 min at 72°C and 31 cycles of 30 sec at 94°C, 40 sec at 61°C, 2 min at 72°C, and 15 min at 72°C. Specific amplification of the nodulin 26 DNA was confirmed by agarose gel electrophoresis (1% (w/v) agarose in 40 mM Tris-acetate, pH 8.3 and 1 mM EDTA) analysis of PCR products. The PCR product was cloned into *BamH*I and *Not*I digested pPIC3.5K vector (Invitrogen) (Fig. 2.1), which was transformed into *E. coli* DH5α and positive clones were verified by DNA sequencing of purified plasmid samples by using a Perkin Elmer Applied Biosystems 373 DNA sequencer at the University of Tennessee Molecular Biology Research Facility, Knoxville, TN.

For *Pichia* transformation, the pPIC3.5K plasmid construct containing His_6-nodulin 26 was linearized by digestion with *Sac*I, and the linearized construct was transformed and incorporated into genomic DNA of methylotrophic *P. pastoris* strains (GS115 of which genotype represents *his4*, *AOX1*, *AOX2* and phenotype represents His^-, Mut^+) (Invitrogen) by electroporation using an Electroporator II (Invitrogen) with pulse conditions at 1.5 kV, 200 Ω, 25 μF (Wu and Letchworth, 2004).

Transformants containing His_6-nodulin 26 were selected by growth on histidine-deficient minimal dextrose agar plates containing 250 µg/mL geneticin. Since the *Pichia* host strains have a mutation in the histidinol dehydrogenase gene (*his4*) that prevents them from synthesizing histidine, the transformants containing *HIS4* can be selected (Fig. 2.1). The clones with the highest His_6-nodulin 26 expression were identified by immunoblotting with antibodies against either nodulin 26 C-loop regions (Vincill et al., 2005) or a commercial antibody against the His_6 tag (Thermo Scientific).

His_6-nodulin 26 phosphorylation site mutant (S262D) was amplified by PCR reaction with the primer set shown in figure 2.1, using a construct of nodulin 26 S262D in pRSETA vector prepared as previously described (Lee et al., 1995) as a template. The PCR reaction was performed using the following parameters: 1 cycle of 5 min at 94°C, 5 cycles of 1 min at 94°C, 1 min at 55°C, 1 min at 72°C and 30 cycles of 1 min at 94°C, 1 min at 63°C, 1 min at 72°C, and 1 cycle of 10 min at 72°C. Specific amplification of the phospho-mimic nodulin 26 DNA was confirmed by agarose gel electrophoresis analysis of PCR products. The DNA sequence of "GAT" coding aspartate (D) at 262^{nd} of nodulin 26 instead of wild-type serine (S) was verified by using a Perkin Elmer Applied Biosystems 373 DNA sequencer at the University of Tennessee Molecular Biology Research Facility, Knoxville, TN. Further cloning into pPIC3.5K vector and *Pichia* transformation were followed same as described for wild-type His_6-nodulin 26.

Expression and purification of His_6-nodulin 26 from *Pichia pastoris*

P. pastoris expression clones were cultured and protein expression was induced as previously described (Karlsson et al., 2003). Fifty mL of YPD medium (1% (w/v) yeast extract, 2% (w/v) peptone and 2% (w/v) dextrose) was inoculated with a single colony, and the culture was incubated at 30°C with shaking at 220 rpm overnight. The cells from the 50 mL seed culture were collected by centrifugation at 1,000g in a Sorvall SS-34 rotor at 4°C for 5 minutes, and were resuspended in 20 mL of buffered glycerol complex medium (BGM: 100 mM potassium phosphate, pH 6.0, 1.34% (w/v) yeast nitrogen base, 4×10^{-5}% (w/v) biotin and 1% (w/v) glycerol) (*Pichia* Expression Kit, Invitrogen) by vortexing and transferred into final volume of 400 mL BGM. The culture was grown at 30°C with shaking at 220 rpm for 24 hours. The cells were collected by centrifugation and were resuspended in 1 L of buffered methanol complex medium (BMCM: 100 mM potassium phosphate, pH 6.0, 1.34% (w/v) yeast nitrogen base, 4×10^{-5}% (w/v) biotin and 0.5% (v/v) methanol) (*Pichia* Expression Kit, Invitrogen) to a final cell density of A_{600} = 1.0, and were grown in a 4 L baffled flask at 30°C for 72 hours with shaking at 220 rpm. Expression of the His_6-nodulin 26 was induced by addition of 0.5% (v/v) methanol in the BMCM culture media. To preserve protein induction, 0.5% (v/v) methanol was added to the culture at 24 hours and 48 hours after starting induction. The cells were harvested after 72 hour-induction, and were stored at -80°C until cell extraction.

The cell pellet was resuspended in 40 mL 20 mM Tris-HCl, pH 8.0, 100 mM NaCl, 0.5 mM EDTA, 5% (v/v) glycerol, 1 μg/mL leupeptin, 1 μg/mL pepstatin A, 0.5 mM PMSF. The cells were disrupted by using a French-Press Cell Disrupter (Thermo Scientific) with 3 passages at 1,500 psi, and cell extracts were cleared by centrifugation at 7,000g in a Sorvall SS-34 rotor for 45 minutes at 4°C. The membrane fraction was isolated from the resulting supernatant fraction by ultracentrifugation at 200,000g in a Beckman Ti-60 rotor for 1 hour at 4°C. For stripping, the pellet was resuspended in 20 mL 5 mM Tris-HCl, pH 9.5, 5 mM EDTA, 5 mM EGTA, 4 M Urea and was homogenized using a hand-operated dounce homogenizer by slowly pressing the pestle on to the sample. To remove the urea solution, the sample was centrifuged at 200,000g for 1 hour at 4°C, and was resuspended in 20 mL of 10 mM Tris-HCl, pH 8.0. For solubilization, the urea-stripped membrane pellet was centrifuged at 200,000g for 1 hour at 4°C and resuspended in 20 mL of solubilization buffer (20 mM Tris-HCl, pH 8.0, 100 mM NaCl, 5% (v/v) glycerol, 20 mM imidazole, 3% (w/v) n-octyl-β-D-glucopyranoside (OG)) and was solubilized by gentle shaking at 60 rpm for 24 hours at 4°C.

One mL (packed volume) of Ni^{+}-NTA (nitrilotriacetic acid) resin (Qiagen) was washed and pre-equilibrated in the 3 mL of solubilization buffer. The OG-solubilized sample was centrifuged at 12,000g for 20 minutes, and the supernatant fraction was transferred to a new tube containing the pre-equilibrated Ni^{+}-NTA resin. The solubilized membrane/resin mixture was

incubated by gentle shaking at 60 rpm overnight at 4°C. The mixture was then centrifuged at 3,000g for 2 minutes to pellet the NTA matrix, and the unbound protein fraction in the supernatant fraction was discarded. The pelleted NTA resin was resuspended in 20 mL of wash buffer (20 mM Tris-HCl, pH 8.0, 300 mM NaCl, 35 mM imidazole, 1% (w/v) OG), and was recollected by centrifugation. The washing step was repeated with an additional 20 mL of washing buffer. The NTA-resin mixture was packed into a column, and was washed with an additional 10 mL of washing buffer. His-tagged nodulin 26 was then eluted with elution buffer (20 mM Tris-HCl, pH 8.0, 300 mM NaCl, 500 mM imidazole, 1% (w/v) OG). Fractions (0.5 mL) were collected and analyzed by SDS-PAGE and Western blot using both anti-His_6 (Thermo Scientific / Pierce Antibodies) and anti-nodulin 26 antibodies (Vincill et al., 2005). Fractions containing nodulin 26 were concentrated to 0.5-1.0 mg/mL using a Vivaspin sample concentrator with 50 kDa cutoff (GE healthcare).

The sample was dialyzed for 24 hr at 4°C against 500 mL of 20 mM Tris-HCl, pH 7.8, 0.9% (w/v) OG, 0.1 mM 2-mercaptoethanol and 1 μM leupeptin. The protein concentration was determined by using the BCA protein assay reagent (Thermo Scientific), and the dialyzed nodulin 26 was stored at -80°C until analysis.

Proteoliposome reconstitution

Proteoliposome reconstitution was performed by a rapid dilution protocol as previously described (Dean et al., 1999). Nodulin 26 (200 ~ 250 μg) was combined with 10 mg of bath-sonicated *Escherichia coli* total lipid extracts (Avanti Polar Lipids) in 50 mM Tris-HCl (pH 7.5), and 0.125% (w/v) OG in a final volume of 1.0 mL. Control liposomes were prepared by a similar manner except nodulin 26 was omitted. The mixture was incubated on ice for 30 minutes, and liposomes were formed by rapidly injecting the sample into 20 mL of fluoro-buffer (250 mM sorbitol, 30 mM KCl, 10 mM HEPES-KOH, pH 6.8, 100 μM carboxyfluorescein (CF)) at room temperature. The liposome mixture was incubated for 30 min and the liposomes were pelleted by ultracentrifugation at 100,000g for 1.5 hours at 4°C. The liposome pellet was washed against 5 mL of dye-free fluoro-buffer in order to remove the residual CF present outside liposome vesicles, and was centrifuged again. The washed liposome pellet was resuspended in 1 mL of dye-free fluoro-buffer and was stored at 4°C until analysis.

Ammonia permeability (P_{NH3}) measurements in symbiosome membrane vesicles and proteoliposomes

Permeability measurements for NH_3 uptake in symbiosome vesicles and liposomes were performed as described by Niemietz and Tyerman (2000), using an Applied Photophysics model SX stopped-flow spectrofluorimeter (excitation at

492 nm, emission filtered with 515 cut-off filter) (Applied Photophysics). Both 100 μM CF-loaded symbiosome membrane vesicles and liposome samples (20 μL) in 250 mM sorbitol, 30 mM KCl, 10 mM HEPES-KOH, pH 6.8 were injected into an equivalent volume of 250 mM sorbitol, 30 mM KCl, 10 mM NH_4Cl, 10 mM HEPES-KOH, pH 6.8, and the increase in CF fluorescence resulting from NH_3 uptake and alkalinization of the internal vesicle and liposome space was monitored. Under the conditions of this experiment, changes of the internal pH were linearly correlated with changes of the relative fluorescence. The fluorimeter was controlled by Pro-Data software (Applied Photophysics), and fluorescence data were collected (1000 points) at time intervals of 0.2 s or 0.4 s with a measured dead time of 10 ms. Data from five injections/sample were averaged. A single exponential function was fitted to the time course of relative fluorescence changes by using Prism software (Version 5.01, GraphPad), and rate constant was determined from the curve fit (Equation 2.1).

$$Y = Y_0 + (A-Y_0)(1-\exp^{-kX}) \qquad \text{(Eq. 2.1)}$$

Where Y represents the relative fluorescence, Y_0 is the Y value when X is zero, A is the plateau fluorescence, k is the rate constant, and X is the time.

To determine P_{NH3}, the differential equations described by Boron and DeWeer (1976) were modified based on the parameters of the experimental system used in this study (Equation 2.2 and 2.3).

$$\frac{d[\mathrm{Am}_{\mathrm{total}}]_i}{dt} = SAV\left[P_{NH3}\left([\mathrm{NH}_3]_o - \frac{K_a}{[\mathrm{H}^+]_i + K_a} \bullet [\mathrm{Am}_{\mathrm{total}}]_i\right)\right] \quad \text{(Eq. 2.2)}$$

$$\frac{d[\mathrm{H}^+]_i}{dt} = \frac{-2.303 \bullet [\mathrm{H}^+]_i \bullet SAV}{\beta}\left[-\frac{[\mathrm{H}^+]_i}{[\mathrm{H}^+]_i + K_a} \bullet P_{NH3}\left([\mathrm{NH}_3]_o - \frac{K_a}{[\mathrm{H}^+]_i + K_a} \bullet [\mathrm{Am}_{\mathrm{total}}]_i\right)\right] \quad \text{(Eq. 2.3)}$$

(Boron and De Weer, 1976)

$[Am_{total}]_i$ = total concentration of NH_3 + NH_4^+ inside the liposome space; $[H^+]_i$ = total proton concentration inside the liposome space; K_a is the equilibrium constant defining NH_4^+ deprotonation (pK_a = 9.24); SAV is the surface area to volume ratio of the liposomes ($4\pi r^2 / 4/3\pi r^3 = 3/r$); $[NH_3]_o$ is the external concentration of ammonia; β is the buffer capacity of the liposome space; and P_{NH3} is the ammonia permeability constant.

The diameters of nodulin 26 proteoliposomes and symbiosome membrane vesicles were determined by transmission electron microscopy (TEM with a Zeiss Libra 200 MC model at the University of Tennessee Advanced Microscopy and Imaging Center, Knoxville, TN) followed by uranyl acetate negative staining as described in (Dean et al., 1999). ImageJ software (National Institutes of Health) was used to determine the average vesicle diameters. The diameters of the vesicles were also measured by dynamic light-scattering using a Dynapro

NanoStar instrument (Wyatt Technology). The buffer capacity was measured by monitoring the change in fluorescence (an internal reporter of pH) in response to proton flux via addition of a membrane permeant acid (acetic acid). The pH standard curve for the fluoro-buffer was generated by measuring the relative fluorescence at pH ranging from 6.4 to 7.4 using a Felix32 spectrofluorimeter (Photon Technology International, PTI). Upon addition of 2 mM acetic acid in the liposome vesicles, the fluorescence change was measured and interpolated to obtain change in pH inside vesicles. The buffer capacity (β) of the liposome space was then calculated as follows; $\beta = \Delta [CH_3COOH^-] / \Delta pH$.

The system of differential equations (Equation 2.2 and 2.3) was solved numerically in Mathematica 7 (Wolfram) using the experimental conditions to generate a set of theoretical curves describing the change in intracellular pH as a function for varying P_{NH3}. Rate constants from experimental stopped flow data fit to a single exponential were used to determine P_{NH3} based on fitting to simulated theoretical curves in Mathematica 7 (Wolfram).

Osmotic water permeability (P_f) measurements in symbiosome membrane vesicles and proteoliposomes

The osmotic water permeability (P_f) of symbiosome vesicle and liposome preparations was determined by the light scattering technique as previously described (Niemietz and Tyerman, 1997; Niemietz and Tyerman, 2000). Light scattering experiments were performed using an Applied Photophysics model SX

stopped-flow spectrophotometer at 600 nm with 515 cut-off filter (Applied Photophysics).

Symbiosome vesicles suspended in isosmotic buffer (330 mM sucrose, 5 mM HEPES-KOH, pH 7.0, 100 μM $CaCl_2$ at 370 mOsm) and proteoliposomes suspended in dye-free fluoro-buffer (250 mM sorbitol, 30 mM KCl, 10 mM HEPES-KOH, pH 6.8) were rapidly mixed with a hyperosmotic buffer by using the Applied Photophysics stopped-flow fluorimetry to create a 200 mOsm osmotic gradient across vesicle membranes. The time course of vesicle shrinking as water effluxed from the vesicle interior was followed as an increase in light scattering shown by downward deflection of the stopped-flow trace. The fluorimeter was controlled by Pro-Data software (Applied Photophysics), and data were collected (1000 points) at time intervals of 0.2 s or 1 s. A single exponential function was fitted to the time course of the downward deflection of scattered light linearly correlating to vesicle shrinking, and rate constant was determined from the curve fit. By using the rate constant, P_f was calculated (van Heeswijk and van Os, 1986; Niemietz and Tyerman, 1997). The equation for P_f is:

$$P_f = (V/A)(k)(1/V_w)(1/C_o) \qquad \text{(Eq. 2.4)}$$

where V/A is the volume over surface area of the vesicle, k is the rate constant from the single exponential curve fit, V_w is the partial molar volume of water (18

cm^3/mol), and C_o is the external osmolarity. The osmolarity of all buffers was measured using an Osmette S automatic osmometer (Precision Systems).

Calculation of activation energy (E_a) for ammonia transport

The activation energy was determined as a function of the temperature dependence of the ammonia transport rate by generating Arrhenius plots. Ammonia uptake assay in proteoliposomes and negative control liposomes was performed at various temperatures between 15°C and 30°C. Rate constants were obtained by experimental single exponential curve fits of the ammonia uptake measurements (Equation 2.1). The natural log of the rate constant was plotted versus the inverse of degrees kelvin (T), and the activation energy was calculated by multiplying the slope of the line by the gas constant (R = 8.314 J/mol/kelvin).

Calculation of single channel unit transport conductance (p_{NH3} and p_f)

The single channel rate (p_{NH3} for NH_3 flux and p_f for water transport) per nodulin 26 monomer was determined by standardizing P_{NH3} and P_f to the surface density of nodulin 26 on proteoliposomes by the approach of Dean et al. (1999). The surface area (SA) and volume (V) of the liposome vesicles were calculated from vesicular diameter ($SA = 4\pi r^2$, $V = 4/3\pi r^3$, r = vesicle radius). The number of nodulin 26 molecules per unit vesicle surface area was calculated from the total amount of the nodulin 26 and the total internal volume of liposome vesicles.

The total intravesicular volume was measured by lysing the vesicles with TritonX-100 and determining the total CF fluorescence released from unit volume of vesicles. The fluorescence released from the vesicles was interpolated into a standard CF curve, and the total CF concentration was determined. Thus, the total internal vesicle volume was calculated by using three determinants: 1. the measured total CF concentration, 2. the experimentally loaded concentration of CF (100 μM), and 3. the final volume of the test solution.

The total amount of the nodulin 26 reconstituted into liposomes was quantitated by Western blot with nodulin 26 C-loop-specific antisera (Vincill et al., 2005) comparing to densitometry determinations of purified nodulin 26 standard protein as described in (Dean et al., 1999). The measured amount of the nodulin 26 was divided by theoretical molecular weight of the nodulin 26 (MW = 29867.63 for His_6-nodulin 26) and multiplied by Avogadro constant (6.022×10^{23}), finally resulting in the total number of the nodulin 26 monomers.

The unit transport conductance ($p_{NH3(or\ f)}$) for nodulin 26 was calculated from equation 2.5 based on the unit surface density of nodulin 26 and the determination of the permeability coefficient.

$$p_{NH3(or\ f)} = P_{NH3(or\ f)} / \mathrm{SuD} \qquad \text{(Eq. 2.5)}$$

Where $P_{NH3(or\ f)}$ is the measured permeability coefficient (cm/s), and SuD is the number of nodulin 26 monomers per unit vesicle surface area (nodulin 26

monomers/cm^2). Additionally, assuming one transport channel per nodulin 26 monomer, the p_{NH3} represents the number of ammonia molecules, which is the turnover number per channel (T_{NH3}) as molecules/channel/s (Equation 2.6) (Saparov et al., 2007).

$$T_{NH3} = N_A \times p_{NH3} / V_{NH3} \qquad \text{(Eq. 2.6)}$$

Where T_{NH3} is the turnover number per channel, N_A is the Avogadro constant and V_{NH3} is the molecular volume of NH_3, respectively.

Two-dimensional electrophoresis

Two-dimensional electrophoretic analysis of affinity purified native glutamine synthetase (GS) was performed as described in (Gorg et al., 2000) with minor modifications. Five μg of affinity purified native GS (Masalkar et al., 2010) in 50 μL of 5 mM Tris-HCl, pH 7.5, 6 M urea was resuspended in a final volume of 150 μL for 7 cm ReadyStrip IPG strip, (immobilized linear pH 5-8 gradient from Bio-Rad) with 8 M urea, 2% (w/v) OG, 4% (w/v) CHAPS, 1% (w/v) dithiotreitol (DTT), 0.16% (v/v) Biolytes 5-7, 0.04% (v/v) Biolytes 3-10, and trace bromophenol blue. The strips were placed in strip trays (Bio-Rad) and were covered with 0.5 mL of mineral oil (Sigma). Rehydration and isoelectric focusing (IEF) were performed in a PROTEAN IEF cell apparatus (Bio-Rad) at 20°C using the manufacturer's instructions (Bio-Rad). The strips were passively rehydrated

for 12 hr and subsequently focused using the following five steps; 100 V for 200 Vhr, 500 V for 500 Vhr, 1000 V for 1000 Vhr, 1000 to 8000 V for 1 hr, and maintained at 8000 V for 8000 Vhr. The IPG strips were equilibrated twice for 15 min after IEF with gentle shaking in 5 mL of 50 mM Tris-HCl, pH 6.8, 6 M urea, 20% (v/v) glycerol, and 2% (w/v) SDS. Two percent (2% w/v) DTT was added to the first equilibration step followed by the addition of 2.5% (w/v) iodoacetamide in the second equilibration step. The IPG strips were placed on top of the 8.5% SDS-PAGE gels and were sealed with 0.7% (w/v) agarose in SDS electrophoresis buffer (25 mM Tris base, 192 mM glycine, and 0.1% (w/v) SDS) and second-dimensional separation by SDS-PAGE was performed. The gels were stained with 0.1% (w/v) Coomassie Brilliant Blue R-250 in 50% (v/v) methanol and 10% (v/v) glacial acetic acid, and were destained in 20% (v/v) methanol and 10% (v/v) glacial acetic acid.

In-gel digestion

Proteins purified by CK-25 affinity chromatography (Masalkar et al., 2010) were identified by peptide mass fingerprinting method as described in (Jensen et al., 1999) with minor modifications. After SDS-PAGE and Coomassie blue staining, the stained protein spots were excised from stained gels, and a background control was cut from a blank region of the gel and processed in a parallel manner with the stained protein band samples. The excised gel pieces were washed with occasional vortexing as follows: 100 μL deionized distilled

water (ddH_2O) for 15 min, 100 μL 50% (v/v) acetonitrile for 15 min, brief washes with 100 μL 100% (v/v) acetonitrile, 100 μL 100 mM NH_4HCO_3 for 5 min, and 100 μL of 50 mM NH_4HCO_3 and 50% (v/v) acetonitrile for 15 min.

After the washing and destaining steps, the supernatant was removed, and the excised gel pieces were dried in a SpeedVac centrifuge (Savant). Fifty μL of 10 mM DTT in 100 mM NH_4HCO_3 was added to the dried gel pieces and the sample was incubated at 56°C for 1 hr. After cooling to room temperature, the DTT solution was replaced with the same volume of 55 mM iodoacetamide in 100 mM NH_4HCO_3 to allow alkylation of free sulfhydryl groups. After incubation for 45 min at ambient temperature in the dark with occasional vortexing, the gel pieces were washed with 100 μL of 100 mM NH_4HCO_3 for 5 min, dehydrated by incubation with 100 μL of 100% (v/v) acetonitrile for 5 min, rehydrated in 100 μL of 100 mM NH_4HCO_3 for 5 min, and dehydrated again by addition of the same volume of 100% (v/v) acetonitrile. The liquid solution was removed, and the gel pieces were completely dried in a SpeedVac centrifuge.

TPCK-treated trypsin (Pierce) was used for tryptic digestion of protein samples. Four μL of 0.05 μg/μL trypsin in 10 mM NH_4HCO_3 was added to the gel pieces, and the sample was incubated at 4°C for 1 hr until the trypsin solution was absorbed into the gel pieces. After incubation, residual trypsin solution was removed and the gel pieces were incubated in 50 μL of 25 mM NH_4HCO_3, 2 mM $CaCl_2$ at 37°C for 16 hr. One μL of trifluoroacetic acid (TFA) was added into tryptic digests to kill trypsin activity, and the solution was decanted to a new tube.

Fifty μL of 1% (v/v) TFA in 60% (v/v) acetonitrile was added into the acidified tryptic peptide solution and dried down in the SpeedVac centrifuge.

ZipTip pipette tips (Millipore), which contain C18 spherical silica (15 μm, 200 Å pore size) in a 0.6 μL bed volume, were used for the desalting of the tryptic peptides (Erdjument-Bromage et al., 1998). The tips were washed with 100% (v/v) acetonitrile, and then were equilibrated with 0.1% (v/v) TFA. The dried pellet was resuspended in 15 μL of 0.1% (v/v) TFA, and the peptide solution was bound to the ZipTip which is pre-equilibrated with 0.1% (v/v) TFA. Samples were aspirated by gentle pipetting for 10 cycles using a single channel pipette (Pipetman P10, Gilson). The ZipTip was washed with 10 μL of 0.1% (v/v) TFA and 10% (v/v) acetonitrile twice. The digested peptides were eluted using 5 μL of elution buffer (5 mg/mL saturated α-cyano-4-hydroxy-cinnamic acid in 30% (v/v) acetonitrile and 0.05% (v/v) TFA).

Mass spectrometric peptide fingerprinting

All mass spectra were acquired on a Bruker microflex time-of-flight mass spectrometer (Bruker Daltonics) with a nitrogen laser operating at 337 nm on a positive-ion mode. System operation and data acquisition was performed by using Flex Analysis software (Bruker Daltonics).

Prior to each analysis in the reflectron method, the mass spectrometer was externally calibrated using the calculated masses of peptide calibration standard II (Bruker Daltonics); bradykinin fragment 1-7, angiotensin II and I,

substance P, bombesin, porcine renin substrate tetradecapeptide, ACTH clip fragments 1-17 and 18-39, and somatostatin 28. One μL of desalted sample was spotted directly onto the AnchorChip target plate (Bruker Daltonics) of the mass spectrometer. The acceleration voltage was set to 20 kV, and the pressure in the TOF analyzer was about $6 \times e^{-7}$ bars.

The obtained tryptic digested-peptide mass spectra were analyzed searching the NCBI nonredundant protein database with ProFound provided by the Laboratory of Mass Spectrometry and Gaseous Ion Chemistry available online (http://prowl.rockefeller.edu/prowl-cgi/profound.exe). Peptide masses were assumed to be monoisotopic, and methionine residues were assumed to be partially oxidized. Additionally, the searches were performed with an addition of carbamidomethylation of cysteine residues, and a maximum of two missed cleavages for tryptic digests were allowed. The mass tolerance was set to 0.32 daltons.

Total RNA isolation and quantitative real time PCR (Q-PCR)

Total RNA was isolated from soybean plant tissue samples by using the Plant RNA Purification Reagent (Invitrogen) followed by RNAse-free DNase I treatment using the DNA-free™ kit (Ambion). Four μg of total RNA was reverse-transcribed into cDNA with the SuperScript™ first-strand synthesis system for reverse transcription-PCR (Invitrogen). Q-PCR was performed with 10 ng cDNA sample on an iQ5 Real-Time PCR detection system, and data analysis was

performed by using iQ5 Optical System software (Bio-Rad). *Glycine max* nodulin 26 (*GmNod26*), pyruvate decarboxylase (*GmPDC*), and leghemoglobin (*GmLba*) transcripts were analyzed by using the primer sets in table 2.2. The *Glycine max* CDPK-related protein kinase (*GmCRK*) gene was used as an internal reference for standardization as described in (Libault et al., 2008) (Table 2.2). Q-PCR was performed using the following parameters: 1 cycle of 5 min at 50°C, 1 cycle of 10 min at 95°C, and 45 cycles of 30 sec at 95°C, 45 sec at 48°C and 45 sec at 72°C in a 96-well optical PCR plate (ABgene). Specific amplification of target genes was confirmed both by electrophoresis and by melting curve analysis of PCR products. The relative expression value of each gene was calculated by using the comparative threshold cycle (Ct) method as previously described (Pfaffl, 2001). ΔCt was calculated using Equation 2.7,

$$\Delta Ct = Ct_{(target)} - Ct_{(reference)} \qquad \text{(Eq. 2.7)}$$

where $Ct_{(target)}$ is the Ct value of gene of interest, and $Ct_{(reference)}$ is the Ct value of the soybean CDPK-related protein kinase. $\Delta\Delta$Ct values were calculated using Equation 2.8,

$$\Delta\Delta Ct = \Delta Ct_{(sample)} - \Delta Ct_{(calibrator)} \qquad \text{(Eq. 2.8)}$$

Table 2.2. Primer sets for Quantitative Real Time PCR (Q-PCR)

Soybean gene	Direction	Primer sequences
GmNod26 [a]	forward	5'-TAGTTGTTTCCTTGTTCTCT-3'
	reverse	5'-GAGCGTTGGATTGTTTC-3'
GmPDC [b]	forward	5'-GAGGTTGAAATTCATGATGG-3'
	reverse	5'-GATCGCATCAATCAACC-3'
GmLba [c]	forward	5'-GCAGCAGCTATTAAGAAG-3'
	reverse	5'-ATTTTAACCAACATTTCTATCGAG-3'
GmCRK [d]	forward	5'-GAGCACCATGCCTATC-3'
	reverse	5'-TGGTTATGTGAGCAGATG-3'

a, *Glycine max* nodulin 26; **b,** pyruvate decarboxylase; **c,** leghemoglobin; **d,** putative CDPK-related protein kinase gene (Libault et al., 2008).

where $Ct_{(sample)}$ represents the expression value of the gene of interest calculated by Equation 2.7, and $Ct_{(calibrator)}$ is the expression value of the sample to which other samples in the data set are normalized. Each $Ct_{(calibrator)}$ of individual Q-PCR experiments is indicated in the figure legends. The relative expression value was obtained from ΔCt values by using Equation 2.9,

$$\text{Relative expression} = 2^{-\Delta Ct} \qquad \text{(Eq. 2.9)}$$

Microscopic analysis for soybean nodule

Soybean nodules were dissected into 1 to 2 mm pieces with a razor blade, were placed into 1 mL of Carson's formalin fixative (Fisher Scientific), and were incubated at 4°C overnight. The dissection samples were washed in 100 mM potassium phosphate (pH 6.8) 3 times for 10 minutes each and were postfixed in 2% (w/v) osmium tetroxide, 50 mM KH_2PO_4 (pH 6.8) at room temperature for 90 minutes. The samples were washed in distilled water several times and dehydrated through a graded acetone series as follows: 25% (v/v), 50% (v/v), 75% (v/v), 95% (v/v), 100% acetone for 30 min each, and were incubated in 100% propylene oxide (PO) for 15 min twice. The dehydrated tissue samples were infiltrated with 100% Spurr resin at 68°C for 48 hours after pre-equilibration steps with Spurr mix (Spurr resin and polypropylene).

For sectioning, the tissue blocks were cut into less than 1 μm-thin with an ultramicrotome (OMU3 ultramicrotome, LeicaReichert) using a glass knife. The

thin sections were placed on glass slides and stained with 0.5% (w/v) toluidine blue in 1% (w/v) borax for 2 minutes. The stained sections were then subject to a bright-field optical microscope (Nikon Eclipse E600) at the Advanced Microscopy and Imaging Center of University of Tennessee, Knoxville. For size analysis of infected cells at the core of the nodules, the optical microscope images with 40 x magnification were used to measure perimeters of the infected cells using the ImageJ software (National Institutes of Health).

Immunochemical techniques

Western blot analysis was performed by a modification of previous methods (Weaver et al., 1991; Zhang and Roberts, 1995). After resolution by SDS-PAGE on 12% (w/v) polyacrylamide gels, protein samples were transferred onto Immobilon-P polyvinylidene fluoride membranes (PVDF, Millipore) which was soaked in transfer buffer containing 200 mM glycine, 25 mM Tris-base, 20% (v/v) methanol at 70 ~ 80 mA for 1 hour by using a Bio-Rad Semi-Dry Transfer Cell unit (Bio-Rad). Blotted membranes were incubated for 1 hour in blocking solution containing 7% (w/v) nonfat dry milk in PBS (137 mM NaCl, 2.7 mM KCl, 10 mM Na_2HPO_4, 2 mM KH_2PO_4, pH 7.4). The membrane blots were washed three times for 10 minutes in PBS containing 0.05% (v/v) Tween-20. Primary antibody and secondary antibody incubations were performed for 1 hr at 37°C, in PBS containing 3% (w/v) nonfat dry milk. Nodulin 26-specific antibody was generated against C-loop region of the nodulin 26 (Vincill et al., 2005), and

phosphorylation-specific nodulin 26 antibody was prepared against synthetic phosphorylation epitope containing peptide sequences of C-terminus of nodulin 26 homolog (CEITKNVS(PO_4)FLKG, referred to as GC12P) (Guenther et al., 2003). The secondary antibody consisted of 0.2 μg/mL horse radish peroxidase-labeled goat anti-rabbit IgG (Vector Laboratories). After antibody incubations, the membrane blots were washed three times for 10 minutes in PBS containing 0.05% (v/v) Tween-20. Chemiluminescent detection was performed by incubation of membranes with 10 mL of 1.25 mM luminol, 0.2 mM *p*-coumaric acid, and 0.009% (v/v) hydrogen peroxide in 0.1 M Tris-HCl, pH 8.5 for 1 min. The blots were either immediately exposed to X-ray film (Phenix) or were analyzed by image documentation system, ChemiDoc™ XRS (Bio-Rad). The intensity of the Western blot signals were quantitated by densitometry (ChemiDoc™ XRS, Bio-Rad) analysis using digitally scanned X-ray film and the Quantity One software (Bio-Rad).

For analysis of protein expression in *Xenopus* oocytes, lysates containing yolk-free membrane fractions were generated by method described by Guenther et al. (2003). Oocytes lysates (10 to 20 μg total protein) were resolved by SDS-PAGE on 12% (w/v) polyacrylamide gels, and proteins were transferred to PVDF membranes (Millipore). The blotted membranes were blocked for 1 hour in blocking solution containing 7% (w/v) nonfat dry milk in PBS. The membranes were washed three times for 10 minutes in PBS containing 0.05% (v/v) Tween-20. Incubation of the membranes with monoclonal anti-FLAG M2 antibody

(Stratagene) and nodulin 26 C-loop antibody (Vincill et al., 2005) were performed for 1 hr at 37°C in PBS containing 3% (w/v) nonfat dry milk. Peroxidase-labeled horse anti-mouse IgG (Vector Laboratories) for FLAG peptide detection and goat anti-rabbit IgG (Vector Laboratories) for detection of nodulin 26 were used as secondary antibody incubations for 30 min at 37°C in PBS containing 3% (w/v) nonfat dry milk. After antibody incubations, the membrane blots were washed three times for 10 minutes in PBS containing 0.05% (v/v) Tween-20, and protein signals were detected.

General analytical techniques

Protein visualization on SDS-PAGE gels was done by staining with 0.1% (w/v) Coomassie Blue R-250 (Bio-Rad) in 50% (v/v) methanol and 10% (v/v) glacial acetic acid as described above for two-dimensional electrophoresis, or by staining with silver stain kit (Thermo Scientific) using the manufacturer's instructions. Protein quantitation was performed by using the BCA assay (Thermo Scientific). Bovine serum albumin was used as a standard.

Bioinformatic techniques

Upstream regions of the soybean *nodulin 26* gene (Glyma08g12650.1) were obtained from the soybean genome database of phytozome (http://www.phytozome.net/soybean). The 1.5 kb-long genomic sequences were analyzed for ARE (anaerobic regulatory element) by web-based tool

“PlantCARE,” a database of plant cis-acting regulatory elements (http://bioinformatics.psb.ugent.be/webtools/plantcare/html) (Lescot et al., 2002).

CHAPTER III

RESULTS

Stopped-flow assays for water and ammonia transport in membrane vesicles

In order to perform functional analysis of NH_3 efflux on vesicles containing the membrane channel protein nodulin 26, a stopped flow method based on fluorimetric approaches was developed, and was initially tested by using isolated symbiosome membrane (SM) vesicles. The rationale for the assay is shown in figure 3.1 A. SM vesicles loaded with the 100 μM CF dye were injected with identical dye-free buffer containing an additional 10 mM NH_4Cl. Uptake of NH_3 from the medium into the vesicle is followed by protonation which causes alkalinization of the vesicle interior leading to an increase of CF fluorescence (Fig. 3.1 A). Changes of the intravesicular pH were linearly correlated with changes of the relative fluorescence. The time course of relative fluorescence changes was fit to a single exponential function, and the rate constant was determined from the curve fit (Fig. 3.1 B).

To determine the osmotic water permeability (P_f), a similar approach using a stopped-flow spectrometer was used except that light scattering was used

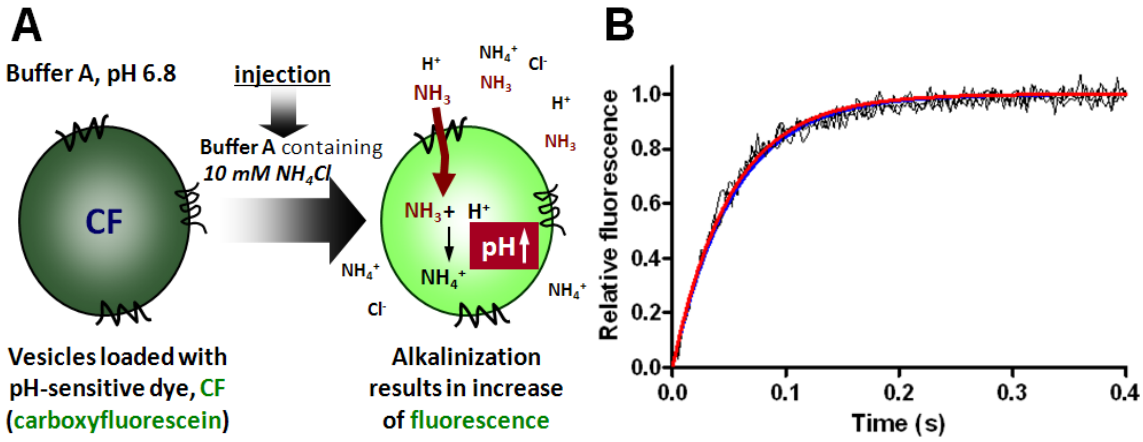

Figure 3.1. Ammonia permeability measurements in membrane vesicles. (A) Schematic representation of ammonia (NH_3) uptake assay, and **(B)** change of fluorescence traces detected by stopped-flow fluorimetry. **(A)** 100 μM CF dye-loaded SM vesicles were injected with identical dye-free buffer containing additional 10 mM NH_4Cl by a stopped-flow device. NH_3 entering SM vesicles results in alkalinization and increases the fluorescence inside the vesicles. (**B)** Changes in CF fluorescence are detected by a stopped-flow fluorimeter, and the relative fluorescence trace was plotted versus time. The red plot represents a nonlinear regression curve fit to a single exponential. The rate constant obtained reflects the rate of NH_3 uptake.

(Niemietz and Tyerman, 2000). SM vesicles suspended in isosmotic buffer were rapidly mixed with a hyperosmotic buffer to create a 200 mOsm osmotic gradient across the membrane (Fig. 3.2 A). The time course of vesicle shrinking as water effluxed from the vesicle interior was followed by an increase in light scattering shown by a downward deflection of the trace. The time course of light scattering changes was fit to a single exponential, and rate constant was determined from the curve fit (Fig. 3.2 B).

To rule out the possibility that the NH_4^+ permeable nonselective cation channel (NSCC) on the SM confounds measurements of the ammonia (NH_3) transport activity in SM vesicles, the rate of fluorescence changes were compared in the presence of variable concentrations of divalent cations such as calcium ($CaCl_2$) and magnesium ($MgCl_2$) which are known blockers of the nonselective cation channel (Tyerman et al., 1995; Roberts and Tyerman, 2002). $CaCl_2$ at concentrations ranging from 0.1 μM to 10 mM and $MgCl_2$ at concentrations from 1 mM to 10 mM did not affect NH_3 uptake across the SM vesicles (Fig. 3.3) suggesting that the stopped flow approaches are specific for measuring NH_3 uptake without interference from NH_4^+.

Purification of recombinant nodulin 26 expressed from *Pichia pastoris* and reconstitution into proteoliposomes (This work and the ammonia permeability analysis of nodulin 26 were part of a publication, (Hwang et al., 2010).)

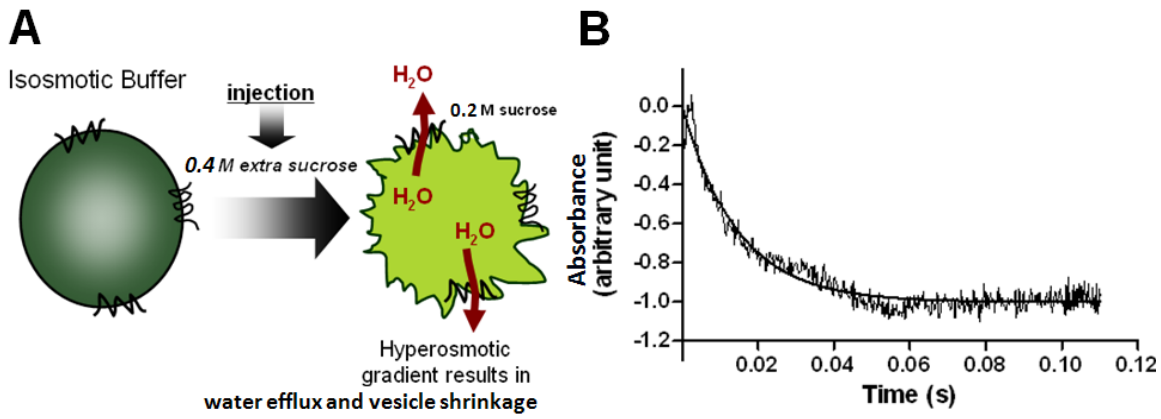

Figure 3.2. Water permeability measurements in membrane vesicles. (A) Schematic representation of water transport assay, and **(B)** change of scattered light detected by stopped-flow spectrometry. **(A)** SM vesicles suspended in isosmotic buffer were rapidly mixed with a hyperosmotic buffer containing 0.4 M extra sucrose by a stopped-flow device. Osmotic gradient across the SM results in water efflux and vesicle shrinkage. (**B)** The time course of vesicle shrinking was followed by increase in light scattering shown by downward deflection of the trace. A single exponential function was fitted to the time course of light scattering changes, and a rate constant, reflecting the rate of water efflux, was determined from the curve fit. The solid line represents a nonlinear regression curve fit to single exponential.

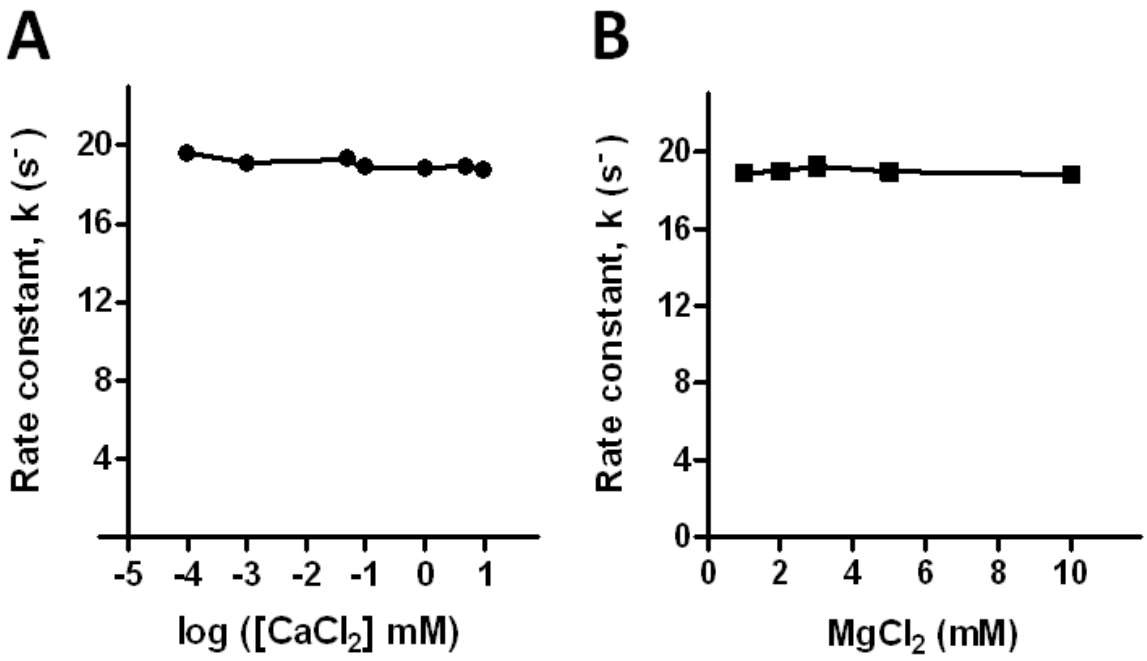

Figure 3.3. Effects of nonselective cation channel blocks on NH_3 uptake assay with symbiosome membrane (SM) vesicles. **(A)** and **(B)** Comparison of NH_3 uptake represented by rate constant, k (s^{-1}). The rate constant was determined by a single exponential curve fit of fluorescence changes following NH_3 efflux into carboxyfluorescein (CF)-loaded SM vesicles at 23°C in the presence of $CaCl_2$ **(A)** or $MgCl_2$ **(B)**. Error bars show standard error of the mean of three replicates, (*n*=3).

The presence of a facilitated pathway for NH_3 on isolated symbiosome vesicles and the finding by other groups that some aquaporins are permeable to ammonia (Jahn et al., 2004; Litman et al., 2009; Ludewig and Dynowski, 2009) led to the hypothesis that nodulin 26 could be an ammonia permeable channel that fluxes fixed NH_3 from the symbiosomes. To test this hypothesis, an approach for the expression and purification of recombinant nodulin 26 using *Pichia pastoris* expression system was devised to allow analysis of quantitative NH_3 transport properties of purified nodulin 26 by reconstitution into proteoliposomes.

The nodulin 26 ORF was fused in-frame with six histidines (His_6) at the N-terminus generating a nodulin 26 cDNA with the coding sequence with an additional six His leader sequence (His_6-nod26). His_6-nod26 was incorporated into the chromosomal *AOX1* (alcohol oxidase enzyme) locus of the methylotrophic yeast *P. pastoris* (Fig. 2.1) and was expressed in *Pichia* cultures by addition of methanol. For purification, His_6-nod26 was solubilized from a microsomal membrane fraction by solubilization in octyl glucopyranoside (OG) and was fractionated by chromatography on Ni-NTA agarose (Fig. 3.4). The highly purified protein band with an apparent molecular weight of 27 kDa was identified as nodulin 26 based on Western blot analysis with both anti-His_6 and anti-nodulin 26 antibodies (Fig. 3.4).

Single unilammelar vesicle liposomes consisting of purified *E. coli* lipids were prepared by bath sonication, and the purified nodulin 26 protein was

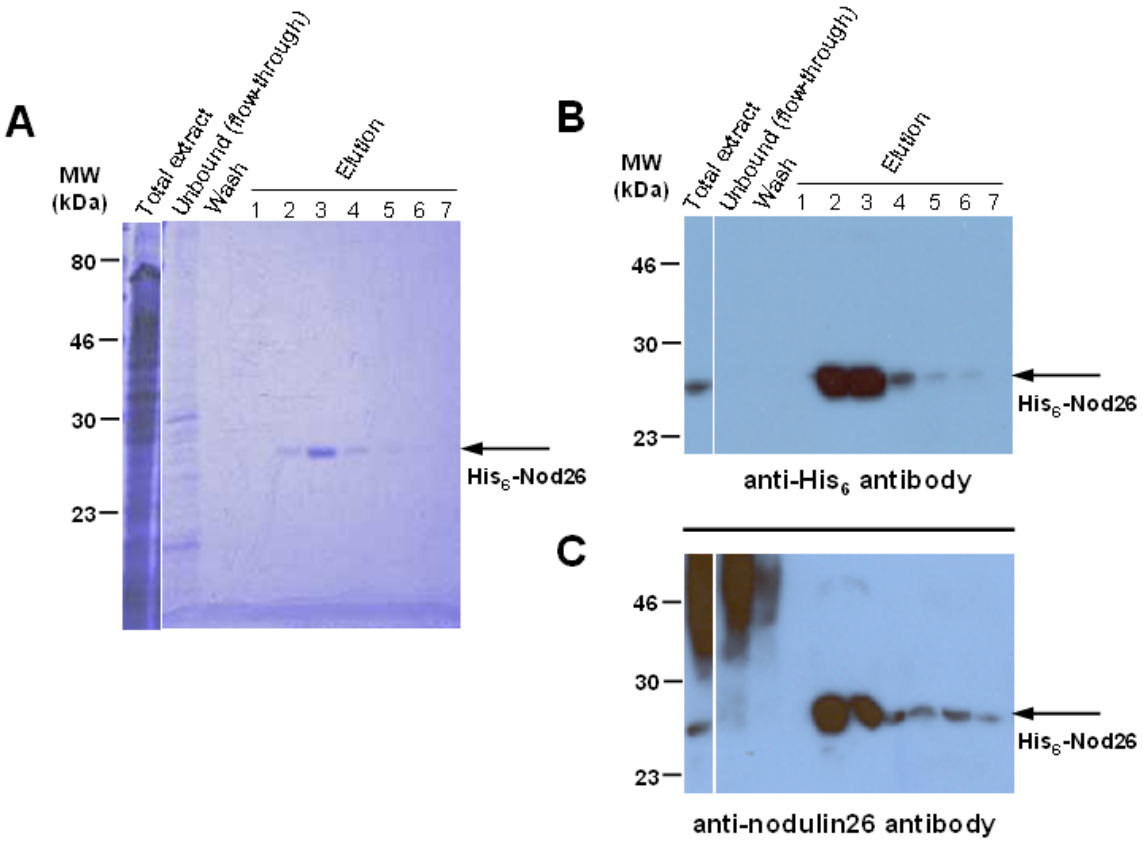

Figure 3.4. Purification of His_6-nodulin 26 from *P. pastoris* on Ni-NTA resins. From the left, total *P. pastoris* extract, unbound fraction after incubation with the Ni-NTA resins, supernatant after washing, and Ni-NTA imidazole eluent fractions, respectively were resolved by SDS-PAGE on a 12% (w/v) polyacrylamide gel. **(A)** Coomassie blue stained gel. **(B)** Anti-His_6 and **(C)** anti-nod26 Western blots. Arrow indicates theoretical molecular weight of His_6-nod26 on the gel and blots.

reconstituted into the liposomes by rapid dilution of the purified His_6-nod26 protein/OG mixture in a 100 μM CF containing buffer to load the pH sensitive dye in the liposome preparations (Fig. 3.5). Reconstitution of His_6-nod26 was verified and quantified by Western blot with anti-nodulin 26 antibody (Fig. 3.5). The incorporation of His_6-nod26 was quantitated by densitometric assay following Western blot analysis, by using a standard curve generated by known concentrations of the purified His_6-nod26 (Fig. 3.6).

Ammonia permeability properties of reconstituted nodulin 26 proteoliposomes

The ammonia permeability properties of the CF-loaded nodulin 26 proteoliposomes were measured by using stopped-flow fluorimetry upon injection into NH_4^+ containing buffers. Uptake of NH_3 is followed by protonation which results in alkalinization of the liposome space which is accompanied by an increase in CF fluorescence (Fig. 3.7). Data from three to five injections per sample were averaged. To determine ammonia permeability co-efficient (P_{NH3}), the differential equations described by Boron and De Weer (1976) were modified based on the parameters of the experimental system discussed in the Materials and Methods (Equation 2.1 and 2.2). From a fit to simulated curves, nodulin 26 proteoliposomes showed a $P_{NH3} = 35.1 \pm 2.84 \times 10^{-3}$ cm/s, a rate that is approximately 3-fold greater than that exhibited by negative control liposomes ($P_{NH3} = 13.8 \pm 0.24 \times 10^{-3}$ cm/s) (Fig. 3.7 A and Table 3.1).

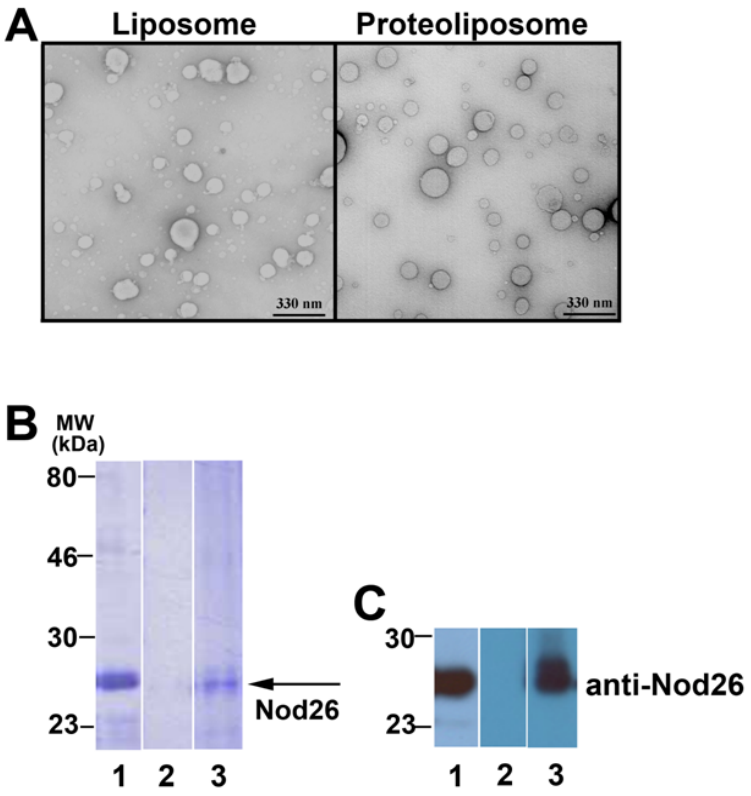

Figure 3.5. Reconstitution of recombinant nodulin 26 into proteoliposomes. (A) Transmission Electron micrograph images of negatively stained nod26-proteoliposomes and control liposomes. Scale bars represent 330 nm. **(B)** Coomassie blue-stained gel and **(C)** Anti-nod26 Western blot of purified His_6-nod26 before reconstitution and liposome preparations after resolution by SDS-PAGE on a 12% (w/v) polyacrylamide gel. Lane 1; purified His_6-nod26 (3 μg) expressed in *P. pastoris*, 2; negative control liposomes, and 3; nod26 proteoliposomes. Arrow indicates predicted molecular weight of His_6-Nod26.

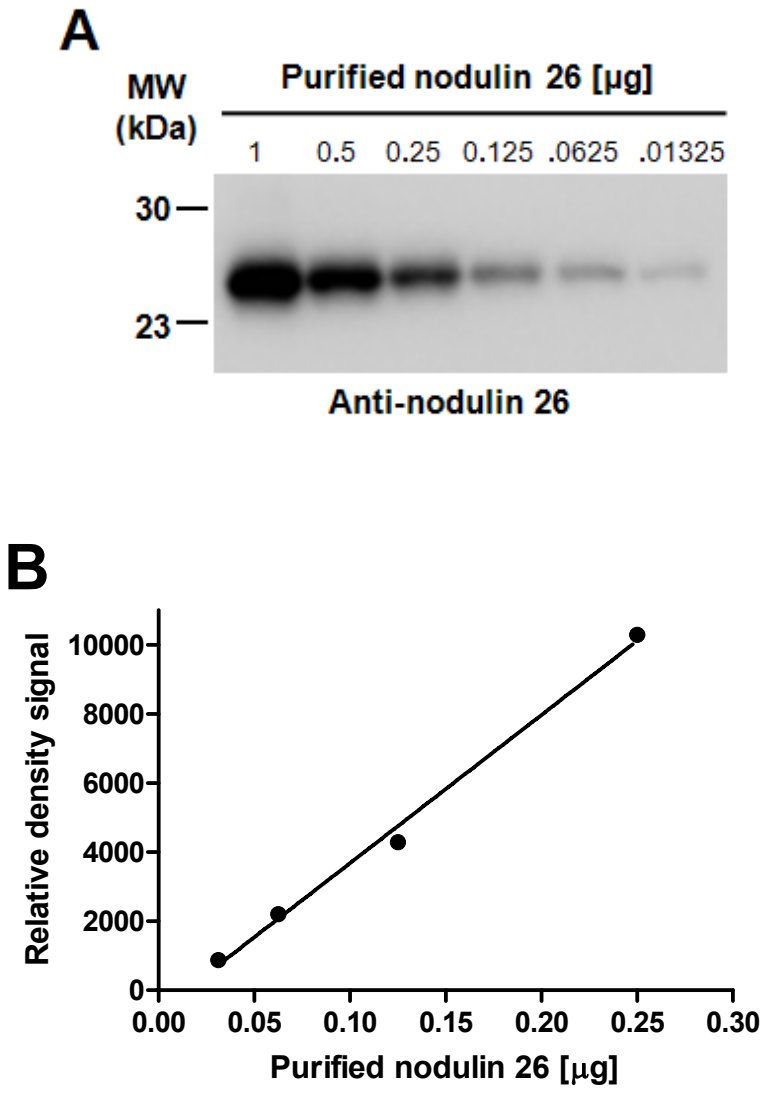

Figure 3.6. Quantitation of nodulin 26 in proteoliposomes by comparing to standard curve. Purified nodulin 26 and proteoliposome were loaded on a 12% (w/v) SDS-PAGE gel, and densitometric assay was performed following Western blot analysis using anti-nodulin 26 antibody. **(A)** Western blot image. **(B)** Standard curve generated by purified nodulin 26 signals, ranging from 0.25 µg to 13.25 ng.

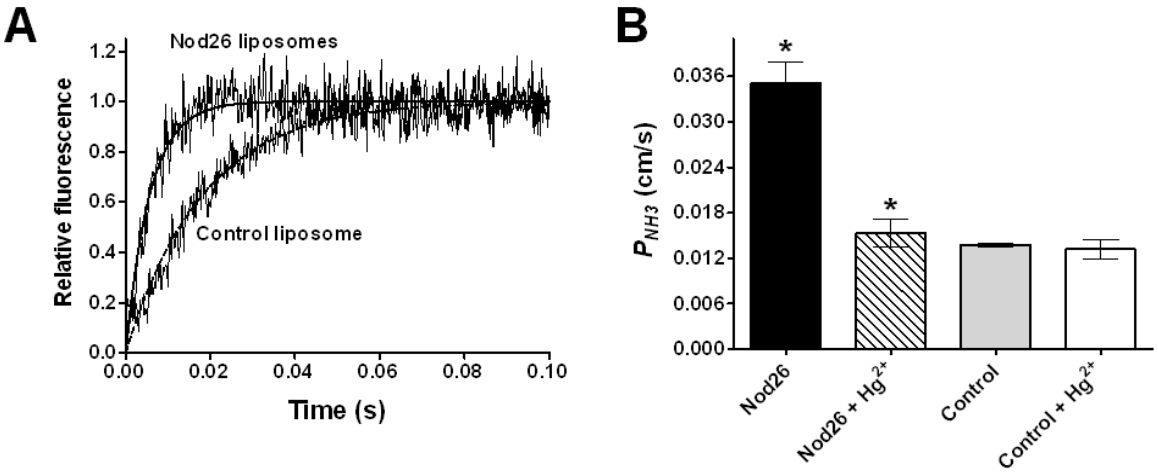

Figure 3.7. Ammonia (NH_3) permeability measurements of nodulin 26-proteoliposomes. **(A)** Time-course of fluorescence increase in CF-loaded nod26 proteoliposomes and negative control liposomes upon injection into 10 mM NH_4Cl was measured by a stopped-flow fluorimetry at 23°C. The data represents an average of five injections and the curve fit to a single exponential is shown. **(B)** Ammonia (NH_3) permeabilities (P_{NH3}) of nod26 proteoliposomes and control liposomes were calculated from stopped flow measurements in the presence or absence of 1 mM $HgCl_2$. The error bars show the standard error of the mean (n=13) for nod26, (n=8) for nod26 with $HgCl_2$, (n=9) for negative control, and (n=4) for negative control with $HgCl_2$. (∗ indicates p value < 0.0001).

Table 3.1. Summary of NH_3 and water permeability properties of liposome preparations.

	Nod26 proteoliposomes	Control liposomes
Diameter (nm)[a]	116 (7.3, n=3)[b]	113 (3.6, n=3)
P_{NH3} (cm/s) x10^{-3} [c]	35.1 (2.84, n=13)	13.8 (0.24, n=9)
P_{NH3} with $HgCl_2$ (cm/s) x10^{-3}	15.3 (1.81, n=8)	13.2 (1.26, n=4)
Hg^{2+}-sensitive [d] P_{NH3} (cm/s)	19.8 $\times$ 10^{-3}	
p_{NH3} (cm^3/subunit/s) x 10^{-14}	1.27 (0.06, n =3)	
NH_3 transported per subunit [e] (S^{-1}) x 10^8	3.06	
E_a (kJ/mol)	38.3	90.4
P_f (cm/s) x10^{-3}	9.45 (0.65, n=19)	5.54 (0.32, n =7)
P_f with $HgCl_2$ (cm/s) x10^{-3}	5.15 (0.32, n =6)	
Hg^{2+}-sensitive [d] P_f (cm/s) x10^{-3}	4.30 $\times$ 10^{-3}	

[a] Between 130 to 220 vesicles were measured and averaged for each liposome preparation tested.

[b] The standard error of the means for the indicated number of measurements is shown parenthetically.

[c] The buffer capacity β for both liposome preparations was 15.9 mM/pH.

[d] The Hg^{2+} sensitive activity was obtained by subtracting the permeability values obtained in the presence of 1 mM $HgCl_2$ from the uninhibited permeability values.

[e] A molar volume of 24.96 cm^3/mol for NH_3 was used for this calculation.

Previous work has shown that water and solute transport through nodulin 26 is inhibited by Hg^{2+}, presumably by modification of critical cysteine sulfhydryls (Rivers et al., 1997; Dean et al., 1999). To verify that transport of NH_3 in nodulin 26 proteoliposomes was mediated by a nodulin 26-based pathway, the effects of Hg^{2+} on transport were investigated (Fig. 3.7). Nodulin 26 proteoliposomes in the presence of 1 mM $HgCl_2$ showed reduced NH_3 uptake to a level observed with negative control liposomes, while the negative control liposomes were not affected by $HgCl_2$ (Fig. 3.7). Another feature of MIP-facilitated transport of water and solutes is a reduced Arrhenius activation energy (E_a) compared to diffusion through a lipid bilayer (Zeidel et al., 1992; King and Agre, 1996). Consistent with this prediction, analysis of the NH_3 permeability of nodulin 26 proteoliposomes as a function of temperature showed a low E_a (38.3 kJ/mol) compared with that of control liposomes (90.4 kJ/mol) (Fig. 3.8 and Table 3.1).

Single channel conductance determination and comparison of ammonia and water permeability

In order to compare the relative selectivity of water and ammonia transport of nodulin 26, light scattering stopped-flow experiments with the proteoliposomes were performed to determine the osmotic water permeability (P_f) as an index of liposome shrinkage as described previously (Niemietz and Tyerman, 1997; Niemietz and Tyerman, 2000). This enables direct comparison of the P_{NH3} and P_f constants for the same liposome preparations. As revealed

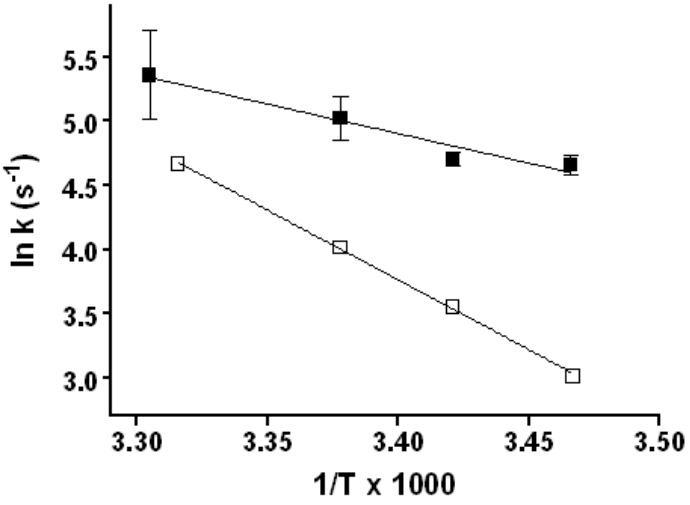

Figure 3.8. Arrhenius plots of NH_3 uptake from nodulin 26 proteoliposomes (■) and negative control liposomes (□). The natural log of the rate constants (ln k) were determined from the single exponential curve fits of fluorescence traces. Error bars show standard error of the mean of three to six replicates.

from a previous study (Dean et al., 1999), reconstitution of nodulin 26 into proteoliposomes results in enhanced water permeability which is inhibited by Hg^{2+} (Fig. 3.9).

To standardize and compare the ammonia and water transport rates, single channel transport permeabilities were calculated based on the surface density of nodulin 26 on proteoliposomes. Since the permeability constant is a combination of protein based transport (Hg^{2+}-sensitive) and lipid bilayer diffusion (Hg^{2+}-insensitive), the calculation of the single channel rate was based on the Hg^{2+}-sensitive fraction of ammonia or water transport (Table 3.1). By this approach, a single channel ammonia permeability, p_{NH3} for nodulin 26 of 12.7 ($\pm$ 0.6) $\times$ 10^{-15} cm^3/subunit/s (n=3) was calculated (Table 3.1). Based on previous measurements, the single channel water permeability, p_f, for nodulin 26 is 3.8 $\times$ 10^{-15} cm^3/subunit/s (Dean et al., 1999), suggesting a 3.3-fold preference for the transport of ammonia. This is supported by the P_{NH3}/P_f ratio (4.6-fold) measured in the present study which includes a preference for NH_3 as a transport substrate (Table 3.1). In addition, assuming one transport channel per nodulin 26 monomer, the single channel ammonia conductance of nodulin 26 represents a permeability of 3.06 x 10^8 NH_3 molecules per channel per second (Table 3.1).

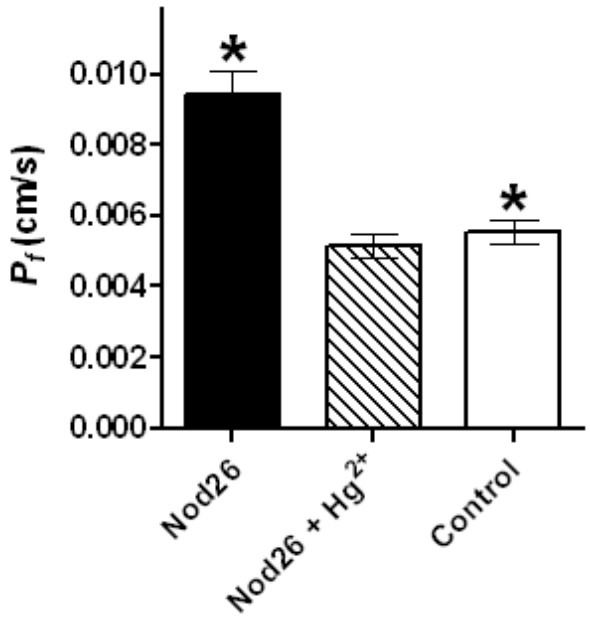

Figure 3.9. Osmotic water permeability measurements of nodulin 26 proteoliposomes. The osmotic water permeabilities (P_f) of nod26 proteoliposomes in the presence or absence of 1 mM $HgCl_2$ and negative control liposomes were determined as described in equation 3. Error bars show standard error of the mean (n=19) for nod26, (n=6) for nod26 with $HgCl_2$, and (n=7) for control. * indicates p value < 0.002.

Interaction of nodulin 26 with glutamine synthetase

This is a collaboration between me and Pintu Masalkar. Portions of this work were published in (Masalkar et al., 2010). Below, I have summarized my contributions to this study.

Figure 3.10 A shows the proposed SM topology of soybean nodulin 26 based on the conserved "hourglass" fold characteristic of the MIP family (Wallace and Roberts, 2004). The cytosolic C-terminal domain of nodulin 26 consists of a hydrophilic 24 amino acid extension (Weaver et al., 1991), which is conserved in group I members of the nodulin 26-like intrinsic protein (NIP) subfamily (Wallace et al., 2006). Previous studies (Girsch and Peracchia, 1991; Noda and Sasaki, 2005; Yu et al., 2005; Rose et al., 2008) show that the C-terminal extensions of MIPs can serve as a binding site for protein-protein interaction with various cytosolic proteins.

To test if the nodulin 26 cytosolic C-terminal domain is a site for a protein interaction, an affinity chromatography approach was designed. An affinity resin consisting of a synthetic peptide (CK-25) containing the nodulin 26 C-terminal sequence immobilized to an agarose resin was incubated with soybean nodule extracts. After washing unbound fraction, a tightly-bound major 40 kDa protein was eluted by using 6 M urea (Fig. 3.10 B). This was the only detectable protein band in the urea eluent. Resolution by 2D-electrophoresis (2DE) showed that the 40 kDa protein band observed in one dimensional SDS-PAGE actually

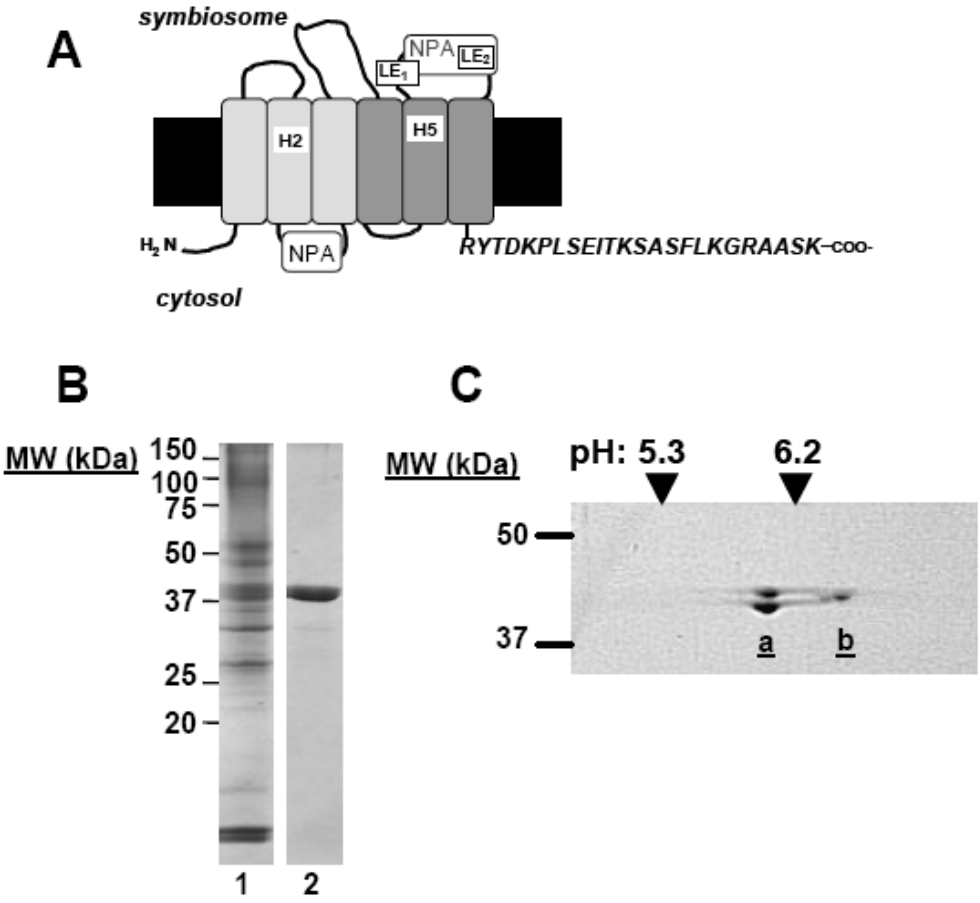

Figure 3.10. Isolation of soybean nodule proteins interacting with the C-terminal domain of nodulin 26. (A) A diagram showing the topology of soybean nod 26 in the SM. The conserved NPA loops and the amino acid positions that comprise the ar/R selectivity filter (H2, H5, LE_1 and LE_2) are indicated. The sequence of the C-terminal cytosolic domain is shown. (**B)** Results of affinity chromatography of a soluble extract of 28-d nodules on the nod26 C-terminal peptide affinity resin. **Lane 1**, soybean nodule extract (10 µg protein). **Lane 2**, affinity resin-bound protein eluted with 6 M urea. **(C)** Results of two dimensional gel electrophoresis of 3 µg of the affinity resin purified protein from panel **B**. The position of pH markers in the first dimension and the molecular weight standards in the second dimension are shown. The lower case **a** and **b** designations show the position of migration of soybean GS_1 β and γ isoforms respectively based on Morey et al. (2002).

consists of a collection of protein spots with distinct isoelectric points (*pI*) and slightly different molecular weights (Fig. 3.10 C).

The 40 kDa protein band was subject to in-gel digestion using trypsin (Jensen et al., 1999), and the tryptic digests were analyzed by MALDI-TOF mass spectrometry (MS) (Fig. 3.11). Analysis of the peptide mass fingerprint identified soybean cytosolic glutamine synthetase $GS_1\beta1$ with a strong expectation score (E value = 6.1×10^{-5}, 56 % sequence coverage). A list of peptide fragments detected by the MS analysis are shown in table 3.2. MS/MS analysis of 1610.022 dalton (Da) tryptic digest confirmed the identification with a peptide sequence as of 277^{th}-HKEHIAAYGEGNER-290^{th} characteristic of soybean $GS_1\beta1$. In addition, the theoretical molecular weight of soybean $GS_1\beta1$ (M_r = 38,759) is consistent with the 40 kDa molecular weight of the protein band observed on the SDS-PAGE gel (Fig. 3.10 B).

Soybean nodules contain four cytosolic GS_1 isoforms ($GS_1\beta1$, $GS_1\beta2$, $GS_1\gamma1$, and $GS_1\gamma2$) that are distinguished by molecular weight and *pI*s (Morey et al., 2002). As discussed above, the 40 kDa protein band observed in one dimensional SDS-PAGE turned out to be a combination of bands with distinct *pI*s and molecular weights (Fig. 3.10 C) consistent with the presence of four soybean GS_1 isoforms. The 2DE result suggests that the four β and γ isoforms of GS_1 interact with the C-terminal nodulin 26 peptide.

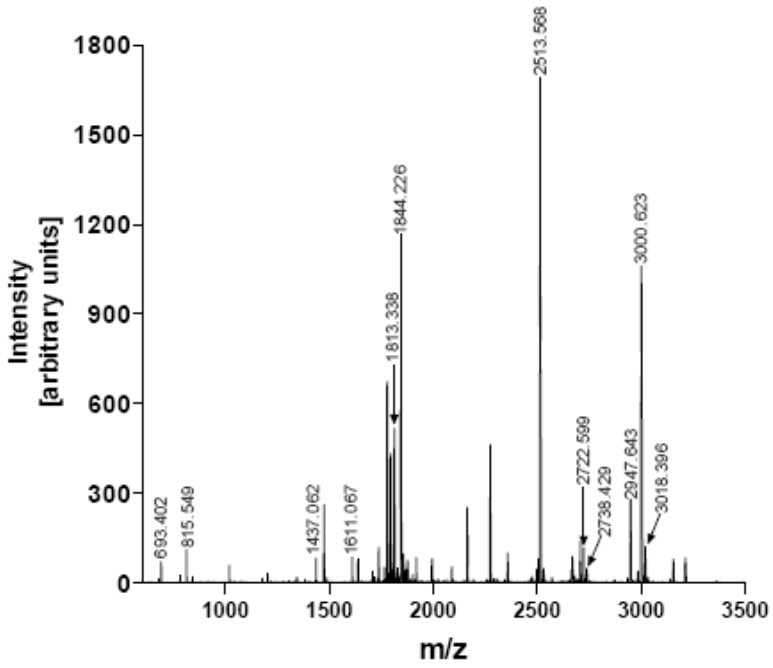

Figure 3.11. Identification of the 40kDa protein as soybean cytosolic glutamine synthetase. MALDI-TOF spectra of protonated tryptic peptides (MH^+) of the 40kDa protein isolated by affinity chromatography on nod26 peptide agarose. The 40kDa protein was resolved by electrophoresis as in Figure 3.8 B and was subjected to in gel tryptic digestion and mass spectroscopic analysis. The Y-axis shows the intensity as arbitrary units. The mass to charge ratio is plotted on the X-axis.

Table 3.2. Mass analysis table of 40 kDa protein tryptic peptides from MALDI-TOF

Measured mass (Da)[a]	Predicted mass (Da)[a]	Error (Da)[b]	Residue i ndices[c]	Sequence[d]
692.392	692.385	.007	219-223	YILER
785.382	785.334	.048	327-332	GYFEDR
814.532	814.491	.041	268-275	AAIDKLGK
1436.042	1435.755	.287	39-52	TLPGPVSDPSELPK
1610.022	1609.759	.263	277-290	HKEHIAAYGEGNER [e]
1737.602	1737.854	-.252	276-290	KHKEHIAAYGEGNER
1779.212	1778.902	.310	19-34	VIAEYIWIGGSGMMMDLR
1812.332	1812.039	.293	224-240	ITEIAGGGVVVSFDPKIPK
1843.212	1842.901	.312	296-311	HETADINTFLWGVANR
2356.362	2356.172	.190	85-106	GNNILVICDAYTPAGEPIPTNK
2512.562	2512.273	.289	85-107	GNNILVICDAYTPAGEPIPTNKR
2512.562	2512.273	.289	84-106	RGNNILVICDAYTPAGEPIPTNK
2668.442	2668.374	.068	84-107	RGNNILVICDAYTPAGEPIPTNKR
2946.632	2946.479	.153	113-137	VFSHPDVVAEVPWYGIEQEEEYTLLQK
2999.612	2999.392	.220	53-79	WNYDGSSTGQAPGEDSEVILYPQAIFR
3017.392	3017.416	-.023	138-165	DIQWPLGWPVGGFPGPQGPYYCGVGADK

[a] The experimental mass of each peptide from the MALDI-TOF experimental spectrum is shown together with the theoretical mass of the corresponding tryptic digest peptide from soybean GS_1 β 1. Each mass is reported in Daltons.

[b] The error between the experimental and theoretical masses of each peptide is shown.

[c] The amino acids of soybean GS_1 β1 corresponding to each peptide are shown.

[d] The derived primary sequence of each soybean GS_1 β1 peptide is shown.

[e] The peptide sequence confirmed by MS/MS analysis.

Regulation of nodulin 26 selectivity by CDPK phosphorylation

As mentioned in the introduction, nodulin 26 is a major target for a CDPK which resides on the SM (Weaver et al., 1991; Weaver and Roberts, 1992). With respect to nodulin 26's water transport activity, previous work revealed that phosphorylation of nodulin 26 enhances its osmotic water permeability (P_f) (Guenther et al., 2003). However, the effects of phosphorylation on ammonia transport activity (P_{NH3}) of nodulin 26 have not been studied.

The phosphorylation state of nod 26 on isolated SM vesicles can be controlled by treatment with $CaCl_2$ and ATP, which triggers CDPK catalyzed nod26-specific phosphorylation in situ, or by treatment with alkaline phosphatase (AP) which dephosphorylates the protein (Fig. 3.12 A). In order to test the comparative effects of phosphorylation on water and NH_3 permeability, isolated and CF-loaded SM vesicles were incubated with Ca^{2+} and ATP for phosphorylation of nodulin 26 or alkaline phosphatase (AP) for dephosphorylation, and transport activities were analyzed by stopped-flow measurements (Fig. 3.12 B and C). Phosphorylation and dephosphorylation of nodulin 26 on the SM vesicles were verified by Western blot analysis using nodulin 26-specific and phospho-nodulin 26-specific antibodies (Fig. 3.12 A).

To investigate the effects of the phosphorylation and dephosphorylation of nodulin 26 on ammonia and water transport activities, stopped-flow kinetic analyses were performed (Fig. 3.12). To correct for nonselective diffusive permeability, the value for Hg^{2+}-treated SM vesicles was used as a background

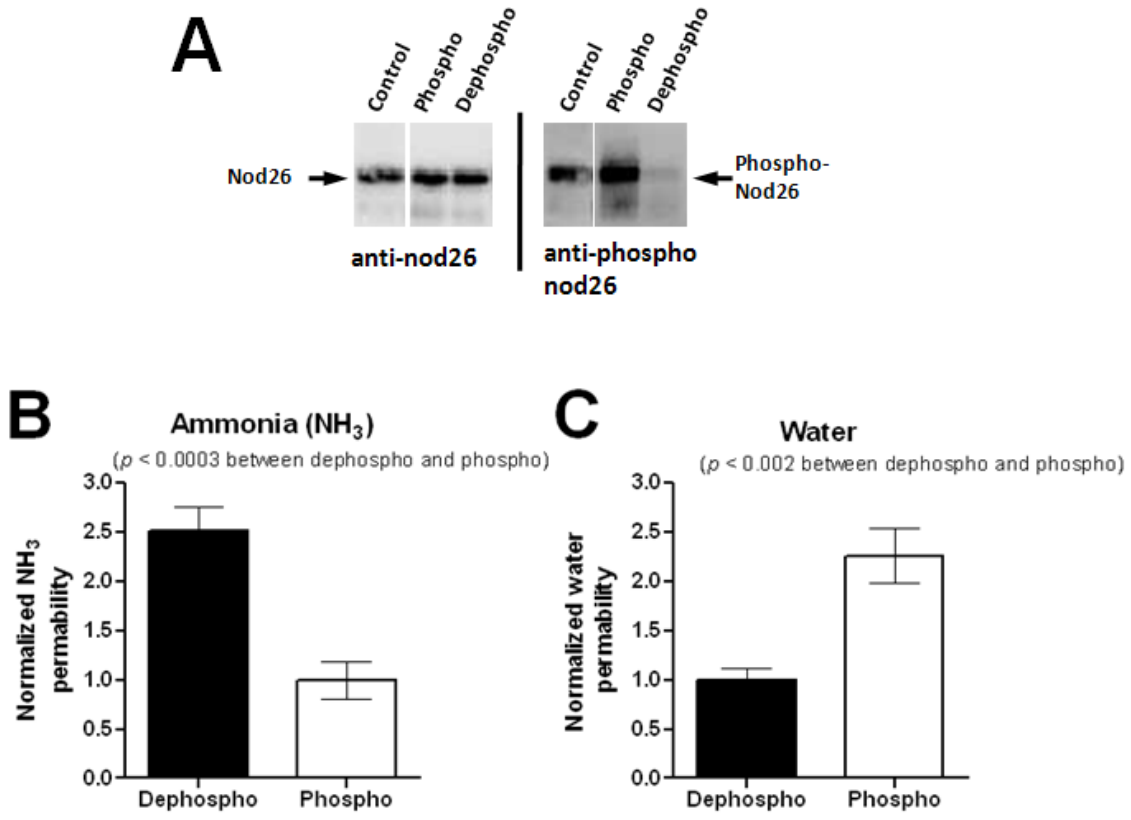

Figure 3.12. Comparison of NH_3 and water permeability of SM vesicles after Ca^{2+}/ATP phosphorylation and alkaline phosphatase-mediated dephosphorylation. CF-loaded SM vesicles (control) were dephosphorylated by using alkaline phosphatase (AP) (Dephospho) and phosphorylated by Ca^{2+}/ATP treatment (Phospho). **(A)** Vesicles after treatments were analyzed by Western blot assay using nodulin 26- and phospho-nodulin 26-specific antibodies. **(B and C)** Corrected and normalized Hg^{2+}-sensitive permeabilities of SM vesicles containing phospho- (open bars, □) and dephospho-nodulin 26 (closed bars, ■). CF-loaded SM vesicles were analyzed for both ammonia **(B)** and water **(C)** transport by using same preparations. Error bars show standard error of the mean, SEM (n=7 to 18).

control. The P_{NH3} of the SM vesicles with dephosphorylated nodulin 26 was enhanced up to 2.5-fold, compared to phosphorylated nodulin 26 (Fig. 3.12 B). Conversely, phosphorylation of nodulin 26 resulted in 2.3-fold increase of the P_f of the SM vesicles, compared to dephosphorylation treatment (Fig. 3.12 C). Consistent with these observations, proteoliposomes containing wild-type and a phospho-mimic mutant (expressed and purified from *Pichia*) showed reduced permeability to NH_3 upon substitution of Ser262 with an Asp residue (Fig. 3.13). These results support the hypothesis that CDPK-dependent phosphorylation can regulate nodulin 26 channel selectivity, with phosphorylation favoring water transport over ammonia transport.

Regulation of nodulin 26 phosphorylation by environmental cues

From the previous section it is clear that nodulin 26 has at least two possible transport activities that are potentially modulated by phosphorylation: ammonia transport and water transport. Because of its high SM concentration**,** nodulin 26 is responsible for the unusually high water permeability of the symbiosome (Rivers et al., 1997; Dean et al., 1999). Considering the fact that the symbiosome is the major organelle in the nonvacuolated infected cell, this high water permeability could serve an osmoregulatory role in cell cytosolic volume homeostasis and osmotic adjustment. In a previous study, it has been confirmed that nodulin 26 phosphorylation increases under osmotic stresses such as salinity and drought, and the enhanced phosphorylation on nodulin 26

Figure 3.13. Comparison of NH_3 permeability of proteoliposomes reconstituted with nodulin 26 wild-type and phospho-mimic mutant. Nodulin 26 phospho-mimic mutant containing 262nd Asp(D) instead of Ser(S) was purified from *Pichia* expression clone culture and was reconstituted into proteoliposomes. **(A)** Western blot of purified wild-type and phospho-mimic His_6-nodulin 26 with anti-nod26 antibodies. As a control, an isolated soybean SM fraction was compared on left end of the panel. Arrows indicate nodulin 26 corresponding to the proposed molecular weight including the N-terminal His_6-tag. **(B)** Hg^{2+}-sensitive ammonia permeabilities (P_{NH3}) of wild-type (closed bar, ■) and phospho-mimic (open bar, □) nodulin 26 were compared. Permeability was normalized against wild-type nodulin 26. Error bars show the standard error of the mean (*n*=6 to 8).

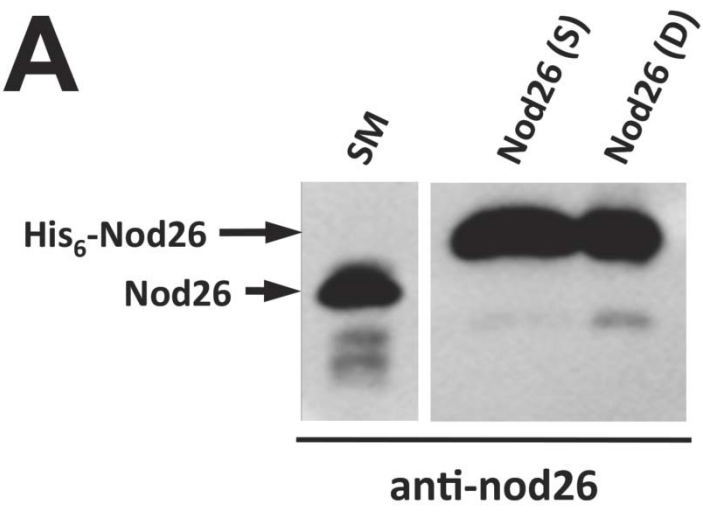
A
SM
Nod26 (S)
Nod26 (D)
His6-Nod26
Nod26
anti-nod26

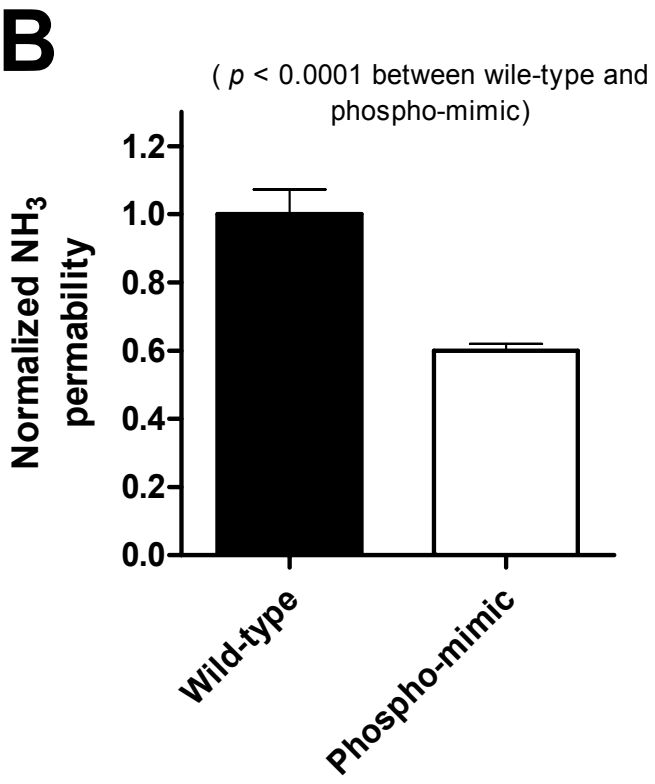
B
(p < 0.0001 between wile-type and phospho-mimic)
Normalized NH3 permability
1.2
1.0
0.8
0.6
0.4
0.2
0.0
Wild-type
Phospho-mimic

results in an increase in water permeability rate that could be part of the response to the nodule to osmotic cues (Guenther et al., 2003). Nodules are very sensitive to these osmotic stresses and show a rapid and reversible decrease in the rate of nitrogen fixation due to the limitation of oxygen diffusion into the core of the nodule (Roberts et al., 2010). In response to hypoxia stress, due to flooding, nodules show the opposite response, exhibiting an increase in the rate of gas diffusion into the nodule core. To explain these observations, an osmoregulatory model was proposed through which movement of water into the interstitial spaces modulates gas diffusion into the nodule core by regulating cell turgor and shape and apoplastic water content, opening or closing intercellular pathways for O_2 movement (Hunt and Layzell, 1993).

To investigate and compare effects of these opposite environmental stimuli on nodulin 26 phosphorylation in response to flooding stress, nodulated soybean roots were subject to water logging. Protein expression versus phosphorylation of the nodulin 26 was analyzed by Western blot assay with anti-nodulin 26 and anti-phospho-nodulin 26 antibodies (Fig. 3.14 and 3.15). Flooding resulted in no significant changes in the overall level of nodulin 26 protein over the time course of the water logging treatment (Fig. 3.14), whereas phosphorylation levels of the nodulin 26 resulted in acute response of decrease as early as 1 hour after treatment and maintain decreased level up to 7-fold less than 0 hour control until 12 hours after flooding stress (Fig. 3.14). The

Figure 3.14. Expression of nodulin 26 and its phosphorylation state in soybean root nodules under flooding stress. 36 day-old nodulated soybean plants were subjected to flooding stresses for 1, 2, 3, 6, and 12 hours (hr) by complete submersion of root parts in water. **(A)** Membrane samples (20 μg/well) isolated from flooding stressed soybean nodules were resolved by electrophoresis by SDS-PAGE on 12% (w/v) polyacrylamide gels, and were stained by Coomassie blue **(top panel)** or were analyzed by Western blot (WB) for nodulin 26 protein content (by anti-Nod26) and phosphorylation state (by anti-phospho Nod26) **(bottom panels)**. **(B)** Densitometry comparison of the relative amounts of nodulin 26 protein and the relative phosphorylation state of nodulin 26 under flooding stress. The data were normalized to the average signal obtained for 0 hr control plants. The error bars show standard error of the mean (*n*=3 to 6).

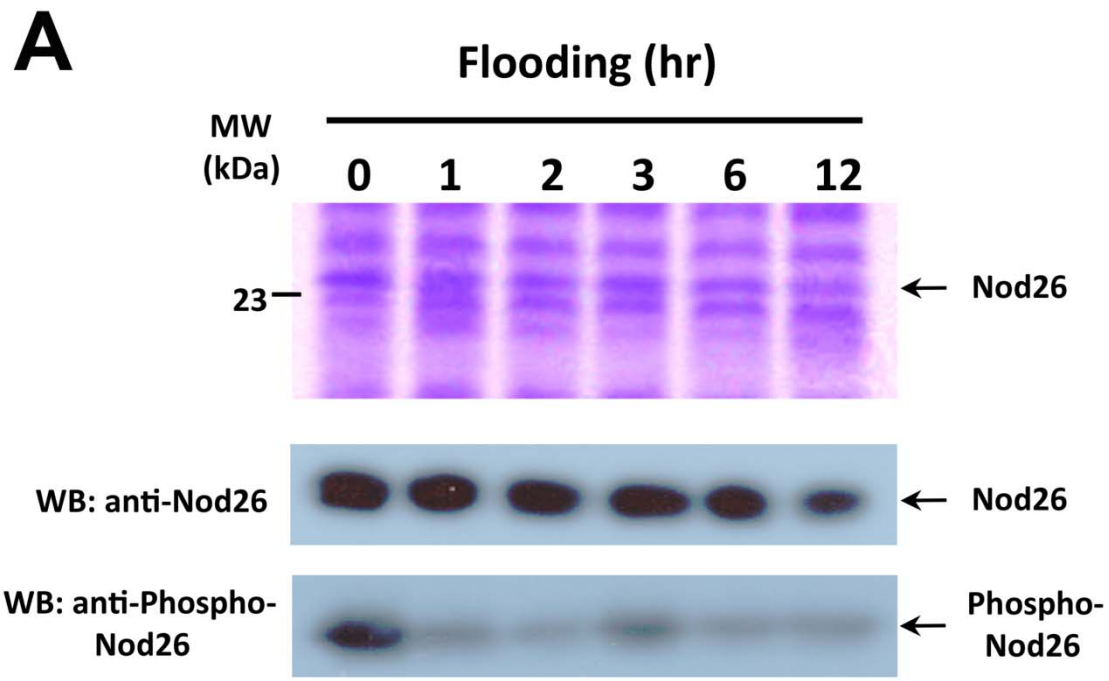
A
Flooding (hr)
MW
(kDa)
0
1
2
3
6
12
23
Nod26
WB: anti-Nod26
Nod26
WB: anti-Phospho-
Nod26
Phospho-
Nod26

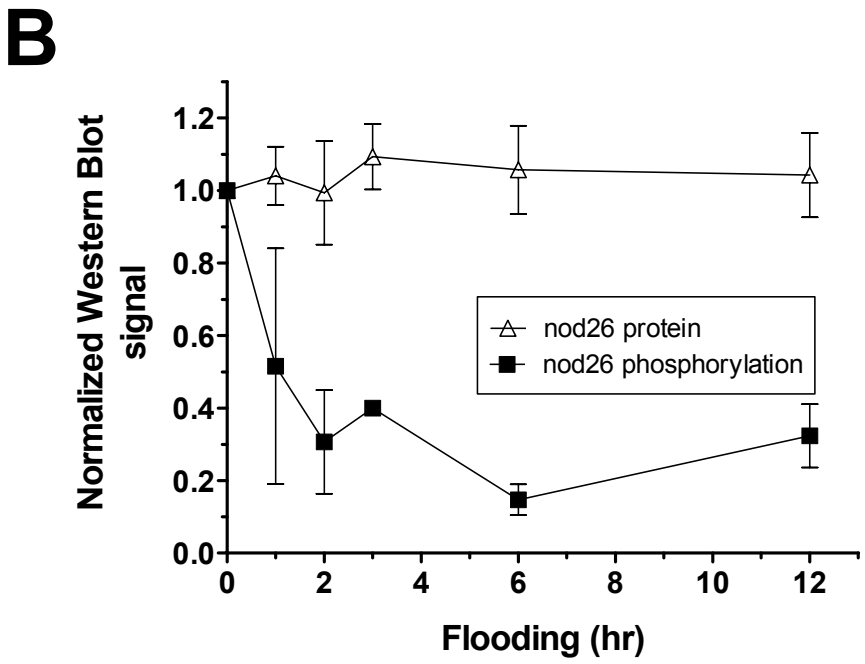
B
Normalized Western Blot
signal
1.2
1.0
0.8
0.6
0.4
0.2
0.0
0
2
4
6
8
10
12
Flooding (hr)
nod26 protein
nod26 phosphorylation

Figure 3.15. Expression and comparison of nodulin 26 and its phosphorylation state under long-term flooding stress. 36 day-old nodulated soybean plants were treated with flooding and nodulin 26 protein and phosphorylation were assayed as described in figure 3.14. **(A)** Membrane samples (20 μg/well) isolated from normoxic control and flooding-treated soybean nodules and were resolved by SDS-PAGE on 12% (w/v) polyacrylamide gels and were analyzed for nodulin 26 protein content (by anti-Nod26) and phosphorylation state (by anti-phospho Nod26) by Western blot. **(B and C)** Densitometric analysis of the relative amounts of nodulin 26 protein and its phosphorylation state under flooding stress **(B)** and in normoxic control nodules **(C)**. The data were normalized to the average signal obtained for 0 hr control plants. The error bars show the standard error of the mean of three replicates (*n*=3).

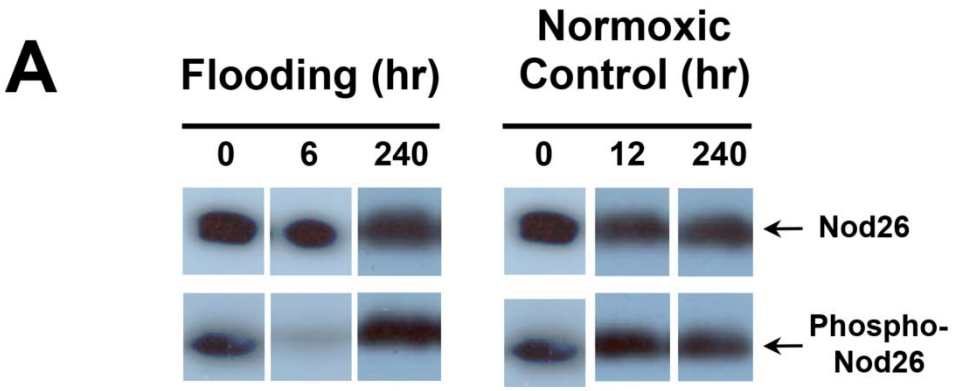
A
Flooding (hr)
Normoxic Control (hr)
0
6
240
0
12
240
Nod26
Phospho-Nod26

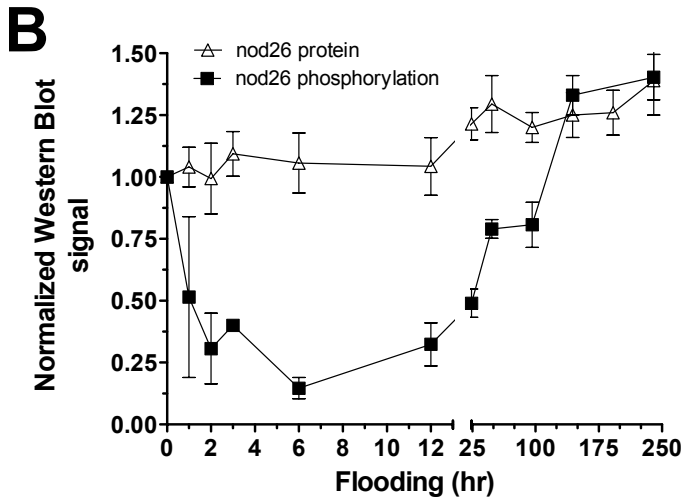
B
nod26 protein
nod26 phosphorylation
Normalized Western Blot signal
1.50
1.25
1.00
0.75
0.50
0.25
0.00
0
2
4
6
8
10
12
25
100
175
250
Flooding (hr)

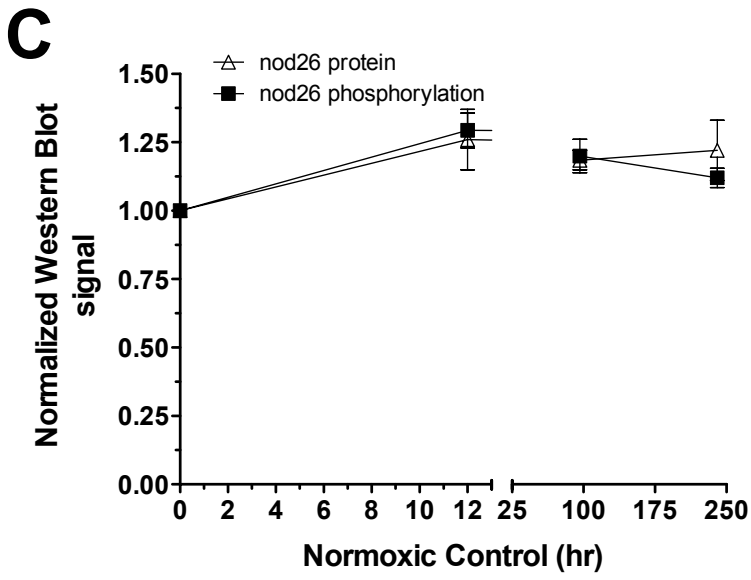
C
nod26 protein
nod26 phosphorylation
Normalized Western Blot signal
1.50
1.25
1.00
0.75
0.50
0.25
0.00
0
2
4
6
8
10
12
25
100
175
250
Normoxic Control (hr)

phosphorylation state eventually recovered after 6 days as the soybean plants adapt to the sustained hypoxic environment driven by flooding (Fig. 3.15).

Since the key stress associated with water logging is oxygen deprivation due to the low permeability of molecular O_2 in water, it was tested whether direct exposure of nodulated soybeans to hypoxia leads to a similar influence on the phosphorylation state of nodulin 26. Nodulated soybean plants were exposed to hypoxia conditions by using an anaerobic jar system. As predicted, exposure of nodulated roots to a hypoxic environment resulted in a rapid decrease in the phosphorylation levels of nodulin 26 (Fig. 3.16). Thus, the effects of flooding appear to be the result of low O_2 tension.

Since transport activity of nodulin 26 for water and ammonia is apparently conversely affected by phosphorylation (Fig. 3.12) it can be proposed that environmental signals that decrease nodulin 26 phosphorylation might also affect nodulin 26 permeability. To test this hypothesis, stopped-flow analysis with SM vesicles isolated from flooding-treated soybean nodules was performed (Fig. 3.17). Stopped-flow measurements following flooding treatment showed a decrease in osmotic water permeability while with a corresponding increase in ammonia permeability (Fig. 3.17), correlating with dephosphorylation effects on nodulin 26 transport activities under flooding. Taken together, these observations suggest that phosphorylation of nodulin 26 may play a role in osmotic and metabolic regulation in response to developmental (Guenther et al., 2003) and environmental cues.

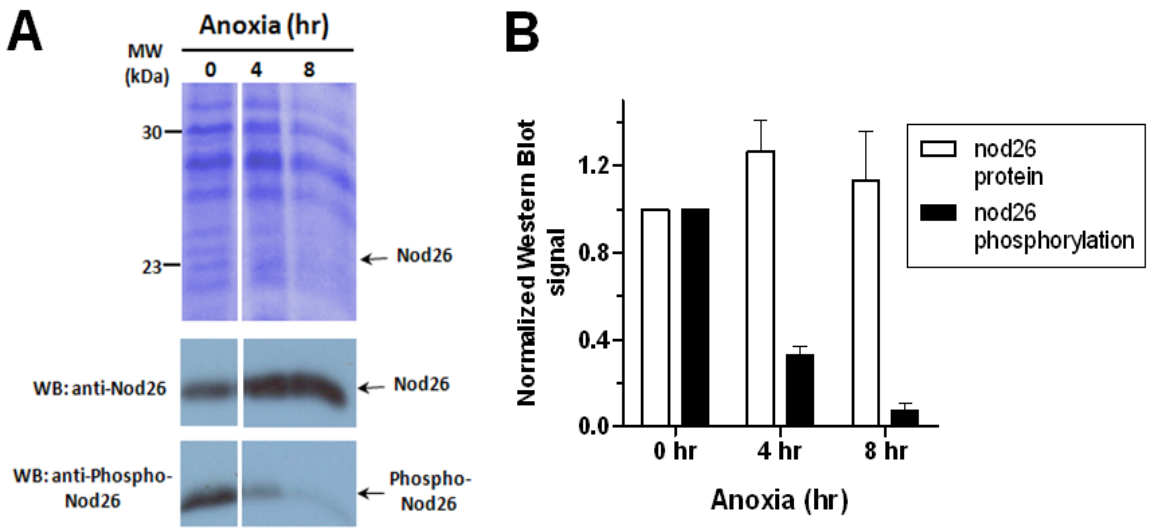

Figure 3.16. Expression and comparison of nodulin 26 and its phosphorylation state under anaerobic stress. 36 day-old nodulated soybean plants were subjected to low oxygen stress using an anaerobic jar system. **(A)** Membrane samples (20 μg/well) isolated from normoxic control and hypoxic soybean nodules were resolved by SDS-PAGE on 12% (w/v) polyacrylamide gels. **Top panel**, Coomassie blue stained gel. **Bottom panels**, Western blot analysis for nodulin 26 protein content (by anti-Nod26) and phosphorylation state (by anti-phospho Nod26). **(B)** Densitometric analysis of the relative amounts of nodulin 26 protein and its phosphorylation state under low oxygen stress. The data were normalized to the average signal obtained for 0 hr control plants. The error bars show the standard error of the mean of three replicates (*n*=3).

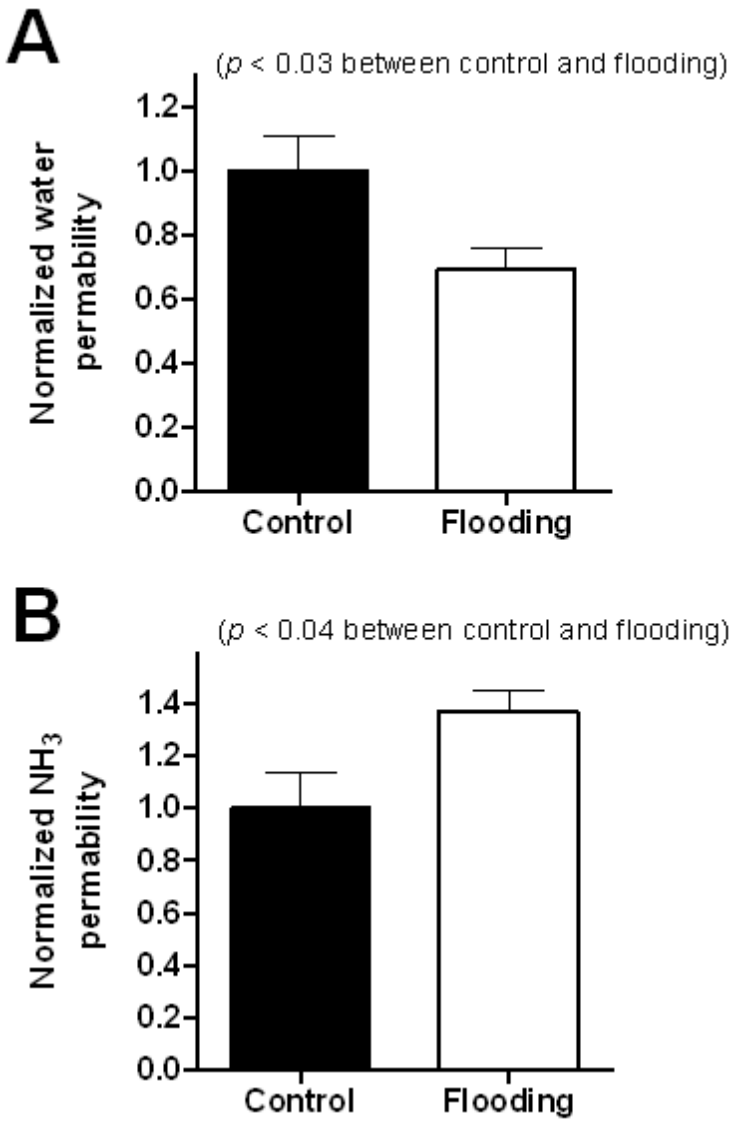

Figure 3.17. Water and ammonia permeabilities of SM vesicles isolated from flooding stressed nodules. Corrected Hg^{2+}-sensitive water **(A)** and ammonia **(B)** permeabilities of SM vesicles isolated from 6 hr-flooding stressed nodules (open bars, □) were normalized and compared to control SM vesicles (closed bars, ■). The error bars show the standard error of the mean (*n*=7 to 14).

Comparison of the effects of environmental signals on nodulin 26 phosphorylation and transport

The effects of environmental stimuli on nodulin 26 phosphorylation are summarized in figure 3.18. Water deficit and flooding/hypoxia stresses exert converse effects on the phosphorylation state of nodulin 26 on symbiosome membranes (Fig. 3.18). For example, exposure of nodulated roots to drought or salinity results in hyperphosphorylation of serine 262 of nodulin 26 (Fig. 3.18). In contrast, flooding or hypoxia stress results in the opposite effect with dephosphorylation observed rapidly. In the case of flooding stress, soybean nodules eventually adapt and resume nitrogen fixation (Roberts et al., 2010), and the observation that the phosphorylation status eventually recovers is consistent with long-term adaptation. The converse effects of water deficit and flooding/hypoxia are also consistent with the opposing effects of these environmental stimuli on the critical gas diffusion barrier of the nodule (Roberts et al., 2010). Hypoxia/flooding stimulates increased diffusion through the gas diffusion barrier (Hunt et al., 1987; Weisz and Sinclair, 1987; Parsons and Day, 1990) whereas water deficit/osmotic stress restricts diffusion through the barrier (Parsons and Day, 1990; Serraj et al., 1994; Del Castillo and Layzell, 1995). A potential role of nodulin 26 as an aquaglycero-ammoniaporin in regulating this process will be discussed further in the discussion section of this thesis.

To test further whether nodulin 26 phosphorylation is correlated with modulation of the gas diffusion barrier, the effects of culturing nodules in various

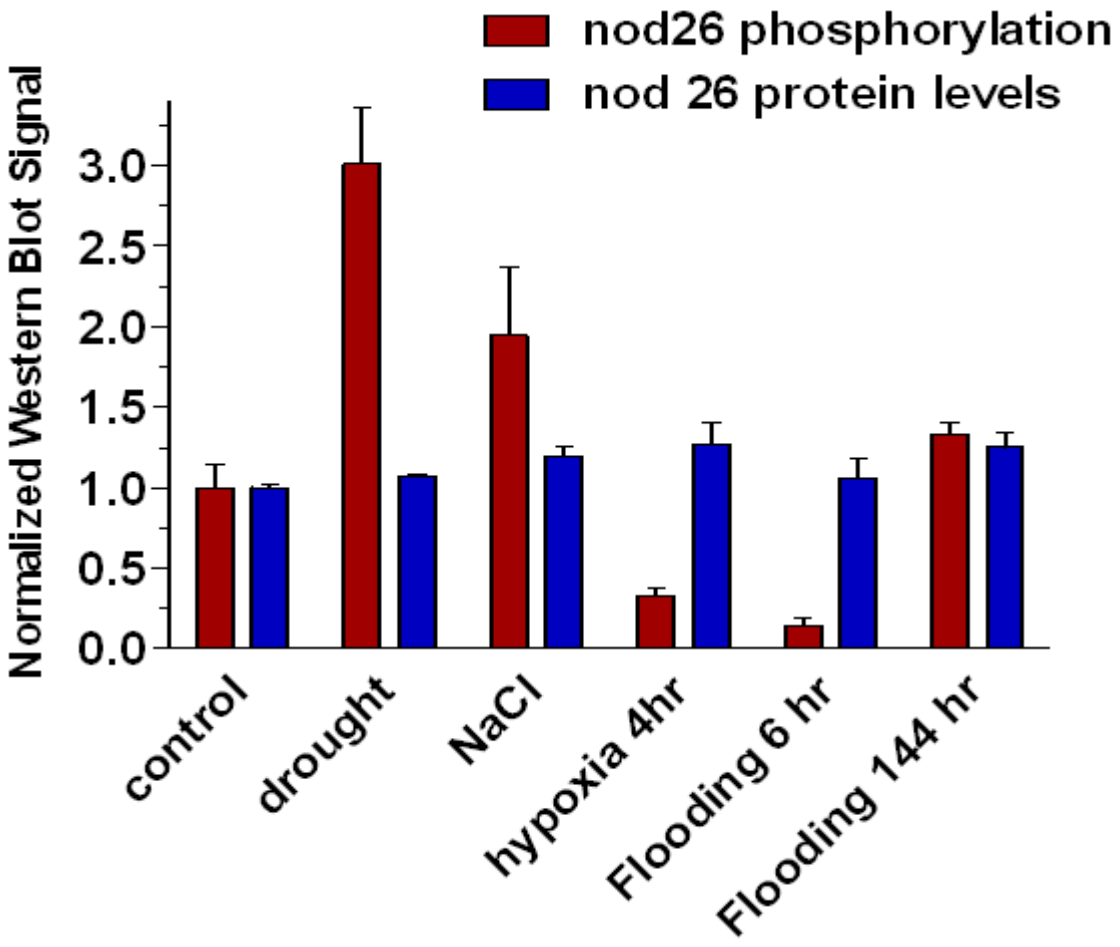

Figure 3.18. Comparison of nodulin 26 protein expression and its phosphorylation state under various environmental stimuli. Normalized Western blot signals of nodulin 26 protein (blue bars) and phosphorylation (red bars) state under osmotic stresses (drought and 0.2 M NaCl), flooding, and hypoxia were compared. Data was normalized to the average signal obtained by control plants. The error bars show the standard error of the mean of three replicates (*n*=3).

pO_2 concentrations was tested. Previous work shows that regulation of the gas diffusion barrier is inversely proportional to the pO_2 of the media. For example, sub-ambient pO_2 results in opening of the gas diffusion barrier to sustain respiration under hypoxia conditions (Weisz and Sinclair, 1987). In contrast, supra-ambient pO_2 restricts the gas diffusion barrier to block inactivation of nitrogenase (Weisz and Sinclair, 1987; King and Layzell, 1991).

Nodulated soybean plants were exposed to ambient, supra-ambient (50% O_2) and sub-ambient (2% O_2) oxygen for four hours. Exposure of nodulated roots with sub-ambient (2%) O_2 resulted in a decrease of phosphorylation of nodulin 26 consistent with the results of flooding, while supra-ambient (50%) O_2 enhanced the levels of nodulin 26 phosphorylation compared to ambient controls (Fig. 3.19). These results support the observation with environmental stress stimuli and suggest that phosphorylation of nodulin 26 is accompanied by conditions that lower gas/O_2 diffusion into the nodule core.

Oxygen sensing as a signal for the induction of *nodulin 26* expression

As suggested by its name, *nodulin 26* was first described as a gene that is induced as a part of the nodule developmental program in soybean (Fortin et al., 1987). However, although it is clear that nodulin 26 is expressed during nodule development, the developmental cues that trigger soybean *nodulin 26* (*GmNod26*) gene expression are still not understood. Unlike other nodulin genes, nodulin 26 has no nodule-specific *cis*-acting element and it has been

Figure 3.19. Expression and comparison of nodulin 26 and its phosphorylation state under different oxygen concentrations. 36 day-old nodulated soybean plants were treated with 2% or 50% oxygen for 4 hrs. **(A)** Membrane samples (20 μg/well) isolated from normoxic control, 2% O_2-treated and 50% O_2-treated soybean nodules were resolved by SDS-PAGE on 12% (w/v) polyacrylamide gels, and were analyzed by Western blot analysis for nodulin 26 protein content (by anti-Nod26) and phosphorylation state (by anti-phospho Nod26). **(B)** Densitometric analysis of the relative amounts of nodulin 26 protein and its phosphorylation state under different O_2 concentrations. The data were normalized to the average signal obtained by control plants. The error bars show the standard error of the mean of three biological replicates (*n*=3).

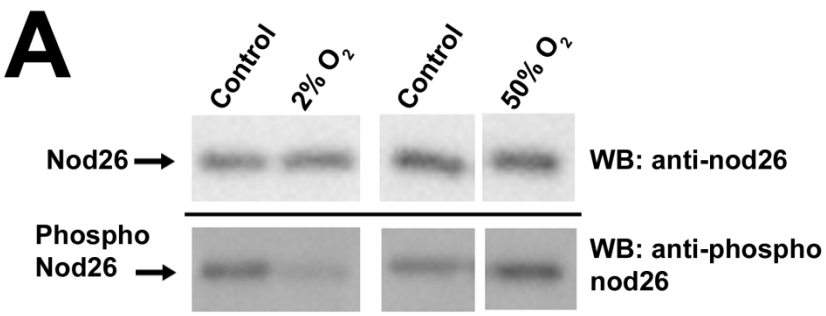
A
Control
2% O2
Control
50% O2
Nod26
WB: anti-nod26
Phospho Nod26
WB: anti-phospho nod26

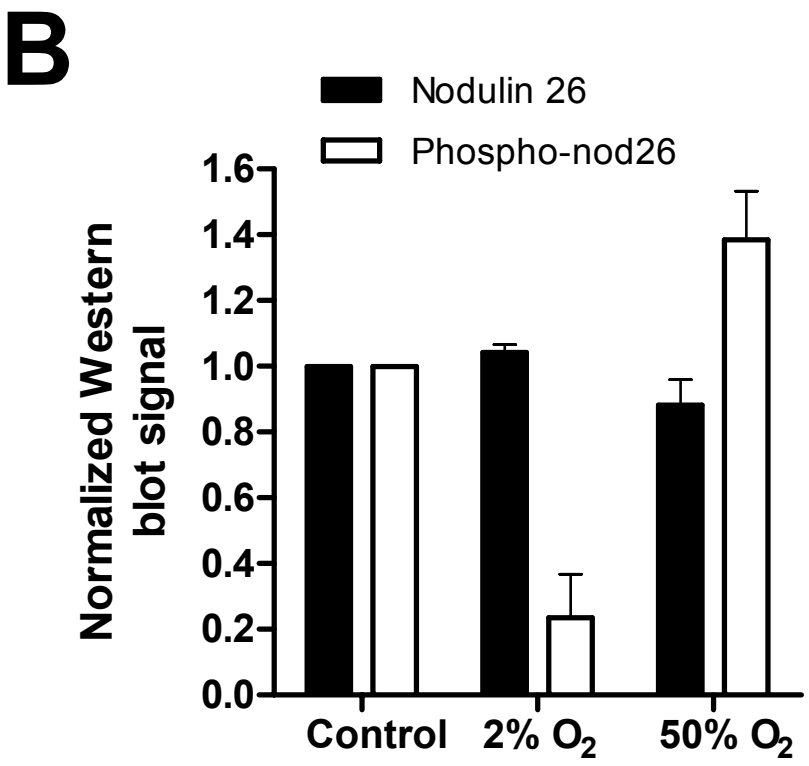
B
Nodulin 26
Phospho-nod26
Normalized Western blot signal
1.6
1.4
1.2
1.0
0.8
0.6
0.4
0.2
0.0
Control
2% O2
50% O2

suggested that the *nodulin 26* gene is controlled by a *trans*-negative regulatory element (Miao and Verma, 1993). It is important to determine which additional physiological regulatory factors and inducible cues regulate *nodulin 26* gene expression in a spatially and temporally regulated fashion during nodule development.

To determine whether specific regulatory motifs in promoter regions would affect *nodulin 26* expression, 1.5 kb genomic DNA sequences upstream of the coding region of the *nodulin 26* were analyzed. This resulted in discovery of the presence of four putative AREs (Anaerobic Response Elements) that could act as *cis*-acting regulatory elements (Dolferus et al., 2001) (Fig. 3.20). AREs are essential *cis*-acting elements for anaerobic induction of the anaerobic polypeptide genes. These 4 AREs which consist of "TGGTTT" are located in predicted promoter regions of the *nodulin 26* and are identical to the GT-motifs found in *Adh1* gene of *Zea mays* (Mohanty et al., 2005) and *AtNIP2;1* gene of *Arabidopsis* (Choi and Roberts, 2007), which are classic anaerobic response polypeptide genes (Sachs et al., 1996).

Nodule development is accompanied by the establishment of a microaerobic environment within the nodule core which is composed of the nitrogen fixing infected cells (Layzell et al., 1990). There has been also evidence showing that up-regulation of certain genes during nodule development is correlated with the establishment of low oxygen conditions, including several

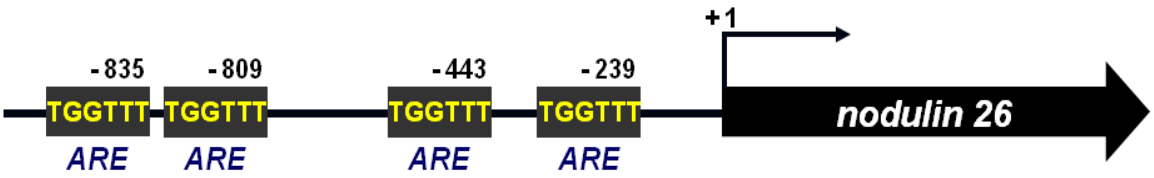

Figure 3.20. *In-silico* analysis of promoter regions of *nodulin 26* for identification of *cis*-acting anaerobic regulatory elements (AREs). Upstream regions of the soybean *nodulin 26* gene (Glyma08g12650.1) were obtained from the soybean genome database of phytozome (http://www.phytozome.net/soybean). The 1.5 kb-long genomic sequences were analyzed for ARE by web-based tool "PlantCARE," a database of plant cis-acting regulatory elements (http://bioinformatics.psb.ugent.be/webtools/plantcare/html) (Lescot et al., 2002). The black boxes represent AREs found in *nodulin 26* promoter regions. The numbers indicate the order of DNA base pairs of 3'-end in the black boxes, beginning from initiator ATG sequences.

transporter genes (Colebatch et al., 2004). Based on these observations, *nodulin 26* gene expression in response to low O_2 signals was investigated.

Nodulin 26 gene expression was analyzed by Q-PCR assay of unnodulated soybean root tissues under conditions of hypoxia induced by water logging (Fig. 3.21). The root portion of uninfected seedlings was completely submerged, and nitrogen gas (N_2) was supplied into the water during the flooding treatment to reduce dissolved O_2 content. The dissolved oxygen content of the media was measured and was consistently lower than 2.5% indicating establishment of hypoxic conditions (Table 2.1). Q-PCR analysis revealed that transcript level of *nodulin 26* increased 11.3-fold under flooding conditions compared to the 0 hour control (Fig. 3.21 A). The changes in *nodulin 26* expression reached a maximum at 1 hr after flooding and returned to basal levels after 12 hr-flooding (Fig. 3.21 A). As an indicator for anaerobic conditions, pyruvate decarboxylase (*GmPDC*) gene expression levels were investigated and showed the predicted increase under hypoxic flooding conditions (Fig. 3.21 B). The expression pattern of *GmPDC* is consistent with that of *nodulin 26*, suggesting that highly up-regulation of transcript levels of both *nodulin 26* and *GmPDC* are due to hypoxia induced by water logging.

The responsiveness of nodulin 26 to low O_2 was confirmed by direct induction of anaerobiosis using an anaerobic jar system. Q-PCR analysis revealed up-regulation of *nodulin 26* expression up to 13-fold under hypoxic conditions (Fig. 3.22 A). As an indicator for establishment of anaerobic

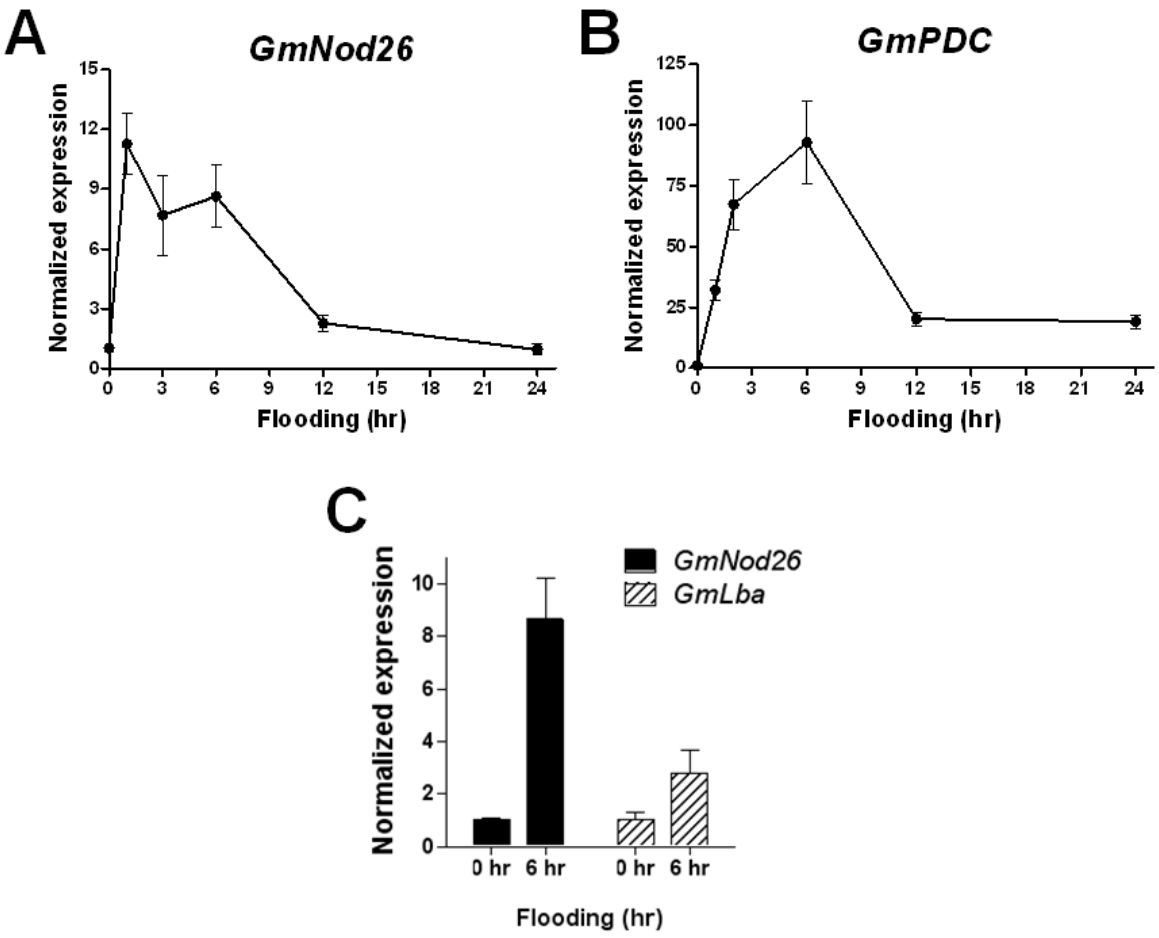

Figure 3.21. Q-PCR analysis of gene expression levels in root tissues under flooding stress. Uninfected 15 day-old soybean seedlings were subjected to flooding stress by complete submersion of roots in water under hypoxic conditions. **(A)** Expression analysis of *GmNod26*. **(B)** Expression analysis of *GmPDC*. **(C)** Comparison of normalized expression of *GmNod26* (closed bars) and *GmLba* (hatched bars) genes at 0 hr and 6 hr after flooding. The data were normalized to the transcript levels in 0 hr-normoxic control. The error bars indicate the SEM (*n*=5 to 6 for **A** and **B**, *n*=3 to 6 for **C**).

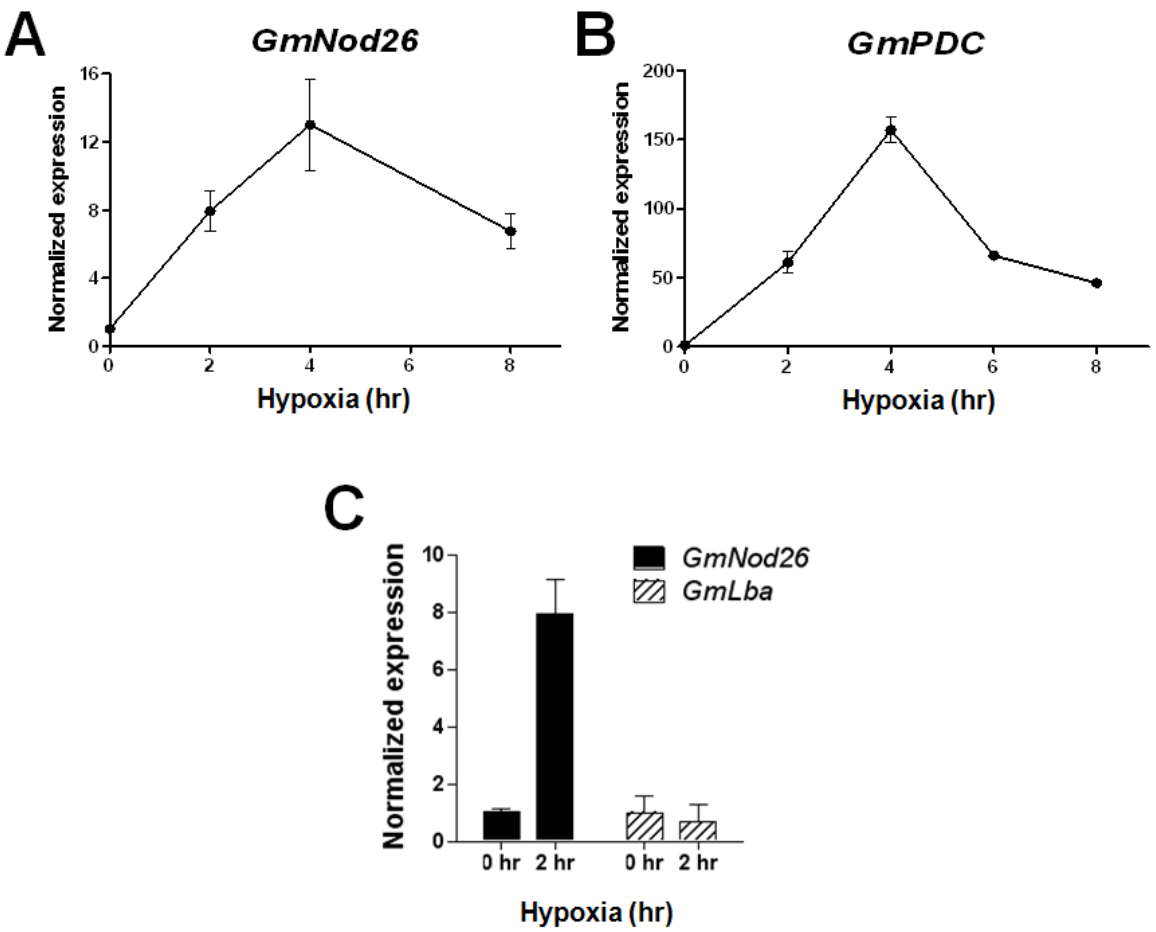

Figure 3.22. Q-PCR analysis of gene expression levels in root tissues under anaerobiosis. Uninfected 15 day-old soybean seedlings were subjected to anaerobic conditions by using anaerobic jars. **(A)** Expression analysis of *GmNod26*. **(B)** Expression analysis of *GmPDC*. **(C)** Comparison of normalized expression of *GmNod26* (closed bars) and *GmLba* (hatched bars) genes at 0 hr and 2 hr-hypoxia. The data were normalized to the gene expression levels in 0 hr-normoxic control nodules. The error bars indicate the SEM (*n*=3 to 6).

environment, *GmPDC* was investigated (Fig. 3.22 B). An increase in *GmPDC* expression corresponds to up-regulation of *GmNod26* transcripts, suggesting that soybean root tissues were under hypoxic conditions (Fig. 3.22 B).

Leghemoglobin (*GmLba*) is a classical late nodulin gene that is exclusively up-regulated during nodule organogenesis and development in soybean (Marcker et al., 1984). Gene expression of *GmLba* is controlled by two *cis*-acting regulatory elements (She et al., 1993), and the *GmLba* contains 2 AREs at their promoters within 1.5kb. Q-PCR analysis showed that flooding results in a small up-regulation of *GmLba* transcript (Fig. 3.21 C) whereas hypoxia showed no apparent induction of *GmLba* (Fig. 3.22 C).

Overall, these data confirmed that *nodulin 26* is up-regulated under conditions of hypoxia/anoxia, suggesting the hypothesis that low O_2 environment could be a signal that induces *nodulin 26* expression. This differs from other late nodulin genes such as *GmLba* which have other developmental signals and cues.

CHAPTER IV

DISCUSSION

The present research project provides new insight into the functional transport and regulatory properties of soybean nodulin 26 in symbiotic nitrogen-fixing nodules. Observations provide evidence that nodulin 26 is an "aquaglycero-ammoniaporin" that is specifically localized to the SM, the symbiotic interface between the plant host and the bacteroid symbiont, where it could play a potential role in osmoregulatory and metabolic functions in the symbiosis. First, purified nodulin 26 reconstituted into liposomes possesses ammonia (NH_3) transport activity with a low activation energy (E_a = 38.3 kJ/mol) and a high single channel conductance (p_{NH3} = 1.27 ± 0.06 x 10^{-14} cm^3/subunit/s, n=3). Second, nodulin 26 serves as a docking site for cytosolic glutamine synthetase on the surface of the symbiosome membrane, and could assist fast assimilation of fixed NH_3. As discussed further below, this could prevent ammonia toxicity and futile cycling. Third, phosphorylation of nodulin 26 exerts opposite effects on the regulation of ammonia and water transport activities. Additionally, phosphorylation of nodulin 26 in mature N_2-fixing nodules is tightly controlled by various environmental osmotic stimuli associated with the rate of N_2-fixation as

well as modulation of the oxygen diffusion barrier inside nodules, suggesting regulation of its channel activity and selectivity during these conditions.

Ammonia permease activity of soybean nodulin 26

Based on the similar properties in molecular volume between water (12.4 cm^3/mol) and NH_3 (13.8 cm^3/mol) and the similarities in their dipole moments (1.471 D for NH_3 and 1.854 D for H_2O), it could be suggested that aquaporins in general should transport both NH_3 and water. However, previous studies of the transport selectivities of several aquaporins show that this is not true, and they have the ability to select for water or ammonia transport based on the amino acids comprising the ar/R selectivity filter (Holm et al., 2005; Beitz et al., 2006; Dynowski et al., 2008). The ar/R region is composed of four amino acids forming the narrowest constriction within the pore and determines the selectivity of MIP/aquaporin channels. The importance of the ar/R pore has been emphasized for the determination of selectivity and transport activity of all plant aquaporins (Wallace and Roberts, 2004; Ludewig and Dynowski, 2009).

In a previous study, molecular dynamics simulations followed by experimental observations were performed on various site directed mutants of the water-specific aquaporin, AtPIP2;1, to determine which ar/R residues determine NH_3 versus water transport (Dynowski et al., 2008). The results showed that several NIP-like mutants of both the NIP I and NIP II ar/R subclasses exhibit the ability to complement yeast ammonia auxotrophs

suggesting that MIPs could potentially flux ammonia (Dynowski et al., 2008). In the present study, it is shown that purified soybean nodulin 26 possesses facilitated transport activity for NH_3 and reveals an approximately four-fold stronger preference for this substrate over water. Additionally, the use of purified nodulin 26 liposomes allowed a determination of the single channel rate (p_{NH3}) for ammonia transport. The calculated p_{NH3} of nodulin 26 (1.27×10^{-14} cm^3/s) is comparable to the value obtained by another ammonia transporting aquaporin, *Rattus norvegicus* AQP8 (rAQP8) ($p_{NH3} = 2.7 \times 10^{-14}$ cm^3/s) (Saparov et al., 2007). The single channel NH_3 transport activity (p_{NH3}) provides an estimation of the amount of ammonia that each nodulin 26 monomer is able to transport per unit time. Provided that one monomeric nodulin 26 has one transport channel, the single channel conductance for NH_3 transport corresponds to a permeability of 3×10^8 NH_3 molecules per channel per second.

What features of the nodulin 26/NIP I ar/R allow ammonia transport? The ar/R region of nodulin 26 consists of Trp (H2), Val (H5), Ala (LE_1) and Arg (LE_2), which are distinct from water-specific AQP1 (Phe (H2), His (H5), Cys (LE_1) and Arg (LE_2)) (Fig. 4.1). These substitutions in nodulin 26 result in a more hydrophobic and wider pore which previously has proposed to allow the transport of larger solutes (including glycerol) (Wallace et al., 2002; Wallace et al., 2006).

The ar/Rs of nodulin 26 (WVAR) (Wallace and Roberts, 2004) and other NH_3 transport MIPs, such as rat AQP8 ar/R (HIAR) and human AQP8 ar/R (HIGR) (Liu et al., 2006) shows that compared to water-selective AQP1, they

Figure 4.1. Membrane topology of the soybean nodulin 26 and architecture of the ar/R selectivity region. (A) Topology of the soybean nodulin 26 is represented with the regions predicted to form the ar/R tetrad highlighted in red within yellow-background boxes. Six helical transmembrane spanning domains are connected by 5 loop compartments (A - E). NPA motifs from each loop B and E region are indicated by blue within light-yellow boxes, which form a seventh pseudo transmembrane domain. A nodulin 26 phosphorylation site which is located at C-terminal Ser262 is highlighted in red with an asterisk (*). **(B)** Comparison of the ar/R selectivity filters of AQP1, nodulin 26, and TIP2;1 and AQP8. Residue side chains are indicated by color codes with blue for basic hydrophilic, yellow for hydrophobic, and white for neutral hydrophilic. AQP1 is shown with water molecule (sky blue) bound. The AQP1 model is based on the crystal structure (PDB: 1J4N) of Sui et al. (2001), while nodulin 26 and TIP2;1 ar/R are based on homology modeling (Wallace and Roberts, 2004).

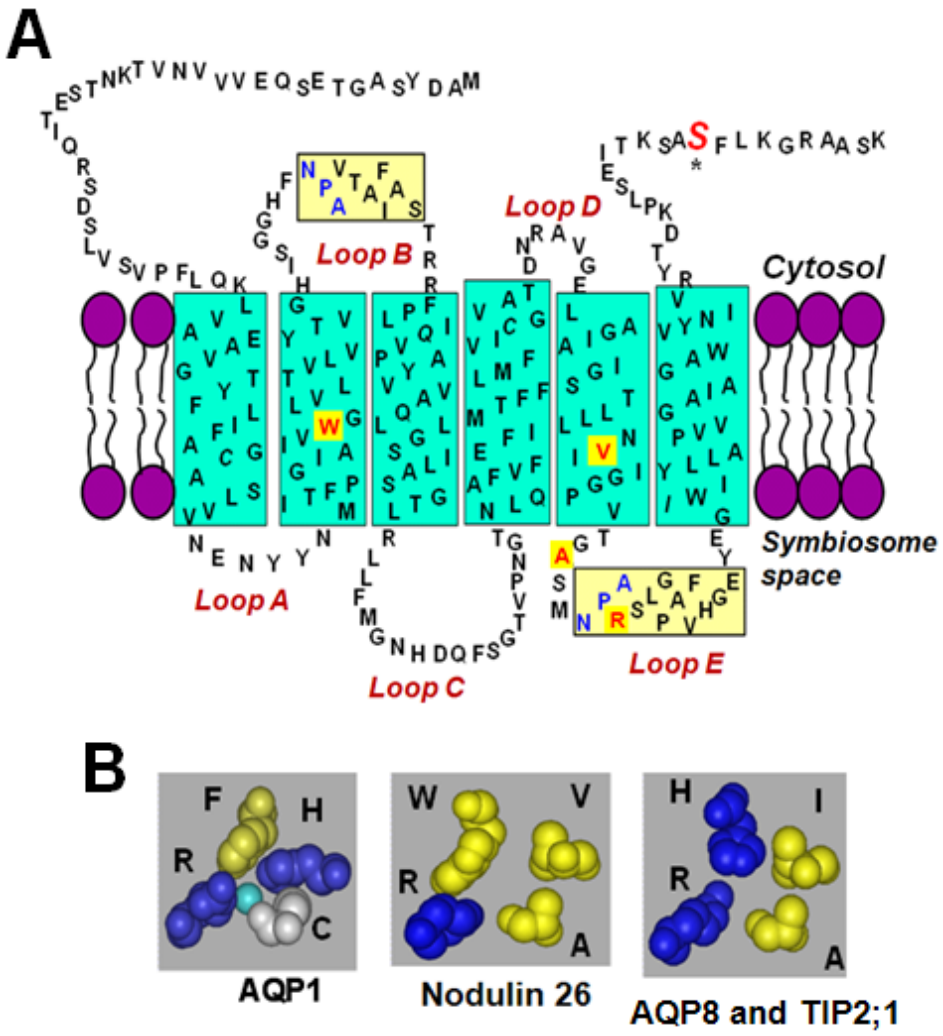
A
Loop A
Loop B
Loop C
Loop D
Loop E
Cytosol
Symbiosome space
B
AQP1
Nodulin 26
AQP8 and TIP2;1

share a small hydrophobic residue (Val or Ile) at H5 rather than His which is characteristic of water-selective aquaporins (Sui et al., 2001). Similarly, wheat TIP2;1, which also exhibits ammonia transport properties (Jahn et al., 2004), shares identical ar/R residues (His (H2), Ile (H5), Ala (LE_1) and Arg (LE_2)) with AQP8 (Fig. 4.1 B). How the structural features of these ar/R residues allow NH_3 permeability in these subclasses of MIP proteins remains unresolved.

Functional aspects of nodulin 26 associated with fixed-NH_3 flux on the symbiosome membrane in the soybean nodule

In previous work by Niemietz and Tyerman, a Hg^{2+}-sensitive facilitated NH_3 transport activity was detected in soybean SM vesicles, and it was proposed to constitute a protein-based NH_3 efflux pathway across the symbiosome (Niemietz and Tyerman, 2000). Soybean nodulin 26 is a SM-specific nodulin protein and constitutes a large portion of total protein mass of this specialized membrane (Fortin et al., 1987; Weaver et al., 1991; Rivers et al., 1997). Based on the high concentration of nodulin 26 on the symbiosome membrane and the calculated single channel rate for NH_3 transport (p_{NH3}), NH_3 movement through nodulin 26 can account for the measured NH_3 flux across the symbiosome membrane (Hwang et al., 2010).

Based on previous work and the present findings, soybean nodulin 26 appears to be the principal protein on the SM responsible for water and NH_3 permeabilities. With respect to ammonia permeability, it is attractive to propose a

role for nodulin 26 as a potential efflux pathway for fixed NH_3 from the symbiosome. The efflux of fixed nitrogen from the symbiosome space to the infected cell cytosol can occur by one of two potential pathways (Fig. 4.2): (1) NH_4^+ efflux by an inwardly rectified, voltage-activated nonselective cation channel (NSCC) (Tyerman et al., 1995) (Fig. 4.2 A); or (2) NH_3 efflux facilitated by nodulin 26 (Fig. 4.2 B). The relative contribution of these pathways depends upon the concentration gradient of NH_4^+ and NH_3, and the pH of the symbiosome space and cytosolic compartments, as well as the resting potential of the symbiosome membrane (Niemietz and Tyerman, 2000). These parameters are controlled by the activity of an energizing H^+-pumping ATPase on the membrane (Udvardi and Day, 1989) (see Fig. 4.2). For example, when a highly active H^+-ATPase hyperpolarizes and acidifies the symbiosome space this would favor efflux of fixed nitrogen in the form of charged NH_4^+ by voltage-dependent activation of the NSCC (Tyerman et al., 1995). In contrast, low ATPase activity would result in reduced SM potential and higher pH of the symbiosome space, which would lead to a higher NH_3/NH_4^+ concentration ratio and a closed NSCC which would favor NH_3 efflux via nodulin 26 across the symbiosome membrane.

One potential issue with having two pathways of NH_4^+/NH_3 movement across the SM is the issue of toxicity, which is a potential outcome of wasteful "ammonia futile cycling" (Britto et al., 2001). During active nitrogen fixation, charged NH_4^+ accumulates in the acidic symbiosome space (Streeter, 1989). Movement of the NH_4^+ into the more alkaline cytosolic compartments, however,

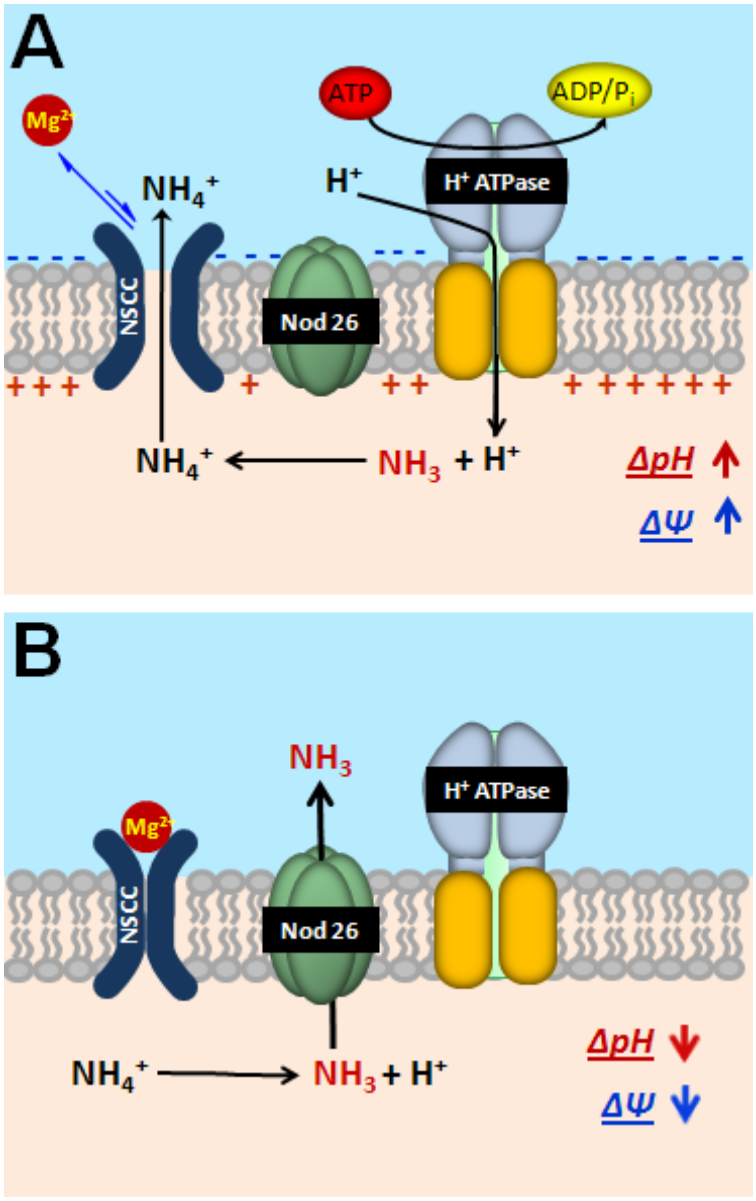

Figure 4.2. Two different pathways of fixed ammonia/ammonium efflux on symbiosome membrane. (A) H^+-ATPase pump hyperpolarizes the SM which leads to voltage activation of NSCC which transports ammonium ion (NH_4^+) into the infected cell cytosol. **(B)** Nodulin 26 would provide a facilitated NH_3 transport path when NSCC is closed.

causes deprotonation and generation of uncharged NH_3, a substrate which can reenter back to the symbiosome space via nodulin 26 (Fig. 4.3). As a result, such a repetitive pathway would result in futile cycling, waste ATP, and dissipate the SM proton motive force. One potential mechanism to prevent futile cycling would be to facilitate rapid NH_3/NH_4^+ assimilation in the cytosol to block back diffusion of NH_3. As discussed next section, nodulin 26 interaction with cytosolic glutamine synthetase may be a mechanism to prevent futile cycling.

Significance of the interaction of soybean nodulin 26 with cytosolic nodule glutamine synthetase

The role of cytosolic glutamine synthetase (GS_1) in nodules is to serve as the first step in the nitrogen assimilatory pathway by catalyzing the rapid incorporation of fixed NH_3 onto the amino acid glutamate by the following reaction (Miflin and Habash, 2002):

$$\mathbf{ATP + NH_4^+ + glutamate \rightarrow ADP + P_i + glutamine}$$

The significance of GS interaction with nodulin 26 is that the nodulin 26 can serve to localize GS to the surface of the symbiosome membrane. Thus, with respect to two principal roles of nodulin 26 as (1) a facilitated NH_3 transporter and (2) a docking site for GS localization on the SM, a potential model mechanism for interaction of nodulin 26 and GS and its role in nitrogen assimilation is proposed (Fig. 4.4) (Masalkar et al., 2010). The specific interaction of GS with nodulin 26 would aid in the rapid assimilation of reduced

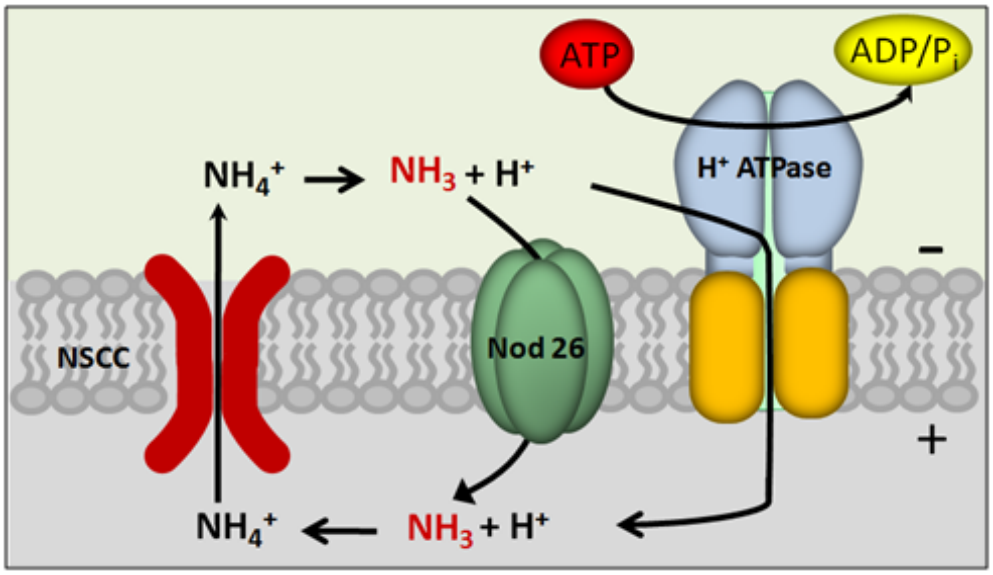

Figure 4.3. Model for NH_4^+/NH_3 futile cycling on the SM. A potential mechanism for ammonia futile cycling through the symbiosome membrane is shown. The symbiosome membrane is energized by an H^+-ATPase which generates a proton gradient by pumping H^+ into the symbiosome space. When the symbiosome membrane is hyperpolarized, the NSCC is activated which directionally transports NH_4^+ into the cytosolic compartment. Since the cytosol is more alkaline than the symbiosome space, NH_4^+ can release a H^+ with NH_3 potentially reentering the symbiosome space through nodulin 26. Maintenance of cytosolic NH_4^+ levels at low concentrations by rapid assimilation via GS would be one approach to prevent this potential metabolite cycling. This figure is taken from Masalkar et al. (2010).

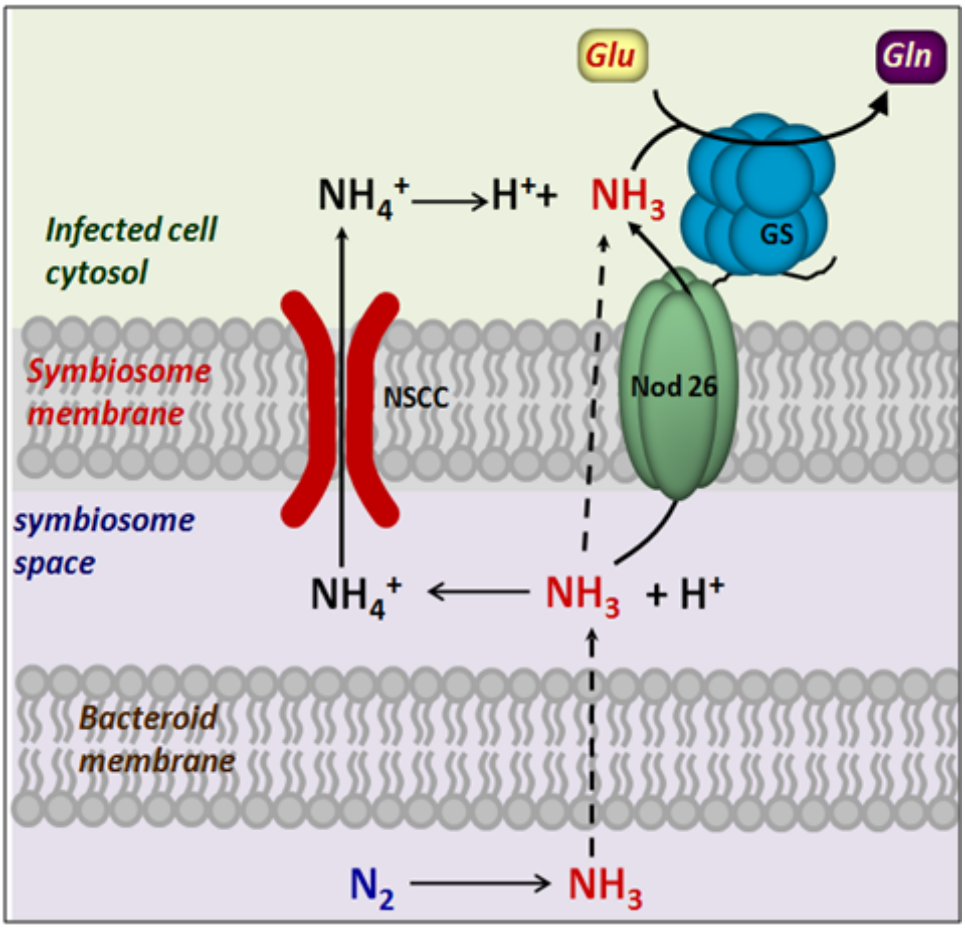

Figure 4.4. Metabolic model for interaction of nodulin 26 and glutamine synthetase and its effect on nitrogen assimilation in nitrogen-fixing nodules. A model for efflux and assimilation of fixed nitrogen in symbiosomes is shown. Three distinct efflux pathways for fixed NH_3/NH_4^+ are represented. Ammonia produced by the action of nitrogenase in the bacteroid moves into the symbiosome space by simple diffusion. NH_4^+ efflux mediated by a non-selective cation channel (NSCC) which is voltage-activated and is inwardly rectified. NH_3 efflux either facilitated by nodulin 26 or diffusive through symbiosome membrane. Binding of glutamine synthetase (GS) to the C-terminal domain increases the concentration of this assimilatory enzyme at the symbiosome surface and also serve as a potential site for rapid assimilation of ammonia traversing nodulin 26. This figure is taken from Masalkar et al. (2010).

nitrogen in the form of uncharged NH_3, which is facilitated through the nodulin 26 channel. Thus, nodulin 26 can be described as a metabolic funnel that couples the transport of fixed nitrogen from the symbiosome and its assimilation in the host cytoplasm (Fig. 4.4). In addition, the rich density of nodulin 26 on the SM could in turn lead to a pronounced localization of GS to the surface of the symbiosome, thus enhancing the rate of NH_3/NH_4^+ assimilation, even if transport occurs through other efflux pathways such as the NSCC (Masalkar et al., 2010).

Thus, the interaction of nodulin 26 with GS could facilitate rapid NH_4^+ assimilation, preventing its accumulation in the cytosol. The maintenance of low cytosolic concentrations of NH_4^+, which are estimated to be 50-fold lower than the NH_4^+ concentration in nitrogen-fixing symbiosomes (Streeter, 1989), would prevent potential futile cycling.

Phosphorylation-dependent regulation of nodulin 26 transport activity

Even before its functional characterization as an aquaglyceroporin (Rivers et al., 1997; Dean et al., 1999), nodulin 26 was first characterized as a SM specific protein that is a major phosphorylation substrate of a SM-associated Ca^{2+}-dependent protein kinase (Weaver et al., 1991; Weaver and Roberts, 1992). Phosphorylation occurs specifically at a single serine, Ser262 within a C-terminal cytosolic domain (Weaver and Roberts, 1992). Analysis of phosphorylation of Ser262 of nodulin 26 *in vivo* shows that it accompanies maturation of the nodule and the onset of nitrogen fixation and is maintained at a

steady state throughout the lifetime of nodule until senescence (Guenther et al., 2003). As discussed in the next section, phosphorylation of nodulin 26 is also very sensitive to environmental and osmotic cues. Overall, it appears as if the protein is a target for calcium-dependent regulation in response to developmental and environmental cues.

What are the effects of phosphorylation on nodulin 26 function? Previous work with other MIPs shows that they can be a common target for posttranslational regulation by phosphorylation. The effects of phosphorylation on transport activity appear to differ from the stimulation of water transport in the case of plants MIPs such as *Pv*TIP3;1 (α-TIP) (Maurel et al., 1995), *So*PIP2;1 (PM28A) (Johansson et al., 1998; Tornroth-Horsefield et al., 2006; Nyblom et al., 2009) and in the case of human AQP2 (Eto et al., 2010), to inhibition of channel activity in AQP4 (Han et al., 1998; Zelenina et al., 2002). In addition, phosphorylation of MIPs has been shown to regulate the water permeability by affecting the membrane localization and trafficking in plant (e.g., *At*PIP2;1 (Prak et al., 2008)) and mammalian cells (e.g., AQP4 (Madrid et al., 2001) and AQP2 (Fushimi et al., 1997)).

However based on the present study, and unlike those cases above, phosphorylation of the soybean nodulin 26 multifunctional aquaglycero-ammoniaporin exerts a dual function which modulates both transport rate and selectivity of permeant molecules. Phosphorylation of nodulin 26 results in approximately 2.3-fold stimulation of P_f compared with a dephosphorylated SM.

This is consistent with previous observations (Guenther et al., 2003) and suggests that phosphorylation stimulates the intrinsic water permeability of the protein, similar to positive gating influences of phosphorylation on some aquaporins (Maurel et al., 1995; Johansson et al., 1998; Tornroth-Horsefield et al., 2006; Nyblom et al., 2009; Eto et al., 2010). However, in contrast, phosphorylation of nodulin 26 inhibits NH_3 transport activity by 2.5-fold. The regulation of nodulin 26 selectivity by posttranslational phosphorylation observed in the present study is significant from two perspectives: (1) The ratio of phosphorylated to unphosphorylated nodulin 26 modulates the selectivity of nodulin 26 on the SM in response to environmental cues, which can be directly assayed by determining the P_{NH3}/P_f of isolated SM vesicles (e.g., see Fig. 3.17); and (2) This dual function of phosphorylation in the differential regulation of two distinct transporting molecules is a unique property that has not been previously reported for any other aquaporins or aquaglyceroporins.

The site of phosphorylation of nodulin 26 is serine 262 (Fig. 4.1), a conserved site for type I NIPs which is found in the hydrophilic carboxyl terminal domain facing the cytosol (reviewed in Wallace et al., 2006). A number of aquaporins are phosphorylated within this region (Hoffert et al., 2006; Kadohira et al., 2008; Prak et al., 2008). As described above the effects of phosphorylation on aquaporin function is varied, and can affect trafficking within the cell as well as activity. Less certain is how the phosphorylation of the C-terminal domain could affect the selectivity of the nodulin 26 channel.

A molecular basis for the effects of phosphorylation on aquaporin gating comes from structural and computational analyses of the plant PIP protein SoPIP2;1 (Tornroth-Horsefield et al., 2006; Nyblom et al., 2009). SoPIP2;1 is proposed to be phosphorylated at two sites, one (Ser274) within the C-terminal domain analogous to nodulin 26, and a second site (Ser115) in loop B (see topology nomenclature in Fig. 4.1). Based on structural and MD simulation analyses, SoPIP2;1 can exist in two conformations, an open and a closed state (Tornroth-Horsefield et al., 2006). The closed state is stabilized by folding of loop D over the pore entrance on the cytosolic side. Phosphorylations of serine residues in both the cytosolic C-terminal and loop B regions lead to interactions with loop D resulting in opening of the channel pore and enhancing water transport activity. In the case of the C-terminal phosphoserine 274, interaction and regulation is predicted to occur “in trans” with the C-terminal domain of one subunit interacting with loop D of an adjacent subunit (Nyblom et al., 2009). While the structural details of the nodulin 26 pore and disposition of the loop regions remain undermined, one could hypothesize that phosphorylation of nodulin 26 on the C-terminal serine could interact in a similar fashion affecting solute transport.

Even more uncertain is how phosphorylation could promote water flux while inhibiting ammonia permeability. As noted above, ammonia selectivity of plant aquaporins was proposed to be dependent upon amino acid residues comprising ar/R constriction filter and also other regions of the pore (Dynowski et

al., 2008). However, it is not clear how phosphorylation could alter the pore structure in a manner that would promote water transport while simultaneously inhibiting ammonia transport. High resolution structural analyses of phosphorylated and unphosphorylated nodulin 26 are needed to provide insight into the mechanism of how the phosphorylation of nodulin 26 conversely regulates transport between water and ammonia.

Regulation of nodulin 26 phosphorylation and O_2 diffusion in the soybean nodules in response to environmental stimuli

The functional transport studies performed in this research raise the question: What signals modulate nodulin 26 phosphorylation, and how is this associated with nodule physiology? Nodulin 26 phosphorylation can be regulated by various environmental conditions which influence N_2-fixation activity and respiration in nodules, while protein expression remains unchanged (Fig. 3.14 to 3.16). Nodulin 26 is hyperphosphorylated on serine 262 in response to osmotic stresses such as drought and salinity. In contrast, flooding and hypoxia induces a rapid dephosphorylation, which is restored over time as the plant system adapts to long-term flooding conditions (Fig. 3.15). To understand the significance of these observations, the differential effects of these stresses on nodule physiology and oxygen diffusion need to be considered.

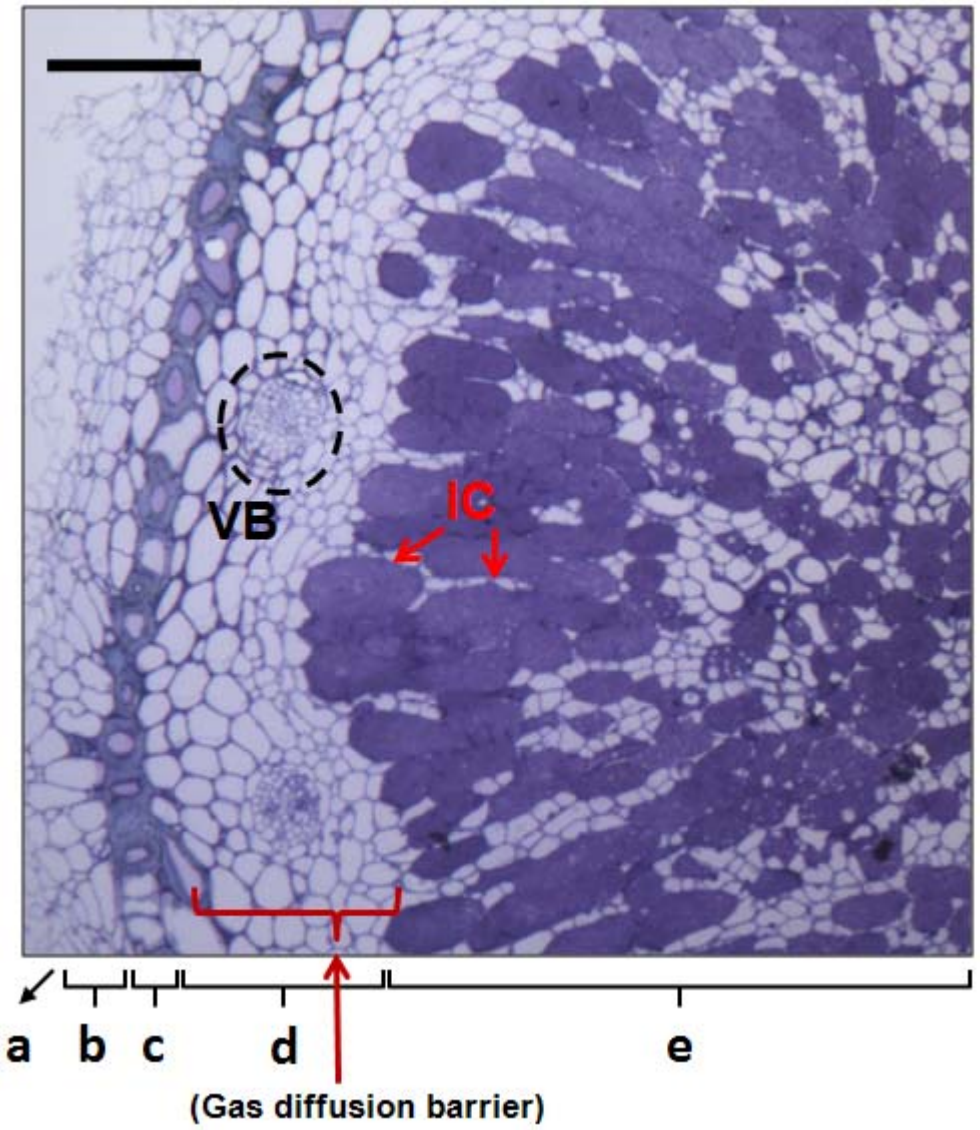

Figure 4.5. Morphology of a mature soybean nodule. Nodule tissue of 35 days old soybean was fixed and sectioned as described in Materials and Methods. Low magnification light micrograph of a nodule. Size bar = 100 µm. **a,** periderm; **b**, outer cortex; **c**, scleroid layer; **d**, inner cortex (including vascular bundle, VB); **e**, central infected zone. The region of the gas diffusion barrier is indicated by a dark red arrow. Enlarged polyploid infected cells (IC) are indicated by red arrows.

The gas diffusion barrier in nodules: To avoid the deleterious effect of free oxygen on bacterial nitrogenase, the central infected zone of the soybean nodule is maintained at a microaerobic state under normal N_2 fixing conditions (approximately 20 nM O_2 concentration, (Layzell et al., 1990)). The nodule has unique structural features that limit gas diffusion which are necessary for the establishment and maintenance of micro aerobic environment (Parsons and Day, 1990; Minchin, 1997). The determinate soybean nodule is mainly composed of a central infected zone which contains the infected cells that contain nitrogen-fixing symbiosomes. This zone is surrounded by a vascularized cortical region containing a scleroid layer (Fig. 4.5). The nodule cortex is a layered tissue comprising a continuous suberized outer boundary, along with an endodermal zone and inner-layers which surround the central infected zone (Dakora and Atkins, 1989; Brown and Walsh, 1994). The inner cortex region found in close proximity to the infected zone consists of relatively smaller cells with restricted intercellular spaces (Witty et al., 1987; Parsons and Day, 1990; Brown and Walsh, 1994).

Measurement of the partial oxygen pressure (pO_2) across the inner structure of the nodule by using an oxygen microelectrode indicated that the oxygen concentration abruptly decreases through the inner cortex region (Tjepkema and Yocum, 1974; Witty et al., 1987). Thus, the inner cortical tissue has been considered to play a role as the main boundary of the gas diffusion barrier inside the nodules (Fig. 4.5). The gas diffusion barrier was proposed to

regulate permeation of O_2 and N_2 into the nodule core as well as CO_2 and H_2 efflux from this region (Sheey et al., 1983; Hunt and Layzell, 1993; Bergersen, 1997; Minchin, 1997; Minchin et al., 2007).

Regulation of the gas diffusion barrier: The osmoregulatory hypothesis: This microaerobic state is dynamic and is maintained and regulated by modulation of O_2 diffusion into the infected zone through the diffusion barrier in response to environmental changes. This in turn regulates the rate of nitrogen fixation by restriction pO_2 and respiratory rates (Hunt and Layzell, 1993).

For instance, under conditions of osmotic stress (water deficit by drought or salinity) nodules reduce O_2 permeability by restriction of the gas diffusion barrier which in turn limits N_2-fixation (Serraj and Sinclair, 1996; Serraj et al., 1999). This may help conserve energy under stress conditions. A similar effect of metabolic signals (low sugar or nitrate) that reduce N_2-fixation has been observed on the gas diffusion barrier (Vessey et al., 1988; Matamoros et al., 1999). Reduction in gas diffusion is accompanied with rapid decrease in intercellular spaces of the inner cortex and infected zone of the nodule (Parsons and Day, 1990; Serraj et al., 1994; Del Castillo and Layzell, 1995; Serraj et al., 1995). High supra-ambient O_2 concentrations have the same effect, presumably to keep pO_2 in the infected zone at an optimal level to allow respiration while preventing nitrogenase inactivation (Hunt et al., 1987; Weisz and Sinclair, 1987; King et al., 1988; Parsons and Day, 1990).

In contrast, under conditions of O_2 deprivation (flooding or hypoxia), in order to support proper O_2 supply and sustain N_2-fixation activity, the gas diffusion barrier along with expansion of intercellular gas-filled spaces enhances gas permeability through the inner cortex into the infected zone of the nodule core (Hunt et al., 1987; Weisz and Sinclair, 1987; Parsons and Day, 1990; Roberts et al., 2010).

To explain the observations of reversible regulation of O_2 permeability in nodules, an osmoregulatory hypothesis was proposed (Purcell and Sinclair, 1994; Denison and Kinraide, 1995; Wei and Layzell, 2006). In this model, the gas diffusion pathway is regulated by reversible osmotically-driven uptake and release of cellular water into the intercellular spaces, as well as changes to cell geometry, which collectively constrict or expand the intercellular space and gas diffusion (Purcell and Sinclair, 1994; Denison and Kinraide, 1995; Wei and Layzell, 2006). Wei and Layzell proposed a specific model for the control of O_2 diffusion into the nodule infected zone, which can be established by coupled movement of K^+ and water (Wei and Layzell, 2006). Stimuli such as water deficit stresses activate K^+ currents (Denison and Kinraide, 1995), which result in efflux of K^+ to the apoplast of the cells in the infected zone. Accumulation of high interstitial [K^+] causes water to move into the intercellular spaces, and thereby restricts the rate of O_2 diffusion into the central zone (Fig. 4.6 A). In contrast, stimuli such as flooding and hypoxia cause the opposite effect with influx of K^+ and water from the apoplast to the cell cytoplasm, and increasing the gas-filled

Figure 4.6. Osmotic and metabolic regulatory model in infected cells of soybean nodules in response to environmental stimuli. A model for osmotic regulation of nodulin 26 in infected cells is shown. **(A)** Under conditions of osmotic stress (drought or salinity) enhanced water channel activity of nodulin 26 by phosphorylation through Ca^{2+} activation of CDPK contributes to bulk flow of water into the intercellular gas-filled spaces, which coincides with movement of K^+. As a result, the flooded-interstitial spaces restrict O_2 diffusion and O_2 permeability to central infected zone of the soybean nodules. Although not shown, nodulin 26 could also affect transcellular flow of water through infected cells, similar to the proposed role of TIPs in vacuoles in other plant cells (Maurel et al., 2008). **(B)** A model for metabolic regulation of nodulin 26 in response to O_2 deficit stress (flooding/hypoxia). External low O_2 availability results in dephosphorylation of nodulin 26 and metabolism shift of the cells to fermentation producing less ATP. The reduction of free ATP decreases H^+-ATPase activity, consequently increasing pH of symbiosome space. Under these conditions, dephosphorylation of the nodulin 26 enhances its NH_3 efflux activity, while NH_4^+ efflux *via* NSCC is down-regulated.

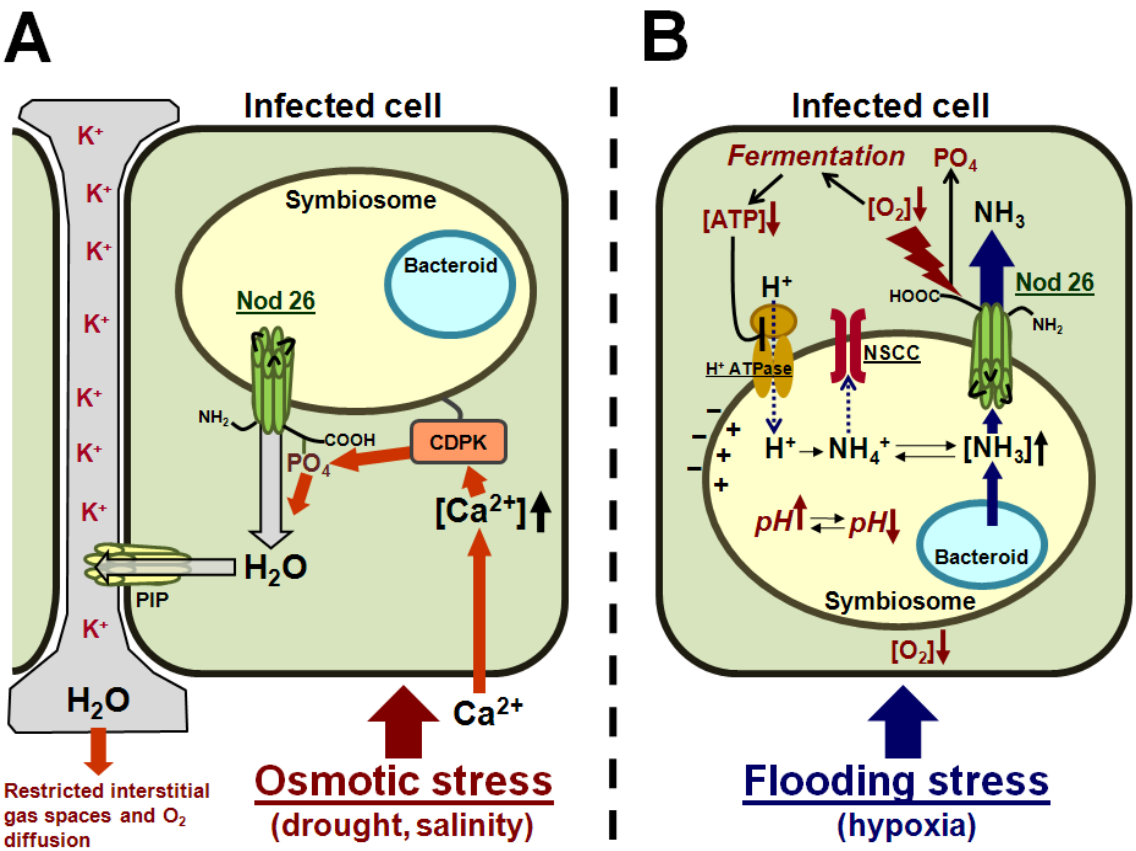
A
Infected cell
K+
Symbiosome
Bacteroid
Nod 26
NH2
COOH
CDPK
PO4
[Ca2+]
H2O
PIP
Ca2+
Restricted interstitial gas spaces and O2 diffusion
Osmotic stress
(drought, salinity)
B
Infected cell
Fermentation
PO4
[ATP]
[O2]
NH3
H+
HOOC
Nod 26
NH2
H+ ATPase
NSCC
H+ → NH4+ ⇌ [NH3]
pH ⇌ pH
Bacteroid
Symbiosome
[O2]
Flooding stress
(hypoxia)

intercellular spaces and O_2 permeability into the nodule infected zone. Water movement between the symplast and the apoplast is in the direction of decreasing water potential driven by K^+ movement between the infected cells and cortical cells, and the intercellular spaces.

Nodulin 26 in osmoregulation and metabolic regulation of the soybean nodule infected cells: As part of the osmoregulatory model, aquaporins have been proposed to aid in directional bulk flow of water in response to ionic osmotic signals (Fleurat-Lessard et al., 2005). With respect to high concentration on the SM (10 to 15% of total protein mass) (Weaver et al., 1991; Dean et al., 1999), nodulin 26 is suggested to be responsible for high water permeability of the symbiosome (osmotic water permeability of the symbiosome, $P_f \geq 0.05$ cm/sec). Since the symbiosomes occupy most of the space in the nonvacuolated infected cell, the symbiosome may play a potential role in the osmoregulation of the infected cell similar to the role of central vacuole in other plant cells (Maurel et al., 2008). Nodulin 26, which is responsible for the high P_f of the symbiosome, would be expected to potentiate this osmoregulatory function by mediating the rapid flux of water to facilitate cytosolic osmotic adjustment of infected cells in response to various environmental cues, and could aid in bulk water flow as part of the osmoregulatory model described in the previous section.

A new working model for this process is proposed (Fig. 4.6 A). Under conditions of normal nodule physiology, nodulin 26 maintains water homeostasis (osmosis) or metabolic NH_3 transport of the symbiosome in infected cells. Under

these conditions, nodulin 26 phosphorylation is regulated at a steady state level in a normal nitrogen fixing nodule. However, under conditions of water deprivation (relevant to osmotic stress from drought or salinity), conditions that are known to activate CDPK in other systems (Patharkar and Cushman, 2000; Saijo et al., 2000), calcium-regulated hyperphosphorylation of nodulin 26 by the SM-CDPK would enhance its aquaporin activity. This would be part of global redistribution of water to the intercellular spaces of the cells of the infected zone and inner cortex, which would help restrict O_2 diffusion into the central infected zone of the nodules.

On the other hand, flooding and hypoxia result in dephosphorylation of nodulin 26 and a decrease in its water transport activity, and conversely, an increase in its ammonia permeability. Accordingly, with respect to this change in selectivity, I propose a new metabolic regulatory model for nodulin 26 in response to O_2-deficit stress (flooding or hypoxia), a model which involves distinct NH_3/NH_4^+ efflux pathways on the symbiosome membrane, since dephosphorylation of nodulin 26 in response to these conditions would address a physiological need to favor its ammonia permease activity to support NH_3 efflux (Fig. 4.6 B). Specifically, flooding-induced acute O_2 deprivation triggers dephosphorylation of nodulin 26 and shifts the energy metabolism in infected cells to fermentation, consequently generating less ATP (Wei and Layzell, 2006). This reduction in free ATP availability causes less energization of the symbiosome membrane due to reduced H^+-ATPase activity, and as a result, pH

of the symbiosome space is increased. Under these conditions, channel activity for NH_4^+ efflux through NSCC is blocked because of the low SM $\Delta\Psi$, and NH_3 efflux through the dephosphorylated nodulin 26 would be favored. In addition, the dephosphorylation of nodulin 26 would decrease the aquaporin activity and osmoregulatory properties of the symbiosome, which could affect the flux of water and possibly the gas diffusion properties of the nodule. While consistent with known nodule physiology and the transport/regulatory properties of nodulin 26, further evidence for these models await genetic studies with model legumes and RNAi or transposon mutagenesis approaches to assess the effects on gas diffusion and nitrogen fixation/assimilation.

Low O_2 as a signal for the induction of *nodulin 26* expression

Expression of nodulin 26 is known to be independent of the entry or presence of rhizobia bacteria moving through the infection threads into the soybean root tissue after inoculation (Fortin et al., 1987). Rather, its expression seems to be dependent upon nodule organogenesis and development based on the previous reports given that expression and protein production of nodulin 26 occur at the immature infected cell during the nodule organogenesis, accompanied with the formation of the symbiosome membrane (Miao and Verma, 1993; Verma and Hong, 1996; Guenther et al., 2003). So far, however, the identity of the physiological regulatory factors and cues inducing *nodulin 26* gene expression with regard to biogenesis of the symbiosome membrane and

the physiological environment of the nodules have not been completely understood. *Nodulin 26* has no nodule-specific *cis*-acting element, and it has been only suggested that nodulin 26 gene would be controlled by *trans*-negative regulatory element which possibly inhibits expression of the nodulin 26 (Miao and Verma, 1993).

In the present study, the finding of presence of 4 AREs in the promoter region of *nodulin 26* provides an idea to better understand regulatory mechanisms of gene expression of *nodulin 26* during nodule development. As consistent with the presence of these AREs, low O_2 signals induce the transcriptional up-regulation of *nodulin 26* in uninfected root tissues.

Based on the results and findings that the expression of genes up-regulated by hypoxia/anoxia coincides with the up-regulation of membrane transporter genes during nodule development (Colebatch et al., 2004), thus, it would be apparently demonstrated that low oxygen concentration is one of multiple factors initiating induction of nodulin 26 transcripts. Apart from this, there could be various regulatory mechanisms which trigger but, also coordinate in multiple ways gene expression of *nodulin 26* in infected soybean roots associated with the formation of mature nodules.

Future directions

In summary, evidence from the present study supports a potential aquaglycero-ammoniaporin role for nodulin 26, and it is proposed that nodulin 26

plays two physiological roles in nitrogen-fixing nodules: 1. An osmoregulatory role (water transport) and 2. A metabolic role (ammonia transport) associated with an interaction of the nitrogen assimilatory enzyme (glutamine synthetase). Further, evidence is provided that the transport selectivity can be conversely regulated by its phosphorylation in response to environmental cues in a manner that would modulate these proposed osmoregulatory and metabolic roles.

To test these models and hypotheses, the following future directions for research are recommended:

1. A more detailed and structural analysis of the molecular basis for water, ammonia and glycerol selectivity of nodulin 26, including how the phosphorylation of the C-terminal region influences pore structure and selectivity.

2. Structural analysis of the nodulin 26/GS interaction and evaluation of the complex formation on regulation of the nodulin 26 transport activities.

3. Genetic studies with model legumes using RNAi or transposon mutagenesis approaches to modulate the expression of nodulin 26 to assess the effects on gas diffusion and nitrogen fixation/assimilation, and the general physiology of the nodule.

4. Use the same genetic approaches with phosphorylation mimic and null mutants of nodulin 26, and fluorescence-tagged nodulin 26 to address the biological role of phosphorylation in nitrogen fixing nodules.

LIST OF REFERENCES

Agre, P. (1997). "Molecular physiology of water transport: aquaporin nomenclature workshop. Mammalian aquaporins." Biol Cell **89**(5-6): 255-257.

Agre, P. (2003). "AQUAPORIN WATER CHANNELS", Nobel Lecture.

Agre, P., Bonhivers, M. and Borgnia, M. J. (1998). "The aquaporins, blueprints for cellular plumbing systems." J Biol Chem **273**(24): 14659-14662.

Agre, P., Saboori, A. M., Asimos, A. and Smith, B. L. (1987). "Purification and partial characterization of the Mr 30,000 integral membrane protein associated with the erythrocyte Rh(D) antigen." J Biol Chem **262**(36): 17497-17503.

Andriankaja, A., Boisson-Dernier, A., Frances, L., Sauviac, L., Jauneau, A., Barker, D. G. and de Carvalho-Niebel, F. (2007). "AP2-ERF transcription factors mediate Nod factor dependent Mt ENOD11 activation in root hairs via a novel cis-regulatory motif." Plant Cell **19**(9): 2866-2885.

Bansal, A. and Sankararamakrishnan, R. (2007). "Homology modeling of major intrinsic proteins in rice, maize and Arabidopsis: comparative analysis of transmembrane helix association and aromatic/arginine selectivity filters." BMC Struct Biol **7**: 27.

Baylis, P. H. (1988). "Water movement through lipid bilayers, pores and plasma membranes: Theory and reality. (Distinquished Lecture Series of the Society of General Physiologists, Volume 4). Alan Finkelstein, John Wiley

and Sons Ltd: New York. 228 pages, £38.45 (1987)." Cell Biochemistry and Function **6**(3): 223-223.

Begum, A. A., Leibovitch, S., Migner, P. and Zhang, F. (2001). "Specific flavonoids induced nod gene expression and pre-activated nod genes of Rhizobium leguminosarum increased pea (Pisum sativum L.) and lentil (Lens culinaris L.) nodulation in controlled growth chamber environments." J Exp Bot **52**(360): 1537-1543.

Beitz, E., Wu, B., Holm, L. M., Schultz, J. E. and Zeuthen, T. (2006). "Point mutations in the aromatic/arginine region in aquaporin 1 allow passage of urea, glycerol, ammonia, and protons." Proc Natl Acad Sci U S A **103**(2): 269-274.

Benedito, V. A., Torres-Jerez, I., Murray, J. D., Andriankaja, A., Allen, S., Kakar, K., Wandrey, M., Verdier, J., Zuber, H., Ott, T., Moreau, S., Niebel, A., Frickey, T., Weiller, G., He, J., Dai, X., Zhao, P. X., Tang, Y. and Udvardi, M. K. (2008). "A gene expression atlas of the model legume Medicago truncatula." The Plant Journal **55**(3): 504-513.

Bergersen, F. J. (1997). "Regulation of nitrogen fixation in infected cells of leguminous root nodules in relation to O₂ supply." Plant and Soil **191**(2): 189-203.

Bergersen, F. J., Turner, G. L., Gibson, A. H. and Dudman, W. F. (1976). "Nitrogenase activity and respiration of cultures of Rhizobium spp. with

special reference to concentrations of dissolved oxygen." Biochim Biophys Acta **444**(1): 164-174.

Boron, W. F. and De Weer, P. (1976). "Intracellular pH transients in squid giant axons caused by CO2, NH3, and metabolic inhibitors." J Gen Physiol **67**(1): 91-112.

Brewin, N. J. (2004). "Plant Cell Wall Remodelling in the Rhizobium–Legume Symbiosis." Crit Rev Plant Sci **23**(4): 293-316.

Britto, D. T., Siddiqi, M. Y., Glass, A. D. and Kronzucker, H. J. (2001). "Futile transmembrane NH4(+) cycling: a cellular hypothesis to explain ammonium toxicity in plants." Proc Natl Acad Sci U S A **98**(7): 4255-4258.

Brown, S. and Walsh, K. (1994). "Anatomy of the Legume Nodule Cortex With Respect to Nodule Permeability." Functional Plant Biology **21**(1): 49-68.

Carbrey, J. M. and Agre, P. (2009). Discovery of the Aquaporins and Development of the Field Aquaporins. E. Beitz, Springer Berlin Heidelberg. **190:** 3-28.

Catalano, C. M., Lane, W. S. and Sherrier, D. J. (2004). "Biochemical characterization of symbiosome membrane proteins from Medicago truncatula root nodules." Electrophoresis **25**(3): 519-531.

Chaumont, F., Moshelion, M. and Daniels, M. J. (2005). "Regulation of plant aquaporin activity." Biol Cell **97**(10): 749-764.

Choi, W. G. and Roberts, D. M. (2007). "Arabidopsis NIP2;1, a major intrinsic protein transporter of lactic acid induced by anoxic stress." J Biol Chem **282**(33): 24209-24218.

Chrispeels, M. J. and Maurel, C. (1994). "Aquaporins: the molecular basis of facilitated water movement through living plant cells?" Plant Physiol **105**(1): 9-13.

Colebatch, G., Desbrosses, G., Ott, T., Krusell, L., Montanari, O., Kloska, S., Kopka, J. and Udvardi, M. K. (2004). "Global changes in transcription orchestrate metabolic differentiation during symbiotic nitrogen fixation in Lotus japonicus." Plant J **39**(4): 487-512.

Cosgrove, D. (1986). "Biophysical control of plant cell growth." Annu Rev Plant Physiol **37**: 377-405.

Crespi, M. and Galvez, S. (2000). "Molecular Mechanisms in Root Nodule Development." J Plant Growth Regul **19**(2): 155-166.

D'Haeze, W., Mergaert, P., Prome, J. C. and Holsters, M. (2000). "Nod factor requirements for efficient stem and root nodulation of the tropical legume Sesbania rostrata." J Biol Chem **275**(21): 15676-15684.

Dakora, F. and Atkins, C. (1989). "Diffusion of Oxygen in Relation to Structure and Function in Legume Root Nodules." Functional Plant Biology **16**(1): 131-140.

Danielson, J. A. and Johanson, U. (2008). "Unexpected complexity of the aquaporin gene family in the moss Physcomitrella patens." BMC Plant Biol **8**: 45.

Day, D. A., Poole, P. S., Tyerman, S. D. and Rosendahl, L. (2001). "Ammonia and amino acid transport across symbiotic membranes in nitrogen-fixing legume nodules." Cell Mol Life Sci **58**(1): 61-71.

de Groot, B. L. and Grubmuller, H. (2001). "Water permeation across biological membranes: mechanism and dynamics of aquaporin-1 and GlpF." Science **294**(5550): 2353-2357.

Dean, R. M., Rivers, R. L., Zeidel, M. L. and Roberts, D. M. (1999). "Purification and functional reconstitution of soybean nodulin 26. An aquaporin with water and glycerol transport properties." Biochemistry **38**(1): 347-353.

Del Castillo, L. D. and Layzell, D. B. (1995). "Drought Stress, Permeability to O2 Diffusion, and the Respiratory Kinetics of Soybean Root Nodules." Plant Physiol **107**(4): 1187-1194.

Denison, R. F. and Kinraide, T. B. (1995). "Oxygen-Induced Membrane Depolarizations in Legume Root Nodules (Possible Evidence for an Osmoelectrical Mechanism Controlling Nodule Gas Permeability)." Plant Physiol **108**(1): 235-240.

Denker, B. M., Smith, B. L., Kuhajda, F. P. and Agre, P. (1988). "Identification, purification, and partial characterization of a novel Mr 28,000 integral

membrane protein from erythrocytes and renal tubules." J Biol Chem **263**(30): 15634-15642.

Dixon, R. and Kahn, D. (2004). "Genetic regulation of biological nitrogen fixation." Nat Rev Micro **2**(8): 621-631.

Dolferus, R., Klok, E. J., Ismond, K., Delessert, C., Wilson, S., Good, A., Peacock, J. and Dennis, L. (2001). "Molecular basis of the anaerobic response in plants." IUBMB Life **51**(2): 79-82.

Dos Santos, P. C., Dean, D. R., Hu, Y. and Ribbe, M. W. (2004). "Formation and insertion of the nitrogenase iron-molybdenum cofactor." Chem Rev **104**(2): 1159-1173.

Dynowski, M., Mayer, M., Moran, O. and Ludewig, U. (2008). "Molecular determinants of ammonia and urea conductance in plant aquaporin homologs." FEBS Lett **582**(16): 2458-2462.

Eady, R. R. and Postgate, J. R. (1974). "Nitrogenase." Nature **249**(5460): 805-810.

Echevarria, M. and Ilundain, A. A. (1998). "Aquaporins." J Physiol Biochem **54**(2): 107-118.

Ehrhardt, D. W., Wais, R. and Long, S. R. (1996). "Calcium spiking in plant root hairs responding to Rhizobium nodulation signals." Cell **85**(5): 673-681.

El Karkouri, K., Gueune, H. and Delamarche, C. (2005). "MIPDB: a relational database dedicated to MIP family proteins." Biol Cell **97**(7): 535-543.

Erdjument-Bromage, H., Lui, M., Lacomis, L., Grewal, A., Annan, R. S., McNulty, D. E., Carr, S. A. and Tempst, P. (1998). "Examination of micro-tip reversed-phase liquid chromatographic extraction of peptide pools for mass spectrometric analysis." J Chromatogr A **826**(2): 167-181.

Eskew, D. L., Jiang, Q., Caetano-Anolles, G. and Gresshoff, P. M. (1993). "Kinetics of Nodule Development in Glycine soja." Plant Physiol **103**(4): 1139-1145.

Esseling, J. J., Lhuissier, F. G. and Emons, A. M. (2003). "Nod factor-induced root hair curling: continuous polar growth towards the point of nod factor application." Plant Physiol **132**(4): 1982-1988.

Eto, K., Noda, Y., Horikawa, S., Uchida, S. and Sasaki, S. (2010). "Phosphorylation of Aquaporin-2 Regulates Its Water Permeability." Journal of Biological Chemistry **285**(52): 40777-40784.

Finkelstein, A. (1987). "Water Movement Through Lipid Bilayer, Pores and Plasma Membranes", Wiley and Sons, New York.

Fleurat-Lessard, P., Michonneau, P., Maeshima, M., Drevon, J. J. and Serraj, R. (2005). "The distribution of aquaporin subtypes (PIP1, PIP2 and gamma-TIP) is tissue dependent in soybean (Glycine max) root nodules." Ann Bot **96**(3): 457-460.

Fortin, M. G., Morrison, N. A. and Verma, D. P. (1987). "Nodulin-26, a peribacteroid membrane nodulin is expressed independently of the

development of the peribacteroid compartment." Nucleic Acids Res **15**(2): 813-824.

Fu, D., Libson, A., Miercke, L. J., Weitzman, C., Nollert, P., Krucinski, J. and Stroud, R. M. (2000). "Structure of a glycerol-conducting channel and the basis for its selectivity." Science **290**(5491): 481-486.

Fushimi, K., Sasaki, S. and Marumo, F. (1997). "Phosphorylation of serine 256 is required for cAMP-dependent regulatory exocytosis of the aquaporin-2 water channel." J Biol Chem **272**(23): 14800-14804.

Girsch, S. J. and Peracchia, C. (1991). "Calmodulin interacts with a C-terminus peptide from the lens membrane protein MIP26." Curr Eye Res **10**(9): 839-849.

Gleason, C., Chaudhuri, S., Yang, T., Munoz, A., Poovaiah, B. W. and Oldroyd, G. E. (2006). "Nodulation independent of rhizobia induced by a calcium-activated kinase lacking autoinhibition." Nature **441**(7097): 1149-1152.

Goldberg, I., Nadler, V. and Hochman, A. (1987). "Mechanism of nitrogenase switch-off by oxygen." J Bacteriol **169**(2): 874-879.

Gonen, T. and Walz, T. (2006). "The structure of aquaporins." Q Rev Biophys **39**(4): 361-396.

Gorg, A., Obermaier, C., Boguth, G., Harder, A., Scheibe, B., Wildgruber, R. and Weiss, W. (2000). "The current state of two-dimensional electrophoresis with immobilized pH gradients." Electrophoresis **21**(6): 1037-1053.

Gualtieri, G. and Bisseling, T. (2000). "The evolution of nodulation." Plant Mol Biol **42**(1): 181-194.

Guenther, J. F., Chanmanivone, N., Galetovic, M. P., Wallace, I. S., Cobb, J. A. and Roberts, D. M. (2003). "Phosphorylation of soybean nodulin 26 on serine 262 enhances water permeability and is regulated developmentally and by osmotic signals." Plant Cell **15**(4): 981-991.

Gupta, A. B. and Sankararamakrishnan, R. (2009). "Genome-wide analysis of major intrinsic proteins in the tree plant Populus trichocarpa: characterization of XIP subfamily of aquaporins from evolutionary perspective." BMC Plant Biol **9**: 134.

Gutierrez, R. A. (2012). "Systems biology for enhanced plant nitrogen nutrition." Science **336**(6089): 1673-1675.

Hachez, C. and Chaumont, F. (2010). "Aquaporins: a family of highly regulated multifunctional channels." Adv Exp Med Biol **679**: 1-17.

Han, Z., Wax, M. B. and Patil, R. V. (1998). "Regulation of aquaporin-4 water channels by phorbol ester-dependent protein phosphorylation." J Biol Chem **273**(11): 6001-6004.

Hanton, S. L., Renna, L., Bortolotti, L. E., Chatre, L., Stefano, G. and Brandizzi, F. (2005). "Diacidic motifs influence the export of transmembrane proteins from the endoplasmic reticulum in plant cells." Plant Cell **17**(11): 3081-3093.

Hill, S. (1988). "How is nitrogenase regulated by oxygen?" FEMS Microbiol Rev **4**(2): 111-129.

Hirel, B., Tétu, T., Lea, P. J. and Dubois, F. (2011). "Improving Nitrogen Use Efficiency in Crops for Sustainable Agriculture." Sustainability **3**(9): 1452-1485.

Ho, S. N. (2006). "Intracellular water homeostasis and the mammalian cellular osmotic stress response." Journal of Cellular Physiology **206**(1): 9-15.

Hoffert, J. D., Pisitkun, T., Wang, G., Shen, R. F. and Knepper, M. A. (2006). "Quantitative phosphoproteomics of vasopressin-sensitive renal cells: regulation of aquaporin-2 phosphorylation at two sites." Proc Natl Acad Sci U S A **103**(18): 7159-7164.

Holm, L. M., Jahn, T. P., Moller, A. L., Schjoerring, J. K., Ferri, D., Klaerke, D. A. and Zeuthen, T. (2005). "NH3 and NH4+ permeability in aquaporin-expressing Xenopus oocytes." Pflugers Arch **450**(6): 415-428.

Hu, Y. and Ribbe, M. W. (2011). "Historic overview of nitrogenase research." Methods Mol Biol **766**: 3-7.

Hubert, J. F., Duchesne, L., Delamarche, C., Vaysse, A., Gueune, H. and Raguenes-Nicol, C. (2005). "Pore selectivity analysis of an aquaglyceroporin by stopped-flow spectrophotometry on bacterial cell suspensions." Biol Cell **97**(9): 675-686.

Hunt, S., King, B. J., Canvin, D. T. and Layzell, D. B. (1987). "Steady and nonsteady state gas exchange characteristics of soybean nodules in relation to the oxygen diffusion barrier." Plant Physiol **84**(1): 164-172.

Hunt, S. and Layzell, D. B. (1993). "Gas Exchange of Legume Nodules and the Regulation of Nitrogenase Activity." Annual Review of Plant Physiology and Plant Molecular Biology **44**(1): 483-511.

Hwang, J. H., Ellingson, S. R. and Roberts, D. M. (2010). "Ammonia permeability of the soybean nodulin 26 channel." FEBS Lett **584**(20): 4339-4343.

Igarashi, R. Y. and Seefeldt, L. C. (2003). "Nitrogen fixation: the mechanism of the Mo-dependent nitrogenase." Crit Rev Biochem Mol Biol **38**(4): 351-384.

Ishibashi, K., Kuwahara, M., Kageyama, Y., Tohsaka, A., Marumo, F. and Sasaki, S. (1997). "Cloning and functional expression of a second new aquaporin abundantly expressed in testis." Biochem Biophys Res Commun **237**(3): 714-718.

Ishibashi, K., Morinaga, T., Kuwahara, M., Sasaki, S. and Imai, M. (2002). "Cloning and identification of a new member of water channel (AQP10) as an aquaglyceroporin." Biochim Biophys Acta **1576**(3): 335-340.

Ishibashi, K., Sasaki, S., Fushimi, K., Uchida, S., Kuwahara, M., Saito, H., Furukawa, T., Nakajima, K., Yamaguchi, Y., Gojobori, T. and et al. (1994). "Molecular cloning and expression of a member of the aquaporin family with permeability to glycerol and urea in addition to water expressed at the

basolateral membrane of kidney collecting duct cells." Proc Natl Acad Sci U S A **91**(14): 6269-6273.

Ishikawa, F., Suga, S., Uemura, T., Sato, M. H. and Maeshima, M. (2005). "Novel type aquaporin SIPs are mainly localized to the ER membrane and show cell-specific expression in Arabidopsis thaliana." FEBS Letters **579**(25): 5814-5820.

Jahn, T. P., Moller, A. L., Zeuthen, T., Holm, L. M., Klaerke, D. A., Mohsin, B., Kuhlbrandt, W. and Schjoerring, J. K. (2004). "Aquaporin homologues in plants and mammals transport ammonia." FEBS Lett **574**(1-3): 31-36.

Jensen, O. N., Wilm, M., Shevchenko, A. and Mann, M. (1999). "Sample preparation methods for mass spectrometric peptide mapping directly from 2-DE gels." Methods Mol Biol **112**: 513-530.

Johanson, U., Karlsson, M., Johansson, I., Gustavsson, S., Sjovall, S., Fraysse, L., Weig, A. R. and Kjellbom, P. (2001). "The complete set of genes encoding major intrinsic proteins in Arabidopsis provides a framework for a new nomenclature for major intrinsic proteins in plants." Plant Physiol **126**(4): 1358-1369.

Johansson, I., Karlsson, M., Shukla, V. K., Chrispeels, M. J., Larsson, C. and Kjellbom, P. (1998). "Water transport activity of the plasma membrane aquaporin PM28A is regulated by phosphorylation." Plant Cell **10**(3): 451-459.

Journet, E. P., El-Gachtouli, N., Vernoud, V., de Billy, F., Pichon, M., Dedieu, A., Arnould, C., Morandi, D., Barker, D. G. and Gianinazzi-Pearson, V. (2001). "Medicago truncatula ENOD11: a novel RPRP-encoding early nodulin gene expressed during mycorrhization in arbuscule-containing cells." Mol Plant Microbe Interact **14**(6): 737-748.

Jung, J. S., Preston, G. M., Smith, B. L., Guggino, W. B. and Agre, P. (1994). "Molecular structure of the water channel through aquaporin CHIP. The hourglass model." J Biol Chem **269**(20): 14648-14654.

Kadohira, I., Abe, Y., Nuriya, M., Sano, K., Tsuji, S., Arimitsu, T., Yoshimura, Y. and Yasui, M. (2008). "Phosphorylation in the C-terminal domain of Aquaporin-4 is required for Golgi transition in primary cultured astrocytes." Biochemical and Biophysical Research Communications **377**(2): 463-468.

Kaiser, B. N., Moreau, S., Castelli, J., Thomson, R., Lambert, A., Bogliolo, S., Puppo, A. and Day, D. A. (2003). "The soybean NRAMP homologue, GmDMT1, is a symbiotic divalent metal transporter capable of ferrous iron transport." Plant J **35**(3): 295-304.

Karlsson, M., Fotiadis, D., Sjovall, S., Johansson, I., Hedfalk, K., Engel, A. and Kjellbom, P. (2003). "Reconstitution of water channel function of an aquaporin overexpressed and purified from Pichia pastoris." FEBS Lett **537**(1-3): 68-72.

King, B. J., Hunt, S., Weagle, G. E., Walsh, K. B., Pottier, R. H., Canvin, D. T. and Layzell, D. B. (1988). "Regulation of o(2) concentration in soybean

nodules observed by in situ spectroscopic measurement of leghemoglobin oxygenation." Plant Physiol **87**(2): 296-299.

King, B. J. and Layzell, D. B. (1991). "Effect of Increases in Oxygen Concentration during the Argon-Induced Decline in Nitrogenase Activity in Root Nodules of Soybean." Plant Physiol **96**(2): 376-381.

King, L. S. and Agre, P. (1996). "Pathophysiology of the aquaporin water channels." Annu Rev Physiol **58**: 619-648.

King, L. S., Kozono, D. and Agre, P. (2004). "From structure to disease: the evolving tale of aquaporin biology." Nat Rev Mol Cell Biol **5**(9): 687-698.

Knight, H., Trewavas, A. J. and Knight, M. R. (1997). "Calcium signalling in Arabidopsis thaliana responding to drought and salinity." Plant J **12**(5): 1067-1078.

Krusell, L., Krause, K., Ott, T., Desbrosses, G., Kramer, U., Sato, S., Nakamura, Y., Tabata, S., James, E. K., Sandal, N., Stougaard, J., Kawaguchi, M., Miyamoto, A., Suganuma, N. and Udvardi, M. K. (2005). "The sulfate transporter SST1 is crucial for symbiotic nitrogen fixation in Lotus japonicus root nodules." Plant Cell **17**(5): 1625-1636.

Layzell, D. B., Hunt, S. and Palmer, G. R. (1990). "Mechanism of Nitrogenase Inhibition in Soybean Nodules : Pulse-Modulated Spectroscopy Indicates that Nitrogenase Activity Is Limited by O(2)." Plant Physiol **92**(4): 1101-1107.

Lee, J. W., Zhang, Y., Weaver, C. D., Shomer, N. H., Louis, C. F. and Roberts, D. M. (1995). "Phosphorylation of nodulin 26 on serine 262 affects its voltage-sensitive channel activity in planar lipid bilayers." J Biol Chem **270**(45): 27051-27057.

Legocki, R. P. and Verma, D. P. (1980). "Identification of "nodule-specific" host proteins (nodoulins) involved in the development of rhizobium-legume symbiosis." Cell **20**(1): 153-163.

Lescot, M., Dehais, P., Thijs, G., Marchal, K., Moreau, Y., Van de Peer, Y., Rouze, P. and Rombauts, S. (2002). "PlantCARE, a database of plant cis-acting regulatory elements and a portal to tools for in silico analysis of promoter sequences." Nucleic Acids Res **30**(1): 325-327.

Libault, M., Farmer, A., Joshi, T., Takahashi, K., Langley, R. J., Franklin, L. D., He, J., Xu, D., May, G. and Stacey, G. (2010). "An integrated transcriptome atlas of the crop model Glycine max, and its use in comparative analyses in plants." Plant J **63**(1): 86-99.

Libault, M., Thibivilliers, S., Bilgin, D. D., Radwan, O., Benitez, M., Clough, S. J. and Stacey, G. (2008). "Identification of Four Soybean Reference Genes for Gene Expression Normalization." The Plant Genome **1**(1): 44-54.

Litman, T., Sogaard, R. and Zeuthen, T. (2009). "Ammonia and urea permeability of mammalian aquaporins." Handb Exp Pharmacol(190): 327-358.

Liu, K., Nagase, H., Huang, C. G., Calamita, G. and Agre, P. (2006). "Purification and functional characterization of aquaporin-8." Biol Cell **98**(3): 153-161.

Ludewig, U. and Dynowski, M. (2009). "Plant aquaporin selectivity: where transport assays, computer simulations and physiology meet." Cell Mol Life Sci **66**(19): 3161-3175.

Luyten, K., Albertyn, J., Skibbe, W. F., Prior, B. A., Ramos, J., Thevelein, J. M. and Hohmann, S. (1995). "Fps1, a yeast member of the MIP family of channel proteins, is a facilitator for glycerol uptake and efflux and is inactive under osmotic stress." EMBO J **14**(7): 1360-1371.

Ma, J. F., Yamaji, N., Mitani, N., Tamai, K., Konishi, S., Fujiwara, T., Katsuhara, M. and Yano, M. (2007). "An efflux transporter of silicon in rice." Nature **448**(7150): 209-212.

Ma, J. F., Yamaji, N., Mitani, N., Xu, X. Y., Su, Y. H., McGrath, S. P. and Zhao, F. J. (2008). "Transporters of arsenite in rice and their role in arsenic accumulation in rice grain." Proc Natl Acad Sci U S A **105**(29): 9931-9935.

Macey, R. I. (1984). "Transport of water and urea in red blood cells." Am J Physiol **246**(3 Pt 1): C195-203.

Madrid, R., Le Maout, S., Barrault, M. B., Janvier, K., Benichou, S. and Merot, J. (2001). "Polarized trafficking and surface expression of the AQP4 water channel are coordinated by serial and regulated interactions with different clathrin-adaptor complexes." EMBO J **20**(24): 7008-7021.

Madsen, E. B., Madsen, L. H., Radutoiu, S., Olbryt, M., Rakwalska, M., Szczyglowski, K., Sato, S., Kaneko, T., Tabata, S., Sandal, N. and

Stougaard, J. (2003). "A receptor kinase gene of the LysM type is involved in legume perception of rhizobial signals." Nature **425**(6958): 637-640.

Maj, D., Wielbo, J., Marek-Kozaczuk, M. and Skorupska, A. (2010). "Response to flavonoids as a factor influencing competitiveness and symbiotic activity of Rhizobium leguminosarum." Microbiological Research **165**(1): 50-60.

Marcker, A., Lund, M., Jensen, E. O. and Marcker, K. A. (1984). "Transcription of the soybean leghemoglobin genes during nodule development." Embo J **3**(8): 1691-1695.

Marschner, H. (1995). "Mineral nutrition of higher plants", 2nd edn. London, Academic Press.

Masalkar, P., Wallace, I. S., Hwang, J. H. and Roberts, D. M. (2010). "Interaction of cytosolic glutamine synthetase of soybean root nodules with the C-terminal domain of the symbiosome membrane nodulin 26 aquaglyceroporin." J Biol Chem.

Matamoros, M. A., Baird, L. M., Escuredo, P. R., Dalton, D. A., Minchin, F. R., Iturbe-Ormaetxe, I., Rubio, M. C., Moran, J. F., Gordon, A. J. and Becana, M. (1999). "Stress-induced legume root nodule senescence. Physiological, biochemical, and structural alterations." Plant Physiol **121**(1): 97-112.

Maurel, C. (2007). "Plant aquaporins: novel functions and regulation properties." FEBS Lett **581**(12): 2227-2236.

Maurel, C., Kado, R. T., Guern, J. and Chrispeels, M. J. (1995). "Phosphorylation regulates the water channel activity of the seed-specific aquaporin alpha-TIP." Embo J **14**(13): 3028-3035.

Maurel, C., Reizer, J., Schroeder, J. I. and Chrispeels, M. J. (1993). "The vacuolar membrane protein gamma-TIP creates water specific channels in Xenopus oocytes." EMBO J **12**(6): 2241-2247.

Maurel, C., Reizer, J., Schroeder, J. I., Chrispeels, M. J. and Saier, M. H., Jr. (1994). "Functional characterization of the Escherichia coli glycerol facilitator, GlpF, in Xenopus oocytes." J Biol Chem **269**(16): 11869-11872.

Maurel, C., Verdoucq, L., Luu, D. T. and Santoni, V. (2008). "Plant aquaporins: membrane channels with multiple integrated functions." Annu Rev Plant Biol **59**: 595-624.

Miao, G. H. and Verma, D. P. (1993). "Soybean nodulin-26 gene encoding a channel protein is expressed only in the infected cells of nodules and is regulated differently in roots of homologous and heterologous plants." Plant Cell **5**(7): 781-794.

Miflin, B. J. and Habash, D. Z. (2002). "The role of glutamine synthetase and glutamate dehydrogenase in nitrogen assimilation and possibilities for improvement in the nitrogen utilization of crops." Journal of Experimental Botany **53**(370): 979-987.

Minchin, F. R. (1997). "Regulation of oxygen diffusion in legume nodules." Soil Biology and Biochemistry **29**(5–6): 881-888.

Minchin, F. R., James, E. K. and Becana, M. (2007). Oxygen Diffusion, Production Of Reactive Oxygen And Nitrogen Species, And Antioxidants In Legume Nodules

Nitrogen-fixing Leguminous Symbioses. M. J. Dilworth, E. K. James, J. I. Sprent and W. E. Newton, Springer Netherlands. **7:** 321-362.

Mitani, N., Yamaji, N. and Ma, J. F. (2008). "Characterization of substrate specificity of a rice silicon transporter, Lsi1." Pflugers Arch **456**(4): 679-686.

Mohanty, B., Krishnan, S. P., Swarup, S. and Bajic, V. B. (2005). "Detection and preliminary analysis of motifs in promoters of anaerobically induced genes of different plant species." Ann Bot (Lond) **96**(4): 669-681.

Monahan-Giovanelli, H., Pinedo, C. A. and Gage, D. J. (2006). "Architecture of infection thread networks in developing root nodules induced by the symbiotic bacterium Sinorhizobium meliloti on Medicago truncatula." Plant Physiol **140**(2): 661-670.

Moreau, S., Thomson, R. M., Kaiser, B. N., Trevaskis, B., Guerinot, M. L., Udvardi, M. K., Puppo, A. and Day, D. A. (2002). "GmZIP1 encodes a symbiosis-specific zinc transporter in soybean." J Biol Chem **277**(7): 4738-4746.

Moreau, S., Verdenaud, M., Ott, T., Letort, S., de Billy, F., Niebel, A., Gouzy, J., de Carvalho-Niebel, F. and Gamas, P. (2011). "Transcription

reprogramming during root nodule development in Medicago truncatula." PLoS One **6**(1): e16463.

Morey, K. J., Ortega, J. L. and Sengupta-Gopalan, C. (2002). "Cytosolic glutamine synthetase in soybean is encoded by a multigene family, and the members are regulated in an organ-specific and developmental manner." Plant Physiol **128**(1): 182-193.

Niemietz, C. M. and Tyerman, S. D. (1997). "Characterization of Water Channels in Wheat Root Membrane Vesicles." Plant Physiol **115**(2): 561-567.

Niemietz, C. M. and Tyerman, S. D. (2000). "Channel-mediated permeation of ammonia gas through the peribacteroid membrane of soybean nodules." FEBS Lett **465**(2-3): 110-114.

Noda, Y. and Sasaki, S. (2005). "Trafficking mechanism of water channel aquaporin-2." Biol Cell **97**(12): 885-892.

Nyblom, M., Frick, A., Wang, Y., Ekvall, M., Hallgren, K., Hedfalk, K., Neutze, R., Tajkhorshid, E. and Tornroth-Horsefield, S. (2009). "Structural and functional analysis of SoPIP2;1 mutants adds insight into plant aquaporin gating." J Mol Biol **387**(3): 653-668.

Obermeyer, G. and Tyerman, S. D. (2005). "NH4+ currents across the peribacteroid membrane of soybean. Macroscopic and microscopic properties, inhibition by Mg2+, and temperature dependence indicate a SubpicoSiemens channel finely regulated by divalent cations." Plant Physiol **139**(2): 1015-1029.

Oldroyd, G. E. and Downie, J. A. (2008). "Coordinating nodule morphogenesis with rhizobial infection in legumes." Annu Rev Plant Biol **59**: 519-546.

Ou Yang, L.-J., Udvardi, M. and Day, D. (1990). "Specificity and regulation of the dicarboxylate carrier on the peribacteroid membrane of soybean nodules." Planta **182**(3): 437-444.

Parsons, R. and Day, D. A. (1990). "Mechanism of soybean nodule adaptation to different oxygen pressures." Plant, Cell & Environment **13**(6): 501-512.

Patharkar, O. R. and Cushman, J. C. (2000). "A stress-induced calcium-dependent protein kinase from Mesembryanthemum crystallinum phosphorylates a two-component pseudo-response regulator." The Plant Journal **24**(5): 679-691.

Pfaffl, M. W. (2001). "A new mathematical model for relative quantification in real-time RT-PCR." Nucleic Acids Res **29**(9): e45.

Poole, P. and Allaway, D. (2000). "Carbon and nitrogen metabolism in Rhizobium." Adv Microb Physiol **43**: 117-163.

Postgate, J. R. (1998). "Nitrogen Fixation", Nitrogen Fixation, Cambridge UK.

Prak, S., Hem, S., Boudet, J., Viennois, G., Sommerer, N., Rossignol, M., Maurel, C. and Santoni, V. (2008). "Multiple phosphorylations in the C-terminal tail of plant plasma membrane aquaporins: role in subcellular trafficking of AtPIP2;1 in response to salt stress." Mol Cell Proteomics **7**(6): 1019-1030.

Preston, G. M. and Agre, P. (1991). "Isolation of the cDNA for erythrocyte integral membrane protein of 28 kilodaltons: member of an ancient channel family." Proc Natl Acad Sci U S A **88**(24): 11110-11114.

Preston, G. M., Carroll, T. P., Guggino, W. B. and Agre, P. (1992). "Appearance of water channels in Xenopus oocytes expressing red cell CHIP28 protein." Science **256**(5055): 385-387.

Purcell, L. C. and Sinclair, T. R. (1994). "An osmotic hypothesis for the regulation of oxygen permeability in soybean nodules." Plant, Cell & Environment **17**(7): 837-843.

Quigley, F., Rosenberg, J. M., Shachar-Hill, Y. and Bohnert, H. J. (2002). "From genome to function: the Arabidopsis aquaporins." Genome Biol **3**(1): RESEARCH0001.

Radutoiu, S., Madsen, L. H., Madsen, E. B., Felle, H. H., Umehara, Y., Gronlund, M., Sato, S., Nakamura, Y., Tabata, S., Sandal, N. and Stougaard, J. (2003). "Plant recognition of symbiotic bacteria requires two LysM receptor-like kinases." Nature **425**(6958): 585-592.

Rivers, R. L., Dean, R. M., Chandy, G., Hall, J. E., Roberts, D. M. and Zeidel, M. L. (1997). "Functional analysis of nodulin 26, an aquaporin in soybean root nodule symbiosomes." J Biol Chem **272**(26): 16256-16261.

Roberts, D. M., Choi, W. G. and Hwang, J. H. (2010). Strategies for Adaptation to Waterlogging and Hypoxia in Nitrogen Fixing Nodules of Legumes.

Waterlogging Signalling and Tolerance in Plants. S. Mancuso and S. Shabala, Springer Berlin Heidelberg**:** 37-59.

Roberts, D. M. and Tyerman, S. D. (2002). "Voltage-dependent cation channels permeable to NH(+)(4), K(+), and Ca(2+) in the symbiosome membrane of the model legume Lotus japonicus." Plant Physiol **128**(2): 370-378.

Rojek, A., Praetorius, J., Frokiaer, J., Nielsen, S. and Fenton, R. A. (2008). "A current view of the mammalian aquaglyceroporins." Annu Rev Physiol **70**: 301-327.

Rose, K. M., Wang, Z., Magrath, G. N., Hazard, E. S., Hildebrandt, J. D. and Schey, K. L. (2008). "Aquaporin 0-calmodulin interaction and the effect of aquaporin 0 phosphorylation." Biochemistry **47**(1): 339-347.

Roth, E., Jeon K. and Stacey, G. (1988). "Homology in endosymbiotic systems: The term 'symbiosome' in: Molecular Genetics of Plant Microbe Interactions".

Roth, L. E. and Stacey, G. (1989). "Bacterium release into host cells of nitrogen-fixing soybean nodules: the symbiosome membrane comes from three sources." Eur J Cell Biol **49**(1): 13-23.

Sachs, M. M., Subbaiah, C. C. and Saab, I. N. (1996). "Anaerobic gene expression and flooding tolerance in maize." Journal of Experimental Botany **47**(1): 1-15.

Saijo, Y., Hata, S., Kyozuka, J., Shimamoto, K. and Izui, K. (2000). "Over-expression of a single Ca2+-dependent protein kinase confers both cold and salt/drought tolerance on rice plants." Plant J **23**(3): 319-327.

Sakurai, J., Ishikawa, F., Yamaguchi, T., Uemura, M. and Maeshima, M. (2005). "Identification of 33 rice aquaporin genes and analysis of their expression and function." Plant Cell Physiol **46**(9): 1568-1577.

Sandal, N. N. and Marcker, K. A. (1988). "Soybean nodulin 26 is homologous to the major intrinsic protein of the bovine lens fiber membrane." Nucleic Acids Res **16**(19): 9347.

Saparov, S. M., Liu, K., Agre, P. and Pohl, P. (2007). "Fast and selective ammonia transport by aquaporin-8." J Biol Chem **282**(8): 5296-5301.

Sato, S., Nakamura, Y., Kaneko, T., Asamizu, E., Kato, T., Nakao, M., Sasamoto, S., Watanabe, A., Ono, A., Kawashima, K., Fujishiro, T., Katoh, M., Kohara, M., Kishida, Y., Minami, C., Nakayama, S., Nakazaki, N., Shimizu, Y., Shinpo, S., Takahashi, C., Wada, T., Yamada, M., Ohmido, N., Hayashi, M., Fukui, K., Baba, T., Nakamichi, T., Mori, H. and Tabata, S. (2008). "Genome structure of the legume, Lotus japonicus." DNA Res **15**(4): 227-239.

Schmutz, J., Cannon, S. B., Schlueter, J., Ma, J., Mitros, T., Nelson, W., Hyten, D. L., Song, Q., Thelen, J. J., Cheng, J., Xu, D., Hellsten, U., May, G. D., Yu, Y., Sakurai, T., Umezawa, T., Bhattacharyya, M. K., Sandhu, D., Valliyodan, B., Lindquist, E., Peto, M., Grant, D., Shu, S., Goodstein, D.,

Barry, K., Futrell-Griggs, M., Abernathy, B., Du, J., Tian, Z., Zhu, L., Gill, N., Joshi, T., Libault, M., Sethuraman, A., Zhang, X. C., Shinozaki, K., Nguyen, H. T., Wing, R. A., Cregan, P., Specht, J., Grimwood, J., Rokhsar, D., Stacey, G., Shoemaker, R. C. and Jackson, S. A. (2010). "Genome sequence of the palaeopolyploid soybean." Nature **463**(7278): 178-183.

Seefeldt, L. C., Dance, I. G. and Dean, D. R. (2004). "Substrate interactions with nitrogenase: Fe versus Mo." Biochemistry **43**(6): 1401-1409.

Serraj, R., Fleurat-Lessard, P., Jaillard, B. and Drevon, J. J. (1995). "Structural changes in the innercortex cells of soybean root nodules are induced by short-term exposure to high salt or oxygen concentrations." Plant, Cell & Environment **18**(4): 455-462.

Serraj, R., Roy, G. and Drevon, J. J. (1994). "Salt stress induces a decrease in the oxygen uptake of soybean nodules and in their permeability to oxygen diffusion." Physiologia Plantarum **91**(2): 161-168.

Serraj, R. and Sinclair, T. R. (1996). "Inhibition of nitrogenase activity and nodule oxygen permeability by water deficit." Journal of Experimental Botany **47**(8): 1067-1073.

Serraj, R., Sinclair, T. R. and Purcell, L. C. (1999). "Symbiotic N2 fixation response to drought." Journal of Experimental Botany **50**(331): 143-155.

She, Q., Lauridsen, P., Stougaard, J. and Marcker, K. (1993). "Minimal enhancer elements of the leghemoglobinlba andlbc3 gene promoters fromGlycine max L. have different properties." Plant Molecular Biology **22**(6): 945-956.

Sheey, J. E., Minchin, F. R. and Witty, J. F. (1983). "Biological Control of the Resistance to Oxygen Flux in Nodules." Annals of Botany **52**(4): 565-571.

Stacey, G., Libault, M., Brechenmacher, L., Wan, J. and May, G. D. (2006). "Genetics and functional genomics of legume nodulation." Curr Opin Plant Biol **9**(2): 110-121.

Stal, L. J., Severin, I. and Bolhuis, H. (2010). "The ecology of nitrogen fixation in cyanobacterial mats." Adv Exp Med Biol **675**: 31-45.

Streeter, J. G. (1989). "Estimation of ammonium concentration in the cytosol of soybean nodules." Plant Physiol **90**(3): 779-782.

Streng, A., op den Camp, R., Bisseling, T. and Geurts, R. (2011). "Evolutionary origin of rhizobium Nod factor signaling." Plant Signal Behav **6**(10): 1510-1514.

Sui, H., Han, B. G., Lee, J. K., Walian, P. and Jap, B. K. (2001). "Structural basis of water-specific transport through the AQP1 water channel." Nature **414**(6866): 872-878.

Sweet, G., Gandor, C., Voegele, R., Wittekindt, N., Beuerle, J., Truniger, V., Lin, E. C. and Boos, W. (1990). "Glycerol facilitator of Escherichia coli: cloning of glpF and identification of the glpF product." J Bacteriol **172**(1): 424-430.

Szczyglowski, K., Kapranov, P., Hamburger, D. and de Bruijn, F. J. (1998). "The Lotus japonicus LjNOD70 nodulin gene encodes a protein with similarities to transporters." Plant Molecular Biology **37**(4): 651-661.

Tadege, M., Wen, J., He, J., Tu, H., Kwak, Y., Eschstruth, A., Cayrel, A., Endre, G., Zhao, P. X., Chabaud, M., Ratet, P. and Mysore, K. S. (2008). "Large-scale insertional mutagenesis using the Tnt1 retrotransposon in the model legume Medicago truncatula." Plant J **54**(2): 335-347.

Takano, J., Wada, M., Ludewig, U., Schaaf, G., von Wiren, N. and Fujiwara, T. (2006). "The Arabidopsis major intrinsic protein NIP5;1 is essential for efficient boron uptake and plant development under boron limitation." Plant Cell **18**(6): 1498-1509.

Tanaka, M., Wallace, I. S., Takano, J., Roberts, D. M. and Fujiwara, T. (2008). "NIP6;1 is a boric acid channel for preferential transport of boron to growing shoot tissues in Arabidopsis." Plant Cell **20**(10): 2860-2875.

Timmers, A. C., Auriac, M. C. and Truchet, G. (1999). "Refined analysis of early symbiotic steps of the Rhizobium-Medicago interaction in relationship with microtubular cytoskeleton rearrangements." Development **126**(16): 3617-3628.

Tjepkema, J. D. and Yocum, C. S. (1974). "Measurement of oxygen partial pressure within soybean nodules by oxygen microelectrodes." Planta **119**(4): 351-360.

Tornroth-Horsefield, S., Wang, Y., Hedfalk, K., Johanson, U., Karlsson, M., Tajkhorshid, E., Neutze, R. and Kjellbom, P. (2006). "Structural mechanism of plant aquaporin gating." Nature **439**(7077): 688-694.

Tsukaguchi, H., Shayakul, C., Berger, U. V., Mackenzie, B., Devidas, S., Guggino, W. B., van Hoek, A. N. and Hediger, M. A. (1998). "Molecular characterization of a broad selectivity neutral solute channel." J Biol Chem **273**(38): 24737-24743.

Tyerman, S. D., Whitehead, L. F. and Day, D. A. (1995). "A channel-like transporter for NH4+ on the symbiotic interface of N2-fixing plants." Nature **378**(6557): 629-632.

Udvardi, M., Lister, D. and Day, D. (1991). "ATPase activity and anion transport across the peribacteroid membrane of isolated soybean symbiosomes." Archives of Microbiology **156**(5): 362-366.

Udvardi, M. K. and Day, D. A. (1989). "Electrogenic ATPase Activity on the Peribacteroid Membrane of Soybean (Glycine max L.) Root Nodules." Plant Physiol **90**(3): 982-987.

Udvardi, M. K. and Day, D. A. (1997). "Metabolite Transport across Symbiotic Membranes of Legume Nodules." Annu Rev Plant Physiol Plant Mol Biol **48**: 493-523.

Udvardi, M. K., Ou Yang, L., Young, S. and Day, D. A. (1990). "Sugar and Amino Acid Transport Across Symbiotic Membranes from Soybean Nodules." Mol Plant Microbe Interact **3**(5): 334-340.

Udvardi, M. K., Price, G. D., Gresshoff, P. M. and Day, D. A. (1988). "A dicarboxylate transporter on the peribacteroid membrane of soybean nodules." FEBS Letters **231**(1): 36-40.

van Heeswijk, M. P. and van Os, C. H. (1986). "Osmotic water permeabilities of brush border and basolateral membrane vesicles from rat renal cortex and small intestine." J Membr Biol **92**(2): 183-193.

Verma, D. P. and Hong, Z. (1996). "Biogenesis of the peribacteroid membrane in root nodules." Trends Microbiol **4**(9): 364-368.

Vessey, J. K., Pawlowski, K. and Bergman, B. (2005). "Root-based N2-fixing Symbioses: Legumes, Actinorhizal Plants, Parasponia sp. and Cycads." Plant and Soil **274**(1-2): 51-78.

Vessey, J. K., Walsh, K. B. and Layzell, D. B. (1988). "Oxygen limitation of N2 fixation in stem-girdled and nitrate-treated soybean." Physiologia Plantarum **73**(1): 113-121.

Vincill, E. D., Szczyglowski, K. and Roberts, D. M. (2005). "GmN70 and LjN70. Anion transporters of the symbiosome membrane of nodules with a transport preference for nitrate." Plant Physiol **137**(4): 1435-1444.

Wallace, I. S., Choi, W. G. and Roberts, D. M. (2006). "The structure, function and regulation of the nodulin 26-like intrinsic protein family of plant aquaglyceroporins." Biochim Biophys Acta **1758**(8): 1165-1175.

Wallace, I. S. and Roberts, D. M. (2004). "Homology modeling of representative subfamilies of Arabidopsis major intrinsic proteins. Classification based on the aromatic/arginine selectivity filter." Plant Physiol **135**(2): 1059-1068.

Wallace, I. S. and Roberts, D. M. (2005). "Distinct transport selectivity of two structural subclasses of the nodulin-like intrinsic protein family of plant aquaglyceroporin channels." Biochemistry **44**(51): 16826-16834.

Wallace, I. S., Wills, D. M., Guenther, J. F. and Roberts, D. M. (2002). "Functional selectivity for glycerol of the nodulin 26 subfamily of plant membrane intrinsic proteins." FEBS Lett **523**(1-3): 109-112.

Weaver, C. D., Crombie, B., Stacey, G. and Roberts, D. M. (1991). "Calcium-Dependent Phosphorylation of Symbiosome Membrane Proteins from Nitrogen-Fixing Soybean Nodules : Evidence for Phosphorylation of Nodulin-26." Plant Physiol **95**(1): 222-227.

Weaver, C. D. and Roberts, D. M. (1992). "Determination of the site of phosphorylation of nodulin 26 by the calcium-dependent protein kinase from soybean nodules." Biochemistry **31**(37): 8954-8959.

Weaver, C. D., Shomer, N. H., Louis, C. F. and Roberts, D. M. (1994). "Nodulin 26, a nodule-specific symbiosome membrane protein from soybean, is an ion channel." J Biol Chem **269**(27): 17858-17862.

Wei, H. and Layzell, D. B. (2006). "Adenylate-coupled ion movement. A mechanism for the control of nodule permeability to O2 diffusion." Plant Physiol **141**(1): 280-287.

Weisz, P. R. and Sinclair, T. R. (1987). "Regulation of Soybean Nitrogen Fixation in Response to Rhizosphere Oxygen: II. Quantification of Nodule Gas Permeability." Plant Physiol **84**(3): 906-910.

White, J., Prell, J., James, E. K. and Poole, P. (2007). "Nutrient sharing between symbionts." Plant Physiol **144**(2): 604-614.

Whitehead, L. F., Tyerman, S. D. and Day, D. A. (2001). "Polyamines as potential regulators of nutrient exchange across the peribacteroid membrane in soybean root nodules." Functional Plant Biology **28**(7): 677-683.

Wienkoop, S. and Saalbach, G. (2003). "Proteome analysis. Novel proteins identified at the peribacteroid membrane from Lotus japonicus root nodules." Plant Physiol **131**(3): 1080-1090.

Witty, J. F., Skøt, L. and Revsbech, N. P. (1987). "Direct Evidence for Changes in the Resistance of Legume Root Nodules to O2 Diffusion." Journal of Experimental Botany **38**(7): 1129-1140.

Wu, S. and Letchworth, G. J. (2004). "High efficiency transformation by electroporation of Pichia pastoris pretreated with lithium acetate and dithiothreitol." Biotechniques **36**(1): 152-154.

Young, N. D., Debelle, F., Oldroyd, G. E., Geurts, R., Cannon, S. B., Udvardi, M. K., Benedito, V. A., Mayer, K. F., Gouzy, J., Schoof, H., Van de Peer, Y., Proost, S., Cook, D. R., Meyers, B. C., Spannagl, M., Cheung, F., De Mita, S., Krishnakumar, V., Gundlach, H., Zhou, S., Mudge, J., Bharti, A. K.,

Murray, J. D., Naoumkina, M. A., Rosen, B., Silverstein, K. A., Tang, H., Rombauts, S., Zhao, P. X., Zhou, P., Barbe, V., Bardou, P., Bechner, M., Bellec, A., Berger, A., Berges, H., Bidwell, S., Bisseling, T., Choisne, N., Couloux, A., Denny, R., Deshpande, S., Dai, X., Doyle, J. J., Dudez, A. M., Farmer, A. D., Fouteau, S., Franken, C., Gibelin, C., Gish, J., Goldstein, S., Gonzalez, A. J., Green, P. J., Hallab, A., Hartog, M., Hua, A., Humphray, S. J., Jeong, D. H., Jing, Y., Jocker, A., Kenton, S. M., Kim, D. J., Klee, K., Lai, H., Lang, C., Lin, S., Macmil, S. L., Magdelenat, G., Matthews, L., McCorrison, J., Monaghan, E. L., Mun, J. H., Najar, F. Z., Nicholson, C., Noirot, C., O'Bleness, M., Paule, C. R., Poulain, J., Prion, F., Qin, B., Qu, C., Retzel, E. F., Riddle, C., Sallet, E., Samain, S., Samson, N., Sanders, I., Saurat, O., Scarpelli, C., Schiex, T., Segurens, B., Severin, A. J., Sherrier, D. J., Shi, R., Sims, S., Singer, S. R., Sinharoy, S., Sterck, L., Viollet, A., Wang, B. B., Wang, K., Wang, M., Wang, X., Warfsmann, J., Weissenbach, J., White, D. D., White, J. D., Wiley, G. B., Wincker, P., Xing, Y., Yang, L., Yao, Z., Ying, F., Zhai, J., Zhou, L., Zuber, A., Denarie, J., Dixon, R. A., May, G. D., Schwartz, D. C., Rogers, J., Quetier, F., Town, C. D. and Roe, B. A. (2011). "The Medicago genome provides insight into the evolution of rhizobial symbioses." Nature **480**(7378): 520-524.

Yu, X. S., Yin, X., Lafer, E. M. and Jiang, J. X. (2005). "Developmental regulation of the direct interaction between the intracellular loop of connexin 45.6 and

the C terminus of major intrinsic protein (aquaporin-0)." J Biol Chem **280**(23): 22081-22090.

Yurgel, S. N. and Kahn, M. L. (2004). "Dicarboxylate transport by rhizobia." FEMS Microbiol Rev **28**(4): 489-501.

Zardoya, R. (2005). "Phylogeny and evolution of the major intrinsic protein family." Biol Cell **97**(6): 397-414.

Zeidel, M. L., Ambudkar, S. V., Smith, B. L. and Agre, P. (1992). "Reconstitution of functional water channels in liposomes containing purified red cell CHIP28 protein." Biochemistry **31**(33): 7436-7440.

Zelenina, M., Zelenin, S., Bondar, A. A., Brismar, H. and Aperia, A. (2002). "Water permeability of aquaporin-4 is decreased by protein kinase C and dopamine." Am J Physiol Renal Physiol **283**(2): F309-318.

Zhang, Y. and Roberts, D. M. (1995). "Expression of soybean nodulin 26 in transgenic tobacco. Targeting to the vacuolar membrane and effects on floral and seed development." Mol Biol Cell **6**(1): 109-117.

Zhao, X. Q., Mitani, N., Yamaji, N., Shen, R. F. and Ma, J. F. (2010). "Involvement of silicon influx transporter OsNIP2;1 in selenite uptake in rice." Plant Physiol **153**(4): 1871-1877.

VITA

Jin Ha Hwang was born in Seoul, South Korea on December 9th, 1976. He entered the Inha University, Incheon, South Korea in March of 1995 and graduated with a Bachelor of Engineering degree in Biochemical Science Engineering in August of 2002. After graduation with a Bachelor degree, he continued study in graduate school at the Gwangju Institute of Science and Technology and graduated with a Master of Science degree in Life Sciences in August of 2004. After graduation with a Master degree, he moved to the United States of America and entered the University of Tennessee, Knoxville in the graduate school of Genome Science and Technology in August of 2005.

He joined and began his Ph.D. training at Dr. Daniel M. Roberts' laboratory in Biochemistry and Cellular and Molecular Biology at the University of Tennessee, Knoxville. During the period of his graduate work, he worked on the soybean nodulin 26, and contributed new discoveries on its functional and regulatory properties in response to environmental stimuli.